ERASMUS UNIVERSITEIT ROTTERDAM

ORTEC
OPTIMIZE YOUR WORLD

Master thesis Econometrics & Management Science

Specialization: Operations Research & Quantitative Logistics

FINAL VERSION

Carbon Intensity Modeling in Energy Value Chain Optimization

Applied on a Case Study in the Dutch Hydrogen Market

Author:
Erik van der Heide
Erasmus School of Economics (481579)

Supervisor:
prof.dr. Albert Wagelmans
Erasmus School of Economics

Company supervisor:
Floris van den Broek
ORTEC - Optimize Your World

Second assessor:
dr. Riley Badenbroek
Erasmus School of Economics

September 28, 2022 - Erasmus University Rotterdam

Abstract

Companies in the energy sector are setting ambitious targets to become climate neutral. In this process, it is of vital importance that each final product is associated with its inherent carbon intensity (CI). This carbon intensity is a measure of the emissions associated with an energy product accumulated while moving through the energy value chain, from extracting primary energy sources up to the utilization of the final product. Carbon intensity is usually measured in gCO2e/x – grams of CO2-equivalent per mass, volume or energy content of the product. To reduce the carbon intensity of a product, companies have several choices and investment opportunities, for example making a switch to cleaner modes of transport or the installation of carbon capture & storage (CCS) technologies. This thesis aims to design models that find the most cost-efficient solutions for energy value chains while incorporating restrictions on carbon intensities.

The contribution of this thesis is twofold. Firstly, we present a general modeling framework that incorporates optimization over carbon intensity in a four-tier supply, production, storage and customer network with multiple product streams, multiple modes of transport and CCS investment options. Carbon intensity can be calculated post-optimization relatively easily given a set of allocation rules, however optimizing over carbon intensity results in a nonconvex quadratic optimization problem. This problem can be solved to optimality within a few minutes with state-of-the-art solvers for small instances of at most a hundred variables and carbon intensity restriction values that are not so low that they approach infeasibility. Secondly, an application of a hydrogen supply chain network optimization case study in the Netherlands is presented. In this network, emissions from hydrogen production account for about 95% of total emissions, where total emissions also include feedstock preparation and transportation emissions. Therefore, investments in CCS are most effective to reduce carbon emissions. For a linear dynamic model of conventional size of several tens of thousands of variables, it takes under one second to find the optimal network configuration without carbon restrictions. Among different CI restrictions, it generally takes a few seconds to find the first feasible solution, but optimality can rarely be proven within five minutes. Solving the linear version of the model where emissions are minimized serves as a good starting solution, which can be used as a warm start in case the model has trouble finding an initial solution satisfying the CI restrictions.

Keywords: mixed integer nonlinear programming (MINLP), energy value chain optimization, carbon intensity, carbon capture & storage (CCS)

Contents

List of Abbreviations

BG	biomass gasification
BLP	bilinear program
CCS	carbon capture & storage
CCUS	carbon capture, utilization & storage
CG	coal gasification
CH_2	compressed hydrogen
CI	carbon intensity
CO_2	carbon dioxide
GHG	greenhouse gas
H_2	hydrogen
HSCN	hydrogen supply chain network
kWh	kilowatt-hour
LCA	life cycle analysis/assessment
LH_2	liquefied hydrogen
MILP	mixed-integer linear program/programming
MINLP	mixed-integer nonlinear program/programming
MRMT	multi-resource, multi-transport
SMR	steam methane reforming
SRMT	single-resource, multi-transport
SRST	single-resource, single-transport
WE	water electrolysis
WtW	well-to-wheels

Chapter 1

Introduction

According to research from the Intergovernmental Panel on Climate Change, the global temperature on earth has risen approximately 1.09°C in 2011-2020 compared to the pre-industrial age (Pörtner et al., 2022). The probability that in the period 2021-2040 this will increase to over 1.5°C, the targeted global warming limit in the Paris Agreement of 2015, has increased to more than 50%. According to Lamb et al. (2021), global greenhouse gas (GHG) emissions peaked in 2018 at 58 gigatons CO_2-equivalent, of which about 34% originate directly from the energy systems sector. Therefore, it is of crucial importance that energy companies take action to lower their carbon emissions in the coming decades.

Energy systems consist of the supply, storage, distribution and sales of energy products. There exists a wide range of energy sources: crude oil, natural gas, coal, biomass, nuclear plants, wind energy, solar power, etc. Feedstock sources are converted into energy products providing different energy services, such as gas for heating houses or gasoline to fuel cars. The design and optimization of such energy systems are also called energy value chain optimization.

Energy products have certain associated carbon emissions. These can roughly be classified into two categories. First of all, there are scope 1 and 2 emissions, which are respectively direct and indirect emissions originating from operations. These include for example the emissions arising during the production of the feedstock at the source, emissions from processing feedstock into products and emissions from transportation of resources. Secondly, there are scope 3 emissions, which consist of - among others - the use of the energy products sold. Scope 3 emissions can vary greatly between energy products: for instance, burning pure diesel corresponds to different carbon emissions than burning biodiesel, where biomass is blended in.

If one accounts for all the emissions that are associated with a final product in an energy value chain, one can calculate its carbon intensity (CI), also known as emission density. Carbon intensity is a quantity that can be used to express the inherent emissions of a product. It is expressed in gCO_2e/x – grams of CO2-equivalent per volume, mass or energy content of the product. In conventional supply chains, the CI property of a product generally increases as it moves through the network, as the production, manufacturing and transport processes increase the cumulative carbon emissions.

To reduce the carbon intensity of a product, several decisions during value chain optimization can be taken. First of all, the selection of feedstock has a large influence on the CI of a product. For instance, electricity can be produced from coal or natural gas, but wind and solar energy are much cleaner alternatives. Secondly, investments in the technology carbon capture & storage

(CCS) can be considered, which captures CO_2 emissions during material processing and stores them underground. Other carbon reduction strategies include the selection of cleaner production units, other modes of transport and satisfying less demand.

Calculating the CI values post-optimization, i.e., given your optimized material flows, is somewhat ambiguous. The emissions of a factory, for instance, could be distributed among the materials in various ways: based on the volume of the products, their mass, etc. Although this is an important topic, it is mainly an accounting challenge. When CI is included as part of the decision variables in the optimization process, however, we also have challenges of a mathematical nature. As carbon flows in the supply chain are a result of the material flows, we establish a nonlinear problem formulation, something that also appears in the well-studied pooling problem in the petrochemical industry. This thesis project focuses on finding effective modeling and solution techniques for carbon intensity in energy value chains.

The research project is conducted in collaboration with ORTEC. ORTEC is a software and consultancy company, specialized in the optimization of business processes using mathematics and data science. The project is done for the company Shell, which is one of the largest energy suppliers in the world. Shell has the ambition to become a net-zero company by 2050, in steps with society.

1.1 Research Objectives

The main challenge surrounding the modeling of carbon intensity is to find the most suitable formulations and solution methods given the various carbon-related use cases that can be modeled. This gives rise to the following research questions:

1. What is the most effective way to model carbon flows in mixed-integer linear programming production and distribution models in the energy value chain optimization domain?
   (a) How can a restriction on carbon intensity be included?
   (b) How can the option for carbon capture & storage be included?
   (c) What is the degree of nonlinearity under different model configurations?
   (d) Are there multiple equivalent model formulations that differ in terms of performance?
2. What is the performance in terms of running time of large models which include restrictions on carbon intensities?

The carbon flows described in Question 1 should be applicable or adjustable to general energy value chain optimization setups. Questions 1a and 1b concern modeling tricks to incorporate different carbon-related concepts. Question 1c requires investigation of whether the formulations are convex or nonconvex, always nonlinear, and to which degree of nonlinearity. Question 1d digs deeper into how carbon intensity can be modeled. Question 2 mainly concerns how well models with CI restrictions perform on instances of reasonable size which we would encounter in a real-life setting.

Although the primary goal of this thesis is to find effective modeling and solving techniques, the underlining aim of these models is to reduce carbon emissions in energy value chains. Therefore, the business question can be formulated as follows:

What is the most cost-effective way to decrease the carbon intensity of energy products?

1.2 Research Approach

To answer the research questions, this research project is split into two parts. The contribution of the first part is a generalized theoretical framework, which mainly serves to answer the first research question. First, we develop a mixed-integer linear model for a general production and distribution problem incorporating multiple product types (resources), multiple modes of transport and CCS. We consider a four-tier model consisting of supply, production, storage and customer nodes. On top of this linear model, we define how to calculate carbon intensities post-optimization, as well as a set of equations to incorporate carbon intensity during-optimization in a nonlinear fashion. This model is validated using artificially created data. The resulting nonconvex nonlinear model can be solved to optimality using recent solvers, but with stricter CI restrictions the solver cannot prove optimality within a few minutes of running time on models with not more than a hundred variables and constraints.

On top of this general modeling framework, we want to incorporate the concept of carbon intensity into a real-life case study. The contribution of this second part is the addition of carbon intensity to a hydrogen supply chain network optimization model and the corresponding investigation on performance to answer the second research question. The model and data are based on the study by Konda et al. (2011), who consider the configuration of a hydrogen network in the Netherlands, where the main decision is where to locate production plants and what type of production plants to build. It is a pure cost minimization model, and although well-to-tank CO_2 emissions are mentioned, they do not optimize over carbon emissions or carbon intensities. We want to see what other decisions the model makes if these concepts are integrated. Under some assumptions, feasible and even optimal solutions can be found for model sizes of several tens of thousands of variables and constraints.

The hydrogen market is one of the most interesting markets to apply the concept of carbon intensity. Currently, hydrogen production is still classified with a color label, where green hydrogen corresponds to hydrogen produced with renewable energy, gray hydrogen to the production with natural gas and blue hydrogen the production with natural gas where the carbon emissions from the production process are captured by CCS. As every type of energy source and production process has at least some associated carbon emissions, the trend goes towards classifying hydrogen products with an inherent carbon intensity (DNV, 2022).

1.3 Thesis Structure

In the remainder of this thesis, we first elaborate on the exact problem we are facing in Chapter 2, including some commonly used terminology surrounding energy value chains. This also includes which possibilities there are for carbon emission reductions in these chains. Thereafter, in Chapter 3 we give a literature overview of topics related to the problem of carbon intensity modeling. In Chapter 4, we first discuss a four-level supply chain optimization model, as well as how to incorporate carbon intensity into this model. Secondly, a broad description of the case study setup and model is presented. Chapter 5 presents the results of these models and the data used to arrive at these results. Finally, in Chapter 6 we give a conclusion and discuss the research outline and results.

Chapter 2

Problem Description

In this chapter, we discuss the problem of carbon intensity modeling and the related energy value chain optimization topics. In Section 2.1, a schematic overview of a general energy value chain is given, including several related concepts. Section 2.2 presents the mathematical challenges of carbon balancing and the similarities with flow and pooling problems.

2.1 Emissions in Energy Value Chains

Energy value chains are usually specific to a certain topology, depending on what energy sources and energy products are required. Nevertheless, the value chain can be generalized into several interrelated components, which are schematically represented in Figure 2.1.

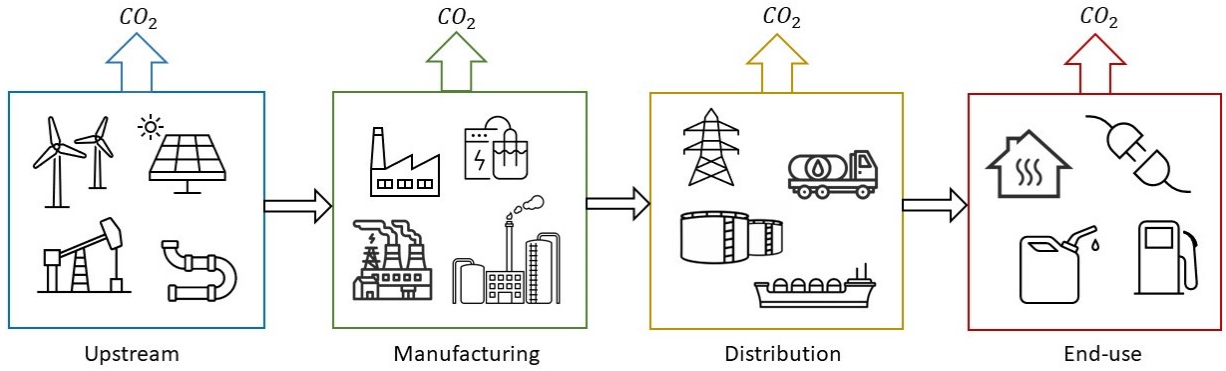

FIGURE 2.1: Schematic overview of an energy value chain.

The energy value chain components from Figure 2.1 are:

- Upstream. This includes all the activities up to the manufacturing stage, for instance digging raw feedstock from the ground, pre-processing the materials and transporting it to the refinery, or generating electricity using windmills and solar panels.
- Manufacturing. This highly depends on the type of energy product that is produced, but most generally this includes processes such as refinery activities, electrolysis and hydrolysis. Generally, these activities happen on the same site and have no long distances in between, but this also depends on the application. For example, the liquefied natural gas chain consists of two distinct manufacturing processes: liquefaction and regasification.

- Distribution and storage. The transportation and inventory of intermediate and final products mainly consist of road, cargo and pipeline infrastructures to storage depots and end-users.
- End-use. The last stage is the final use of the energy product, like heating the house with gas or burning gasoline while driving. Emissions depend on the energy product used, for instance hydrogen is a zero-emission clean fuel at the point of use, while hydrocarbon sources such as oil, gas and coal have a relatively high carbon content.

2.1.1 Emission Reduction Possibilities

Each of the four components in Figure 2.1 has some associated carbon emissions. Some of the main components where carbon emissions can be reduced are:

- Feedstock selection. Using energy feedstock alternatives with a lower carbon content such as biomass save a significant amount of emissions at the end-use stage. Also the processing of feedstock at different locations can vary in direct carbon emissions.
- Selection of production units. As technology advances, investments in cleaner technologies will reduce the emissions at manufacturing units. For instance, cleaner external energy sources can be used at these units in order to convert energy feedstock into intermediate and final products.
- Carbon capture & storage. Another way to save emissions at manufacturing units is the investment in CCS, which is further explained in Section 2.1.3.
- Selection modes of transport. Carbon emissions can be saved by investing in cleaner modes of transport that distribute materials in the network, like replacing diesel trucks with electric trucks.
- Less production. If less demand of the end-user is satisfied, naturally, less CO_2 will be emitted. However, this is not always a viable option, as some minimum production is needed to serve the energy demand of society and still be profitable as a company.

2.1.2 Scope 1, 2 and 3 Emissions

Greenhouse gas emissions can be separated into three categories: scope 1, 2 and 3 emissions. Scope 1 and 2 emissions originate from business operations, while scope 3 emissions are indirect emissions, in this context specifically emissions from the end-use of energy products. Scope 1 emissions consist of direct emissions from operations, like exploration, production, processing and refining. Scope 2 emissions are indirect emissions originating from purchased electricity, steam and heat to run a company's operations. Scope 3 emissions are all other indirect emissions, which mainly consist of the emissions released by the use of energy products by suppliers and customers. Scope 3 emissions typically account for around 95% of all scope 1, 2 and 3 emissions.

2.1.3 Carbon Capture & Storage

Carbon capture & storage is a technology that is able to capture CO_2 that is produced at industrial facilities (Ravi et al., 2017). For instance, if a CCS facility is installed at a fossil fuel power station, it can significantly reduce the associated carbon emissions of electricity. However, CCS facilities also require a baseline energy input to work and have a limited capture rate, which becomes increasingly

expensive if a higher capture rate is desired (Quarton & Samsatli, 2020). After the CO_2 is captured, it is compressed and transported to a storage location, such as a depleted oil or gas field, or injected deep underground. Nowadays, two other emerging technologies exist: one where CO_2 is directly captured from the air, and carbon capture, utilization & storage (CCUS), where CO_2 is used in a range of (chemical) applications. These two are not considered in this research project.

2.1.4 Carbon-To-Serve

Carbon intensity has a lot of similarities with the concept of cost-to-serve. Cost-to-serve is the cost that is needed to deliver one unit of material at a certain location in the supply chain. The cost-to-serve increases going forwards in the network. In the oil industry, this is called a netback, which is the cost of bringing one barrel of oil to the market. In the context of GHG emissions, one could argue that carbon intensity is something analogous to carbon-to-serve. However, it also differs from cost-to-serve, firstly because intermediate acquired energy products already have an associated 'carbon cost', while this does not have to be the case for the cost-to-serve. Secondly, a carbon cost can also be negative because of carbon capture, which is not the case for cost-to-serve. Ideally, we want to do some type of quantitative research that puts a restriction on the cost-to-serve, but this is not well-studied in the literature.

2.1.5 Carbon Intensity

The carbon emissions associated with different stages of a product are studied under different terminology. Firstly, there is life cycle analysis or life cycle assessment (LCA), which accounts for the environmental impact over each stage of the life cycle of a product or service. More specifically in the energy sector, the term well-to-wheels (WtW) is used, which is similar to LCA, but does not include the production and end-of-life of machines, for instance the emissions associated with the installation of a wind park. Well-to-wheels consists of two stages: well-to-tank, which are all processes from extracting primary energy sources to the deliverance of final products, and tank-to-wheel, which consists of the actual burning of the final product by the engines. The carbon intensity of a product can be calculated in different ways, depending on whether you take an LCA or WtW approach, but essentially it corresponds to the GHG emissions associated with the different steps in the supply chain, expressed in gCO_2e/x: grams of CO_2-equivalent per x, where x can be a mass (kg), volume (L) or energy content (MJ or kWh). This measure is more related to a specific product, while the absolute carbon emissions in grams CO_2e per annum (gpta) is a more general measurement.

2.2 Mathematical Challenges

Next, we discuss which mathematical challenges are faced when modeling carbon intensity. First, we discuss carbon balancing at intermediate units, after which we discuss how this problem relates to other flow and pooling problems.

2.2.1 Carbon Balancing

Figure 2.2 gives a sketch of a simplified energy value chain. Starting from the supply nodes (sup.), different types of feedstock are transported to the production unit, where the feedstock is converted into final products. This happens under the supply of some energy source to let the process work. At the production unit, a CCS unit is added as a decision option to let (some of) the produced carbon emissions at the production unit be captured. Once the products are produced, they are stored at a depot, which also needs a (fixed) baseline energy consumption to sustain the products. Finally, the products are distributed over the customer nodes (cust.) from the depot, where the customers have certain demands for each of the products.

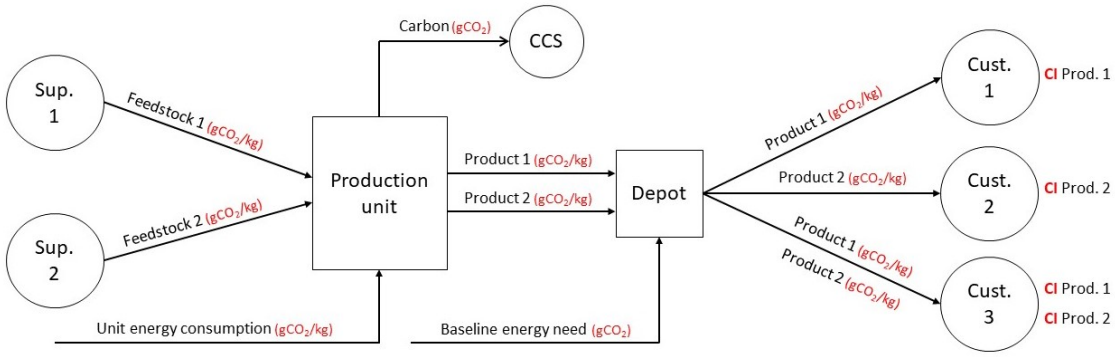

FIGURE 2.2: Schematic flow diagram of a simplified energy value chain.

For the configuration in Figure 2.2, the optimization decisions are how much feedstock to acquire from each supplier, how much product to distribute to each customer and optionally to install a CCS facility. Given the material flows that the model optimizes for, one can calculate the carbon intensity of each product at the customer nodes, given the allocation rules of carbon emissions over the different material streams. The total carbon flow (the material flows times the carbon intensities) that enters an intermediate node must leave the node, distributed over its output flows. We assume there is no loss of energy in the system. How this distribution is done is mostly depending on the process at the unit itself, as carbon flows can for example be distributed based on mass, volume or energy content. The resulting carbon balance constraints in general consist of carbon intensity variables multiplied by materials flows, such that the carbon intensity of a node equals the weighted sum of incoming carbon intensities. At the supply nodes, carbon intensities are still fixed numbers per unit product, but from the intermediate nodes onward, carbon intensities depend on other variables in the system and are therefore also variables.

Carbon intensity can be calculated relatively easily post-optimization once the material flows are known, but including it during-optimization creates nonlinear balance equations. This is because there is some sort of 'shadow network' of carbon flows in the system, which is a result of the material flow network. Because both flow networks influence each other, it is not possible to optimize both the material and carbon flows simultaneously in a linear way, something that also appears in the nonlinear pooling problem. These nonlinearities add significantly to the complexity of the problem: next to the thousand or even tens of thousands of decision variables and constraints that are present in a typical supply chain optimization model, these nonlinear constraints might have a big effect on running times.

2.2.2 Similarities Flow and Pooling Problems

Energy value chain optimization problems consist of some type of network flow, and often some blending and/or pooling activities. For standard flow problems, products are transported from source (supply) to sink (customer) nodes, possibly via transshipment nodes. One such application in the energy sector is the transport of fuels from a refinery to gasoline stations via depot storage. In the blending problem, raw feedstock from several source nodes is blended at sink nodes, in such a way that the attributes of the blends at the sinks meet certain criteria, for instance a minimum and maximum sulfur content of the blend. The pooling problem generalizes both the minimum-cost flow problem and the blending problem (Gupte et al., 2017). The pooling problem combines both concepts, where feedstock from source nodes is blended at in-between 'pooling' nodes, from where it is distributed and blended again at the sink nodes. An example is given in Figure 2.3. The material streams should be optimized in such a way that the sulfur content restrictions at the sinks are respected. For instance, sink 3 cannot be satisfied for 100% by source 3, because then the sulfur content would be 90%, which is above 80%. The nonlinearity arises from the fact that the sulfur content at the sinks depends on material streams from pools, where in turn at the pools the sulfur content depends on the material streams from the sources.

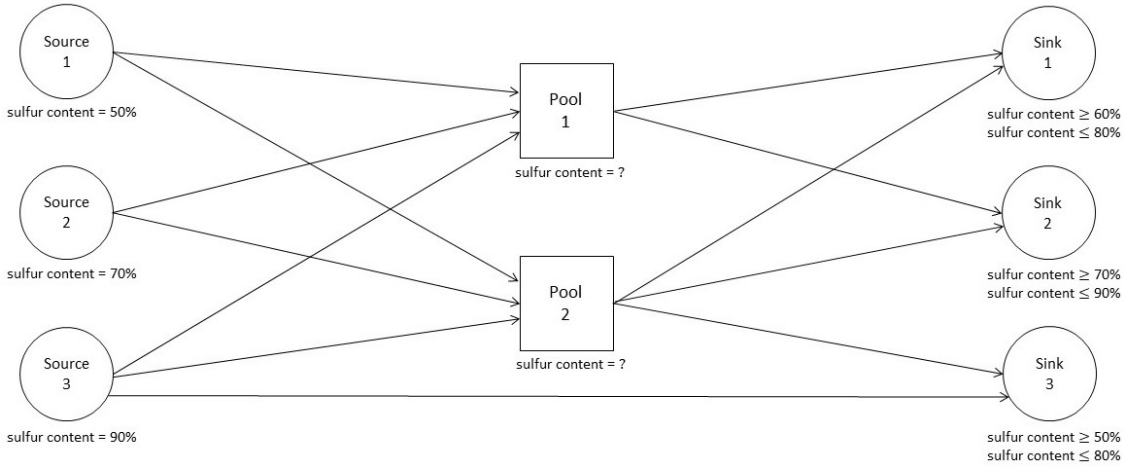

FIGURE 2.3: Example of a pooling problem.

The structure of the pooling problem has several similarities with the carbon intensity modeling problem. The pooling problem is a nonlinear problem, as the attributes of the materials at the pooling nodes depend on the flows from sources to pools, making it an unknown quantity. The carbon intensity of a product at any stage in the supply chain can also be interpreted as an attribute or property of the product. This attribute can change, depending on the type of material handling, mode of transport used, etc. Therefore, we get the same nonlinear structure for which the incoming carbon flow at an intermediate node must equal the outgoing carbon flow. Different than for standard flow problems, carbon flow can also be added along the arcs, in particular by transportation emissions. The constraints on the attributes of the products in the pooling problem can be translated to constraints where the carbon intensities of the products should be lower than a certain threshold.

Chapter 3

Literature Review

The design and optimization of supply chains is a broad field of research that inherits classical problems in optimization, such as facility location problems and network flow problems (Garcia & You, 2015). The goal of supply chain optimization is to design an industry network in such a way that it optimizes certain metrics, like the minimization of operational costs or the maximization of the service rate. Supply chains typically contain components such as production units, storage locations and modes of transport. This chapter discusses concepts of supply chain optimization that are relevant for carbon intensity modeling: energy value chain optimization (Section 3.1), hydrogen supply chain models (Section 3.2) carbon capture & storage (Section 3.3), flow and pooling problems (Section 3.4) and methods to solve nonlinear programming problems (Section 3.5).

3.1 Supply Chain Optimization of Energy Value Chains

Supply chain optimization mainly concerns long-term strategic and mid-term tactical decisions. On a strategic level, this includes network design and facility location problems, and on a tactical level, this includes distribution planning and demand analysis. In the literature, several such case studies in the energy sector have been published, which use mixed-integer linear programming (MILP) modeling. Most studies focus on the value chain optimization of one energy source in particular, such as biofuels like bioethanol (Zamboni et al., 2009), synthetic natural gas (Calderón et al., 2017) or algal biodiesel (Gong & You, 2014). Samsatli and Samsatli (2018) present a multi-objective MILP model to find an optimal way to utilize primary energy sources for different energy uses, including decisions in energy conversion, transportation and storage. This model, also known as the value web model, is one of the largest studied models allowing for various energy resources and network design decisions. Quarton and Samsatli (2020) extend this model by incorporating CCUS. Hydrogen technologies were added too, such as power-to-gas, for which electricity is converted into hydrogen through electrolyzers, as well as the storage of hydrogen. Some papers also consider matheuristics to reduce the computation times of exact models. An example comes from Ruvalcaba-Sandoval et al. (2021), who present a matheuristic for a four-tier supply chain consisting of suppliers, factories, warehouses and customers, where warehouses and their capacities are selected heuristically.

The concept of carbon intensity is not yet widely used in the literature. Studies on carbon intensity are for example from Moro and Lonza (2018), who discuss the carbon intensity of the electricity mix, expressed in gCO_2e/kWh, of countries in the European Union. However, they do not optimize this carbon intensity. Studies that consider multi-objective optimization, for instance

Han et al. (2013) and Zarei et al. (2020), usually maximize profit and minimize carbon emissions in the supply chain, but do not impose a restriction on the carbon intensity of a product. Similarly, Benjaafar et al. (2012) optimize over cost and carbon emissions in traditional lot sizing problems to demonstrate how carbon can be used in decision-making models. Nouira et al. (2016) do not explicitly restrict carbon intensities at the demand side, but look at demand that is sensitive to carbon emissions per unit product. Another common carbon reduction strategy is carbon cap and trading, such as done by Nie et al. (2020). They put carbon limits, i.e., caps, on specific processing units in the supply chain. If these caps are exceeded, carbon permits need to be bought on the trading market, while a surplus on the carbon cap can be traded to increase revenue. This is different from carbon intensity modeling, as it concerns restrictions on the emissions at specific units, rather than restrictions on the accumulated carbon intensity of a product at a stage in the supply chain.

3.2 Hydrogen Supply Chain Models

As our study is performed on a hydrogen case study, we give special attention to hydrogen supply chain network (HSCN) models in the literature. Almansoori and Shah (2006) present a static hydrogen supply chain model with factory, storage and transportation components, also considering different technologies and hydrogen physical products. The same authors extended their model by making it dynamic and incorporating feedstock availability (Almansoori & Shah, 2009) and incorporating fueling stations and demand uncertainty (Almansoori & Shah, 2012). More extensions in different directions to the basic model for different case study regions were proposed in the literature, which are summarized in Table 3.1. All papers have the following four components in common: they consider grid squares, which are the demand locations; multiple physical hydrogen products, usually compressed and liquefied hydrogen; production plants with different production technologies; the option for multiple modes of transport.

TABLE 3.1: Model components present in different hydrogen supply chain network adaptations.

Paper	Storage locations	Plant sizes	Energy sources	Time periods	Scenario analysis	Refuel stations	Uncertainty	Case
Almansoori and Shah (2006)	x	-	-	-	-	-	-	UK
Kim et al. (2008)	x	-	-	-	-	-	x	Korea
Almansoori and Shah (2009)	x	x	x	x	-	-	-	UK
Konda et al. (2011)	x	x	x	x	x	x	-	NL
Almansoori and Shah (2012)	x	x	x	x	x	x	x	UK
Han et al. (2012)	x	-	-	-	-	-	-	Korea
Nunes et al. (2015)	x	-	x	x	-	x	x	UK
Moreno-Benito et al. (2017)	x	x	-	x	-	x	-	UK
Seo et al. (2020)	-	x	x	-	-	x	-	Korea
Robles et al. (2020)	x	-	x	-	-	x	-	France
Cantú et al. (2021)	-	x	x	x	-	-	-	France

Konda et al. (2011) perform a hydrogen infrastructure case study in the Netherlands, which we use in this research project. Another paper that comes close to what we are after is from Almansoori and Betancourt-Torcat (2016), who incorporate emissions constraints in the HSCN model. To overcome the computational burdens of large models, some (mat)heuristical algorithms are considered.

Woo and Kim (2019) combine a nonlinear variant of the HSCN problem with a genetic algorithm structure, and Robles et al. (2020) use genetic algorithms to solve a multi-objective variant of the problem. Cantú et al. (2021) propose a matheuristic where the problem is split into finding locations for facilities and minimizing and operational and transportation costs of those facilities.

3.3 Carbon Capture & Storage

Several studies have been conducted concerning carbon capture & storage. Ravi et al. (2017) designed a framework to optimize the use of CCS in the Netherlands. They develop a MILP model which minimizes the total cost of capturing CO_2 from source locations, choosing capture technologies and pipeline transportation to physical storage sites. Each source of CO_2 can only be captured by one technology and stored at one location. However, a storage location can receive CO_2 transport from multiple locations and a technology can capture CO_2 from multiple sources, although the latter was not included in the model. By using fractional variables on the amount of CO_2 that is captured, next to binary variables if CO_2 is captured, the model is linearized compared to earlier models. A similar study for Northeastern China was performed by Zhang et al. (2018).

Similar studies have been conducted where sources of CO_2 are matched with possible storage locations. For instance, Middleton and Bielicki (2009) develop a MILP model that determines how much CO_2 from certain sources should be distributed to reservoirs, especially under which pipeline infrastructure. Tan et al. (2013) develop a similar, but multi-period model, including injection and storage capacity restrictions. Source-to-sink matching of CO_2 is not necessarily what this thesis focuses on, but the topic is relevant as we also deal with flow problems and CCS variables. A big difference between these papers and our study is that CO_2 emissions are assumed to be fixed in the papers, while they are variables in our models.

3.4 Flow and Pooling Problems

In the literature, several types of flow problems can be found. Examples include the minimum-cost flow problem, where transport from a source to a sink should be done in the least costly way, or the maximum flow problem, which seeks to find the highest possible flow from source to sink (Ahuja et al., 1988). These problems can be formulated as either single- or multi-commodity problems. They are usually solved by mixed-integer linear programming, including column generation and dynamic programming techniques.

The pooling problem, a relevant problem for carbon intensity modeling, is a nonlinear programming problem with bilinear constraints, or bilinear program (BLP). These are strongly $\mathcal{NP}$-hard problems as they generalize the strongly $\mathcal{NP}$-hard linear max-min problem (Hansen & Jaumard, 1992). Several equivalent formulations were proposed, which can solve the BLPs with nonconvex quadratic programming. The P-formulation by Foulds et al. (1992) uses flow variables between nodes and attribute variables to measure the concentration of material properties at the pools. Ben-Tal et al. (1994) proposed the Q-formulation where the flow variables from supply nodes to pooling nodes are replaced with proportion variables, representing the fraction of inflow at a pool from a supply node. Tawarmalani and Sahinidis (2013) extended the Q-formulation into a new

PQ-formulation by adding valid inequalities to the model. Audet et al. (2004) came up with a hybrid formulation that combines the P-formulation and Q-formulation, which is especially useful when considering the generalized pooling problem where edges between pools exist. Finally, Alfaki and Haugland (2013) present a formulation for the generalized pooling problem based on the multi-commodity flow problem.

Solution methods for the pooling problems can be separated into local and global optimization techniques. Local optimization techniques include successive linear programming, which is based on the linear approximation of the bilinear terms by first-order Taylor expansions (Baker & Lasdon, 1985). Another local optimization method by Floudas and Aggarwal (1990) uses Benders' decomposition. Heuristics are also proposed, for instance Audet et al. (2004) use an alternating method, which iteratively freezes the quality variables and optimizes the flows, in combination with a variable neighborhood search framework. Alfaki and Haugland (2014) create a greedy construction heuristic based on the optimization of subgraphs with a single demand node. The problem can be solved globally using reformulation and spatial branch-and-bound frameworks (Audet et al., 2004; Foulds et al., 1992; Quesada & Grossmann, 1995) or Lagrangian duality approaches (Adhya et al., 1999; Almutairi & Elhedhli, 2009).

3.5 Nonlinear Programming Optimization

Mixed-integer nonlinear programming (MINLP) problems are a generalization of MILP problems, where nonlinear terms might appear in the objective and/or in (some of) the constraints. MINLPs have applications in chemical engineering such as the pooling problem, but also in other domains in engineering, network design and medicine. Both convex and nonconvex MINLPs are generally $\mathcal{NP}$-hard, but nonconvex problems are in practice much harder to solve (Burer & Letchford, 2012). As the continuous relaxation of nonconvex MINLPs may lead to a nonconvex feasible region, more has to be done to get a convex relaxation to use in a branch-and-bound framework. One way to go is to replace nonconvex functions with piecewise linear approximations and use a MILP solver (Belotti et al., 2013). Another option to solve MINLPs to optimality is to use spatial branch-and-bound, which replaces nonconvex terms with their convex envelopes and branches on both integer and continuous variables. More recently, branch-and-reduce algorithms were used, which reduce the variable domains stronger compared to spatial branch-and-bound. This framework is implemented inside the commonly used branch-and-reduce optimization navigator (BARON) solver.

Chapter 4

Methodology

In this chapter, we elaborate on the supply chain optimization models that include carbon intensity calculations and constraints. In Section 4.1, we introduce a generalized supply chain optimization model on which the concept of carbon intensity modeling is tested. In Section 4.2, we explain the setup of a hydrogen supply chain optimization case study where CI is incorporated.

4.1 The Multi-Resource, Multi-Transport Supply Chain Model

We start with a stylized supply chain optimization model for energy products, which we call the multi-resource, multi-transport (MRMT) model. The model is multi-resource, meaning multiple materials or products flow through the system, and multi-transport, meaning that multiple modes of transport are defined between nodes in the network. The model has resemblances with the four-tier multi-product supply-chain network by Ruvalcaba-Sandoval et al. (2021). The simpler single-resource, multi-transport (SRMT) model can be found in Appendix A. This section first describes the basic model without accounting for carbon emissions, after which we discuss how carbon emissions and carbon intensity can be incorporated into these models. The option for CCS and linear constraints on carbon emissions, as well as some model assumptions are discussed too.

4.1.1 Indices, Sets, Parameters and Variables

The model is defined on a graph $\mathcal{G} = (\mathcal{V}, \mathcal{E})$, where $\mathcal{V}$ represents the set of nodes (vertices) and $\mathcal{E}$ the set of arcs (edges). Through the network there is a flow of resources, denoted by the set $\mathcal{R}$, which can be feedstock, intermediate or final products. We define resources per unit, which can in practice be kilotons or kilowatt hour for example. The nodes are divided into the sets $\mathcal{V} = \mathcal{S} \times \mathcal{P} \times \mathcal{D} \times \mathcal{T}$. Here, $\mathcal{S}$ is the set of source nodes that generate resources into the system, $\mathcal{P}$ the set of production nodes that convert resources into other resources, $\mathcal{D}$ the set of depot nodes which temporarily store resources and $\mathcal{T}$ the set of target or customer nodes which make resources disappear from the system. It is assumed that depots can store multiple resources and receive inflow from multiple nodes per resource. Next, the set $\mathcal{M}$ represents the set of available modes of transport defined on the arcs. Not every arc can transport every type of resource on every mode of transport, but this is specified by the exact topology of the data considered. To include CCS investment options, we define the set $\mathcal{P}' \subseteq \mathcal{P}$ as the subset of processing units for which such investments are possible. Let $\mathcal{L}$ be the set of levels of investments of CCS, where each level corresponds to a different capacity of CO_2 capture and associated installation cost. Table 4.1 shows the full list of indices and sets.

TABLE 4.1: Indices and sets of the model.

Index & Set	Description
$i, j \in \mathcal{V}$	nodes of the graph $\mathcal{G}$;
$(i, j) \in \mathcal{E}$	arcs of the graph $\mathcal{G}$;
$\mathcal{N}(i)^+ = \{j \in \mathcal{V} \mid (i, j) \in \mathcal{E}\}$	out-neighbors of node $i \in \mathcal{V}$;
$\mathcal{N}(j)^- = \{i \in \mathcal{V} \mid (i, j) \in \mathcal{E}\}$	in-neighbors of node $j \in \mathcal{V}$;
$s \in \mathcal{S} \subset \mathcal{V}$	source nodes (only outflow);
$p \in \mathcal{P} \subset \mathcal{V}$	production nodes (inflow and outflow);
$d \in \mathcal{D} \subset \mathcal{V}$	depot nodes (inflow and outflow);
$t \in \mathcal{T} \subset \mathcal{V}$	target nodes (only inflow);
$r \in \mathcal{R}$	resources (materials);
$m \in \mathcal{M}$	modes of transport defined on the arcs;
$p' \in \mathcal{P}' \subseteq \mathcal{P}$	production nodes on which CCS investment is possible;
$l \in \mathcal{L}$	level of investment in CCS defined on CCS production nodes.

The parameters of the model are presented in Table 4.3. In practice, the list of parameters could be much bigger, especially with more cost, carbon and throughput parameters. However, we have chosen a selection of parameters that suffice to reflect the modeling challenges in these types of models and that serve the test instance as presented in Chapter 5. One parameter requires additional explanation: $yield_{rp}$, the yield of resource $r \in \mathcal{R}$ at production unit $p \in \mathcal{P}$. Yields at a production unit reflect a 'recipe' in which some resources are converted into other resources. For any $r \in \mathcal{R}$, $p \in \mathcal{P}$: if $yield_{rp} \in [-1, 0)$, the resource is used as input at the production unit; if $yield_{rp} \in (0, 1]$, the resource is outputted at the production unit; if $yield_{rp} = 0$, the resource is not used in the production process at the unit. The absolute values of the negative yields sum up to one, just as the positive yields sum up to one. The values represent the fractions in which resources are inputted or outputted: see Table 4.2 for a numerical example, with a schematic representation in Figure 4.1 including a possible resource flow below the arcs.

TABLE 4.2: Example yield data of a production unit.

	Resource				
	R1	R2	R3	R4	R5
Yield	-0.65	-0.20	-0.15	+0.70	+0.30

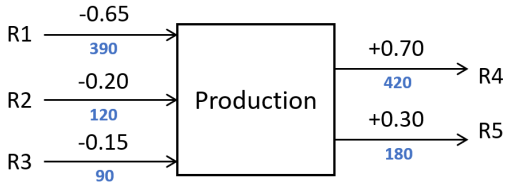

FIGURE 4.1: Schematic example of yield data.

Table 4.4 presents the variables of the model. Not every single possible variable needs to be defined: for example, if some resource $r \in \mathcal{R}$ is not demanded at some target $t \in \mathcal{T}$, we also do not have to define $\boldsymbol{x}_{ritm}$, $i \in \mathcal{N}(t)^-$, $m \in \mathcal{M}$; $\boldsymbol{x}_{rt}$ and $\boldsymbol{CI}_{rt}$. We have defined carbon intensity variables per unit of resource $r \in \mathcal{R}$ on location $i \in \mathcal{V}$. The carbon intensity restrictions are reflected in the parameter CI_{rt}^{max}. Additionally, we define $emissions^{max}$ as an upper bound on the absolute amount of CO_2 emissions in the whole system, instead of carbon intensities which are per amount of resource.

TABLE 4.3: Parameters of the model.

Parameter	Description
$supply_{rs}^{min}$	minimum amount of resource $r \in \mathcal{R}$ in order to use source node $s \in \mathcal{S}$;
$supply_{rs}^{max}$	maximum amount of resource $r \in \mathcal{R}$ available at source node $s \in \mathcal{S}$;
$cost_{rs}$	cost per unit of resource $r \in \mathcal{R}$ deployed from source node $s \in \mathcal{S}$;
$carbon_{rs}$	carbon emissions per unit of resource $r \in \mathcal{R}$ deployed from source node $s \in \mathcal{S}$;
$through_{p}^{max}$	maximum throughput of resources at production node $p \in \mathcal{P}$;
$cost_{p}$	cost per unit of resources handled at production node $p \in \mathcal{P}$;
$carbon_{p}$	carbon emissions per unit of resources at production node $p \in \mathcal{P}$;
$yield_{rp}$	yield of resource $r \in \mathcal{R}$ at production node $p \in \mathcal{P}$;
$through_{d}^{min}$	minimum throughput of resources in order to use depot node $d \in \mathcal{D}$;
$through_{rd}^{max}$	maximum throughput of resource $r \in \mathcal{R}$ at depot node $d \in \mathcal{D}$;
$cost_{d}^{fixed}$	fixed cost to use depot $d \in \mathcal{D}$;
$carbon_{d}^{fixed}$	fixed carbon emissions at depot node $d \in \mathcal{D}$;
$demand_{rt}^{min}$	minimum demand of resource $r \in \mathcal{R}$ to be satisfied at target node $t \in \mathcal{T}$;
$demand_{rt}^{max}$	maximum demand of resource $r \in \mathcal{R}$ to be satisfied at target node $t \in \mathcal{T}$;
$price_{rt}$	price paid per unit of resource $r \in \mathcal{R}$ satisfied at target node $t \in \mathcal{T}$;
$through_{rijm}^{max}$	maximum throughput resource $r \in \mathcal{R}$ at arc $(i,j) \in \mathcal{E}$ using mode $m \in \mathcal{M}$;
$cost_{rijm}$	cost per unit of resource $r \in \mathcal{R}$ transported over arc $(i,j) \in \mathcal{E}$ using mode $m \in \mathcal{M}$;
$carbon_{rijm}$	carbon emissions per unit of resource $r \in \mathcal{R}$ over arc $(i,j) \in \mathcal{E}$ using mode $m \in \mathcal{M}$;
$capture_{pl}^{max}$	CO_2 capture capacity of CCS at production node $p \in \mathcal{P}'$ at level $l \in \mathcal{L}$;
$install_{pl}^{fixed}$	installation cost CCS at production node $p \in \mathcal{P}'$ at level $l \in \mathcal{L}$;
CI_{rt}^{max}	maximum allowed carbon intensity of resource $r \in \mathcal{R}$ at target node $t \in \mathcal{T}$;
$emissions^{max}$	maximum allowed absolute amount of carbon emissions in the whole chain.

TABLE 4.4: Variables of the model.

Variable	Description
$\boldsymbol{x}_{rijm}$	amount of flow of resource $r \in \mathcal{R}$ going over arc $(i,j) \in \mathcal{E}$ using mode $m \in \mathcal{M}$;
$\boldsymbol{x}_{ri}$	total flow of resource $r \in \mathcal{R}$ going through node $i \in \mathcal{V}$;
$\boldsymbol{y}_{rij}$	amount of carbon flow of resource $r \in \mathcal{R}$ going over arc $(i,j) \in \mathcal{E}$;
$\boldsymbol{y}_{ri}$	total carbon flow from resource $r \in \mathcal{R}$ going through node $i \in \mathcal{V}$;
$\boldsymbol{z}_{rs}$	1 if resource $r \in \mathcal{R}$ is supplied from source $s \in \mathcal{S}$, 0 otherwise;
$\boldsymbol{z}_{d}$	1 if depot node $d \in \mathcal{D}$ is used in the network, 0 otherwise;
$\boldsymbol{CI}_{ri}$	carbon intensity per unit of resource $r \in \mathcal{R}$ at node $i \in \mathcal{V}$;
$\boldsymbol{c}_{p}$	amount of CO_2 captured at production node $p \in \mathcal{P}'$;
$\boldsymbol{z}_{pl}$	1 if CCS is installed at location $p \in \mathcal{P}'$ at level $l \in \mathcal{L}$, 0 otherwise.

4.1.2 Linear Program Without Accounting for Carbon Emissions

If we do not account for any carbon flow calculations and restrictions in the model, we arrive at the MILP model as given in (4.1)-(4.25).

$$\max \quad \boldsymbol{revenue} - \boldsymbol{costs} \tag{4.1}$$

$$\text{s.t.} \quad \boldsymbol{x}_{rs} = \sum_{j \in \mathcal{N}(s)^+} \sum_{m \in \mathcal{M}} \boldsymbol{x}_{rsjm} \qquad r \in \mathcal{R},\, s \in \mathcal{S} \tag{4.2}$$

$$\boldsymbol{x}_{rp} = \sum_{i \in \mathcal{N}(p)^-} \sum_{m \in \mathcal{M}} \boldsymbol{x}_{ripm} \qquad r \in \mathcal{R},\, p \in \mathcal{P},\, yield_{rp} < 0 \tag{4.3}$$

$$\boldsymbol{x}_{rp} = \sum_{j \in \mathcal{N}(p)^+} \sum_{m \in \mathcal{M}} \boldsymbol{x}_{rpjm} \qquad r \in \mathcal{R},\, p \in \mathcal{P},\, yield_{rp} > 0 \tag{4.4}$$

$$\boldsymbol{x}_{rd} = \sum_{i \in \mathcal{N}(d)^-} \sum_{m \in \mathcal{M}} \boldsymbol{x}_{ridm} \qquad r \in \mathcal{R},\, d \in \mathcal{D} \tag{4.5}$$

$$\boldsymbol{x}_{rt} = \sum_{i \in \mathcal{N}(t)^-} \sum_{m \in \mathcal{M}} \boldsymbol{x}_{ritm} \qquad r \in \mathcal{R},\, t \in \mathcal{T} \tag{4.6}$$

$$\boldsymbol{revenue} = \sum_{r \in \mathcal{R}} \sum_{t \in \mathcal{T}} price_{rt} \cdot \boldsymbol{x}_{rt} \tag{4.7}$$

$$\boldsymbol{cost}_{sources} = \sum_{r \in \mathcal{R}} \sum_{s \in \mathcal{S}} cost_{rs} \cdot \boldsymbol{x}_{rs} \tag{4.8}$$

$$\boldsymbol{cost}_{prod} = \sum_{p \in \mathcal{P}} \sum_{r \in \mathcal{R}, yield_{rp} < 0} cost_p \cdot \boldsymbol{x}_{rp} \tag{4.9}$$

$$\boldsymbol{cost}_{depots} = \sum_{d \in \mathcal{D}} cost_d^{fixed} \cdot \boldsymbol{z}_d \tag{4.10}$$

$$\boldsymbol{cost}_{transport} = \sum_{r \in \mathcal{R}} \sum_{(i,j) \in \mathcal{E}} \sum_{m \in \mathcal{M}} cost_{rijm} \cdot \boldsymbol{x}_{rijm} \tag{4.11}$$

$$\boldsymbol{costs} = \boldsymbol{cost}_{sources} + \boldsymbol{cost}_{prod} + \boldsymbol{cost}_{depots} + \boldsymbol{cost}_{transport} \tag{4.12}$$

$$\boldsymbol{x}_{rs} \geq supply_{rs}^{min} \cdot \boldsymbol{z}_{rs} \qquad r \in \mathcal{R},\, s \in \mathcal{S} \tag{4.13}$$

$$\boldsymbol{x}_{rs} \leq \min\Big\{ supply_{rs}^{max}, M \Big\} \cdot \boldsymbol{z}_{rs} \qquad r \in \mathcal{R},\, s \in \mathcal{S} \tag{4.14}$$

$$\sum_{r \in \mathcal{R}, yield_{rp} < 0} \boldsymbol{x}_{rp} \leq through_p^{max} \qquad p \in \mathcal{P} \tag{4.15}$$

$$\boldsymbol{x}_{rp} = -1 \cdot yield_{rp} \sum_{r' \in \mathcal{R}, yield_{r'p} > 0} \boldsymbol{x}_{r'p} \qquad r \in \mathcal{R},\, p \in \mathcal{P},\, yield_{rp} < 0 \tag{4.16}$$

$$\boldsymbol{x}_{rp} = yield_{rp} \sum_{r' \in \mathcal{R}, yield_{r'p} > 0} \boldsymbol{x}_{r'p} \qquad r \in \mathcal{R},\, p \in \mathcal{P},\, yield_{rp} > 0 \tag{4.17}$$

$$\sum_{i \in \mathcal{N}(p)^-} \sum_{m \in \mathcal{M}} \boldsymbol{x}_{ripm} = \sum_{j \in \mathcal{N}(p)^+} \sum_{m \in \mathcal{M}} \boldsymbol{x}_{rpjm} = 0 \qquad r \in \mathcal{R},\ p \in \mathcal{P},\ yield_{rp}=0 \qquad (4.18)$$

$$\sum_{i \in \mathcal{N}(d)^-} \sum_{m \in \mathcal{M}} \boldsymbol{x}_{ridm} = \sum_{j \in \mathcal{N}(d)^+} \boldsymbol{x}_{rdjm} \qquad r \in \mathcal{R},\ d \in \mathcal{D} \qquad (4.19)$$

$$\sum_{r \in \mathcal{R}} \boldsymbol{x}_{rd} \geq through_d^{min} \cdot \boldsymbol{z}_d \qquad d \in \mathcal{D} \qquad (4.20)$$

$$\boldsymbol{x}_{rd} \leq \min\left\{through_{rd}^{max}, M\right\} \cdot \boldsymbol{z}_d \qquad r \in \mathcal{R},\ d \in \mathcal{D} \qquad (4.21)$$

$$demand_{rt}^{min} \leq \boldsymbol{x}_{rt} \leq demand_{rt}^{max} \qquad r \in \mathcal{R},\ t \in \mathcal{T} \qquad (4.22)$$

$$\boldsymbol{x}_{rijm} \leq through_{rijm}^{max} \qquad r \in \mathcal{R},\ (i,j) \in \mathcal{E},\ m \in \mathcal{M} \qquad (4.23)$$

$$\boldsymbol{x}_{rijm} \geq 0 \qquad r \in \mathcal{R},\ (i,j) \in \mathcal{E},\ m \in \mathcal{M} \qquad (4.24)$$

$$\boldsymbol{z}_{rs}, \boldsymbol{z}_d \in \{0,1\} \qquad r \in \mathcal{R},\ s \in \mathcal{S},\ d \in \mathcal{D} \qquad (4.25)$$

The objective (4.1) maximizes the profit, which is the revenue minus the total costs. Constraints (4.2)-(4.6) create help variables for the flow of resources through the sources, production units, depots and targets, respectively. Constraints (4.7)-(4.12) specify the revenue and costs of the different components in the network. Constraints (4.13) and (4.14) regulate the minimum and maximum supply of each resource from the sources. The big M that is used is defined as $M = \sum_{r \in \mathcal{R}} \sum_{t \in \mathcal{T}} demand_{rt}^{max}$. Constraints (4.15)-(4.18) control the production of resources at the production nodes. Constraints (4.15) ensure the total inflow of resources at the production node is no more than the allowed maximum inflow. Constraints (4.16) ensure for each incoming resource the right fraction from the total outgoing flow. As the absolute values of the yields of the incoming resources sum up to one, these constraints also ensure the mass balance at the production nodes. Constraints (4.17) ensure the right fraction of outflow for each of the outgoing resources. Constraints (4.18) make sure resources with a zero yield do not flow in and out of a production unit. Constraints (4.19)-(4.21) ensure respectively the flow balance, minimum and maximum throughput restrictions at the depot nodes. The same big M is used as in constraints (4.14). Constraints (4.22) make sure the demand for each resource at the target nodes is satisfied. Constraints (4.23) preserve the maximum arc flows. Constraints (4.24) and (4.25) specify the domain of the variables.

4.1.3 Calculating Carbon Intensities Post-Optimization

Before optimizing over carbon intensities, we should properly define how carbon intensities are calculated. To do so, we start with two numerical examples.

To show the concept of carbon intensity, we start with an example of a production unit. This example is illustrated in Figure 4.2, where the production unit converts resources $R1$, $R2$ and $R3$ into $R4$ and $R5$. The carbon intensity of an incoming resource itself can be the result of averaging carbon intensities of the same resource coming from different locations with a different CI. We calculate the carbon intensities of the outgoing resources by averaging over the fractions of incoming resources and adding the carbon emissions per unit at the production unit. As we calculate carbon intensities

on unit/mass basis, the outgoing resources $R4$ and $R5$ end up having the same carbon intensity. However, a correction factor could be performed if one wants to distribute carbon flows differently over the resources, for example based on the lower heating values of the resources.

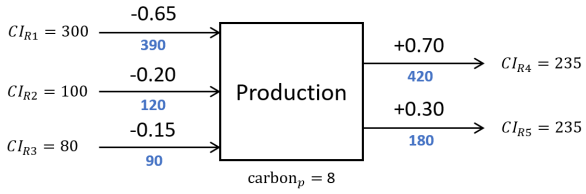

FIGURE 4.2: Carbon intensity calculation example for a production unit (yields above the arrows, resource flows below the arrows).

Figures 4.3 and 4.4 give an example solution for a depot node, where 50 units of resource $R1$ flow in from source node $S1$ and another 50 units from source node $S2$. At the depot, the 100 units are split into 70 units of $R1$ going to target $T1$ and 30 units going to target $T2$. There are two ways to calculate carbon intensities for the same instance, either by averaging carbon intensities at depot nodes as done in Figure 4.3 or by distributing carbon flows over arcs as done in Figure 4.4. We left out the carbon emissions on arcs themselves and do not consider multiple modes of transport in these examples for simplicity. By multiplying or dividing by the number of units of resource at nodes, it is easy to go from one solution to another: both provide us with the same carbon intensity results. How these calculations are done in general by mathematical equations is shown after these examples. The strategy from Figure 4.3 we define as 'Option 1' and the strategy from Figure 4.4 as 'Option 2'.

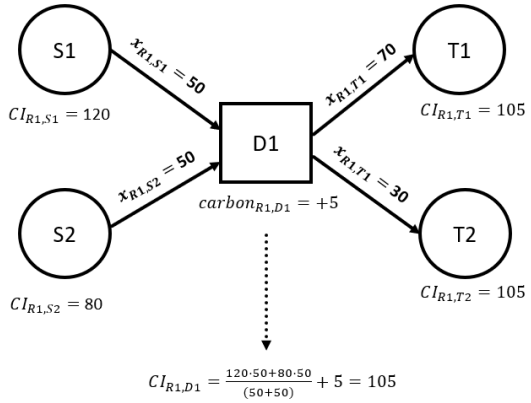

FIGURE 4.3: Depot calculation example using carbon intensities (CI).

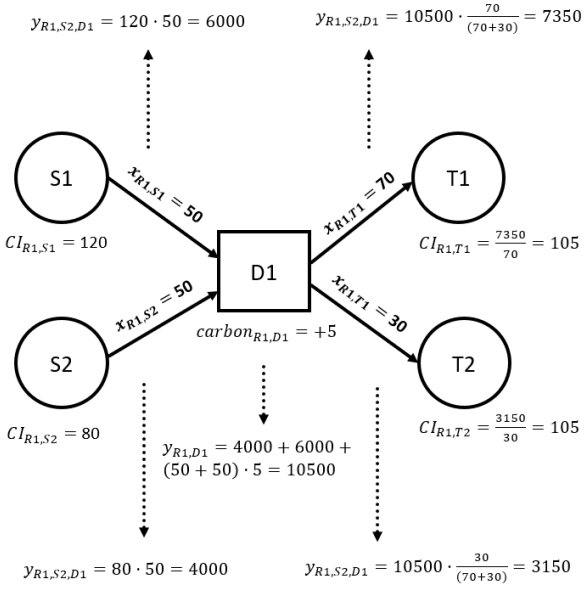

FIGURE 4.4: Depot calculation example using carbon flows (y).

Calculation Option 1: Carbon Intensities at the Nodes Equations (4.26)-(4.30) calculate the carbon intensities per resource and per location post-optimization. To stress the fact that the resource flow variables are already optimized over, they are marked with a bar ($\bar{\boldsymbol{x}}$). For (4.27),

(4.29) and (4.30) the equations are only defined if the denominators are positive, otherwise the carbon intensities are 0.

$$CI_{rs} := carbon_{rs} \qquad r\in\mathcal{R},\, s\in\mathcal{S} \tag{4.26}$$

$$CI_{rp} := \sum_{i\in\mathcal{N}(p)^-} \sum_{m\in\mathcal{M}} (CI_{ri} + carbon_{ripm}) \cdot \frac{\bar{\boldsymbol{x}}_{ripm}}{\bar{\boldsymbol{x}}_{rp}} \qquad r\in\mathcal{R},\, p\in\mathcal{P},\, yield_{rp}<0,\, \bar{\boldsymbol{x}}_{rp}>0 \tag{4.27}$$

$$CI_{rp} := \sum_{r\in\mathcal{R}, yield_{rp}<0} CI_{rp} \cdot (-1 \cdot yield_{rp}) + carbon_p \qquad r\in\mathcal{R},\, p\in\mathcal{P},\, yield_{rp}>0 \tag{4.28}$$

$$CI_{rd} := \sum_{i\in\mathcal{N}(d)^-} \sum_{m\in\mathcal{M}} (CI_{ri} + carbon_{ridm}) \cdot \frac{\bar{\boldsymbol{x}}_{ridm}}{\bar{\boldsymbol{x}}_{rd}} + \frac{carbon_d^{fixed}}{\sum_{r'\in\mathcal{R}} \bar{\boldsymbol{x}}_{r'd}} \qquad r\in\mathcal{R},\, d\in\mathcal{D},\, \bar{\boldsymbol{x}}_{rd}>0 \tag{4.29}$$

$$CI_{rt} := \sum_{i\in\mathcal{N}(t)^-} \sum_{m\in\mathcal{M}} (CI_{ri} + carbon_{ritm}) \cdot \frac{\bar{\boldsymbol{x}}_{ritm}}{\bar{\boldsymbol{x}}_{rt}} \qquad r\in\mathcal{R},\, t\in\mathcal{T},\, \bar{\boldsymbol{x}}_{rt}>0 \tag{4.30}$$

At the sources, equations (4.26) set the carbon intensity for each resource to the initial carbon emissions at the source. At the production units, equations (4.27) first calculate the carbon intensities of the incoming resources as a weighted sum over the preceding nodes. Then, equations (4.28) determine the carbon intensities of the outgoing resources as a weighted sum of the incoming carbon intensities according to the yields, plus the carbon emissions per unit at the production node itself. At the depots, equations (4.29) set the carbon intensity of a resource as the weighted sum of the incoming carbon intensities of incoming resources, plus the fixed carbon emissions at the depot as a share of the total weight of all resources at the depot. At the targets, equations (4.30) set the carbon intensities per resource as the weighted sum of the incoming flows.

Calculation Option 2: Carbon Flows through the Nodes The second option calculates carbon flows explicitly on arcs and calculates the sum of carbon flows that enter each node. This allows us to post-calculate the carbon intensities by (4.31)-(4.37).

$$y_{rsj} := \sum_{m\in\mathcal{M}} (carbon_{rs} + carbon_{rsjm}) \cdot \bar{\boldsymbol{x}}_{rsjm} \qquad r\in\mathcal{R},\, s\in\mathcal{S},\, j\in\mathcal{N}(s)^+ \tag{4.31}$$

$$y_p := \sum_{\substack{r\in\mathcal{R},\\ yield_{rp}<0}} \sum_{i\in\mathcal{N}(p)^-} y_{rip} + carbon_p \cdot \bar{\boldsymbol{x}}_p \qquad p\in\mathcal{P} \tag{4.32}$$

$$y_{rpj} := \sum_{m\in\mathcal{M}} \left(\frac{y_p}{\bar{\boldsymbol{x}}_p} + carbon_{rpjm}\right) \cdot \bar{\boldsymbol{x}}_{rpjm} \qquad r\in\mathcal{R},\, p\in\mathcal{P},\, yield_{rp}>0,\, j\in\mathcal{N}(p)^+,\, \bar{\boldsymbol{x}}_p>0 \tag{4.33}$$

$$y_{rd} := \sum_{i\in\mathcal{N}(d)^-} y_{rid} + carbon_d^{fixed} \cdot \frac{\bar{\boldsymbol{x}}_{rd}}{\sum_{r'\in\mathcal{R}} \bar{\boldsymbol{x}}_{r'd}} \qquad r\in\mathcal{R},\, d\in\mathcal{D},\, \textstyle\sum_{r'\in\mathcal{R}} \bar{\boldsymbol{x}}_{r'd}>0 \tag{4.34}$$

$$y_{rdj} := \sum_{m\in\mathcal{M}} \left(\frac{y_{rd}}{\bar{\boldsymbol{x}}_{rd}} + carbon_{rdjm}\right) \cdot \bar{\boldsymbol{x}}_{rdjm} \qquad r\in\mathcal{R},\, d\in\mathcal{D},\, j\in\mathcal{N}(d)^+,\, \bar{\boldsymbol{x}}_{rd}>0 \tag{4.35}$$

$$y_{rt} := \sum_{i\in\mathcal{N}(t)^-} y_{rit} \qquad r\in\mathcal{R},\, t\in\mathcal{T} \tag{4.36}$$

$$CI_{rt} := \frac{y_{rt}}{\bar{\boldsymbol{x}}_{rt}} \qquad r\in\mathcal{R},\, t\in\mathcal{T},\, \bar{\boldsymbol{x}}_{rt}>0 \tag{4.37}$$

Equations (4.31) calculate the carbon flows per resource on arcs leaving the source nodes. Equations (4.32) calculate the total carbon flow y_p of all entering resources at a unit $p \in \mathcal{P}$, plus the emissions at the unit itself. For ease of notation, we use the variable $\bar{\boldsymbol{x}}_p = \sum_{r' \in \mathcal{R}, yield_{r'p} < 0} \bar{\boldsymbol{x}}_{r'p}$, which is the total amount of units ('mass') going through unit $p \in \mathcal{P}$. Equations (4.33) calculate the carbon flow on outgoing arcs, plus transportation emissions. Equations (4.34) calculate the total carbon flow per resource entering a depot, plus the fraction of fixed emissions at the depot itself. Equations (4.35) distribute the total carbon flows at a depot over the outgoing arcs, plus the emissions from transportation. For depots, it is important that carbon flows from different resources do not 'mix'. Equations (4.37) finally calculate the carbon intensity of each resource at the target nodes.

4.1.4 Optimizing Carbon Intensities During-Optimization

To actually incorporate carbon intensities while optimizing the supply chain, we have to introduce nonlinearities to the model. We propose two sets of bilinear carbon intensity balance constraints, based on the aforementioned two options to post-calculate carbon intensities. Both options, one using carbon intensity variables and one using carbon flow variables, are explained in this section.

Optimization Option 1: Carbon Intensity Balance Equations Adding the balance equations (4.38)-(4.43) to the basic model (4.1)-(4.25) regulates the carbon intensities in the system, where constraints (4.44) put the actual restrictions on carbon intensities 'at the back' of the network. The constraints require the additional variables $\boldsymbol{f}_{rd}$, which represent the fraction of incoming resource $r \in \mathcal{R}$ at depot $d \in \mathcal{D}$ compared to the total amount of resource flowing through the depot.

$$\boldsymbol{CI}_{rs} = carbon_{rs} \qquad r \in \mathcal{R},\, s \in \mathcal{S} \qquad (4.38)$$

$$\boldsymbol{CI}_{rp} \cdot \boldsymbol{x}_{rp} = \sum_{i \in \mathcal{N}(p)^-} \sum_{m \in \mathcal{M}} (\boldsymbol{CI}_{ri} + carbon_{ripm}) \cdot \boldsymbol{x}_{ripm} \qquad r \in \mathcal{R},\, p \in \mathcal{P},\, yield_{rp} < 0 \qquad (4.39)$$

$$\boldsymbol{CI}_{rp} = \sum_{r' \in \mathcal{R}, yield_{r'p} < 0} \boldsymbol{CI}_{r'p} \cdot yield_{r'p} + carbon_p \qquad r \in \mathcal{R},\, p \in \mathcal{P},\, yield_{rp} > 0 \qquad (4.40)$$

$$\boldsymbol{f}_{rd} \cdot \sum_{r' \in \mathcal{R}} \boldsymbol{x}_{r'd} = \boldsymbol{x}_{rd} \qquad r \in \mathcal{R},\, d \in \mathcal{D} \qquad (4.41)$$

$$\boldsymbol{CI}_{rd} \cdot \boldsymbol{x}_{rd} = \sum_{i \in \mathcal{N}(d)^-} \sum_{m \in \mathcal{M}} (\boldsymbol{CI}_{ri} + carbon_{ridm}) \cdot \boldsymbol{x}_{ridm} + carbon_d^{fixed} \cdot \boldsymbol{f}_{rd} \qquad r \in \mathcal{R},\, d \in \mathcal{D} \qquad (4.42)$$

$$\boldsymbol{CI}_{rt} \cdot \boldsymbol{x}_{rt} = \sum_{i \in \mathcal{N}(t)^-} \sum_{m \in \mathcal{M}} (\boldsymbol{CI}_{ri} + carbon_{ritm}) \cdot \boldsymbol{x}_{ritm} \qquad r \in \mathcal{R}, t \in \mathcal{T} \qquad (4.43)$$

$$\boldsymbol{CI}_{rt} \leq CI_{rt}^{max} \qquad r \in \mathcal{R},\, t \in \mathcal{T} \qquad (4.44)$$

Constraints (4.38) set the carbon intensities at the resources as their starting values. Constraints (4.39) calculate the carbon intensities of the incoming resources at production units. Constraints (4.40) distribute the carbon intensities of the incoming resources over the outgoing resources. Constraints (4.41) calculates the fraction of one resource at a depot compared to the other resources

at the same depot, which is needed for constraints (4.42), which are the carbon intensity balancing constraints at the depots. Constraints (4.43) calculate the carbon intensities per resource at the targets. Finally, constraints (4.44) put the restriction on the individual carbon intensities.

Optimization Option 2: Carbon Flow Balance Equations Alternatively, one can calculate carbon flows on the arcs directly and redistribute these flows at the nodes. For this strategy, we reduced the number of variables on the arcs by pooling modes of operation between the same nodes for the same resource. Constraints (4.45)-(4.51) track and restrict carbon flows in the system.

$$\boldsymbol{y}_{rsj} = \sum_{m \in \mathcal{M}} (carbon_{rs} + carbon_{rsjm}) \cdot \boldsymbol{x}_{rsjm} \qquad r \in \mathcal{R},\, s \in \mathcal{S},\, j \in \mathcal{N}(s)^+ \qquad (4.45)$$

$$\boldsymbol{y}_p = \sum_{r \in \mathcal{R},\, yield_{rp} < 0} \sum_{i \in \mathcal{N}(p)^-} \boldsymbol{y}_{rip} + carbon_p \cdot \boldsymbol{x}_p \qquad p \in \mathcal{P} \qquad (4.46)$$

$$\boldsymbol{y}_{rpj} \cdot \boldsymbol{x}_p = \boldsymbol{y}_p \cdot \sum_{m \in \mathcal{M}} \boldsymbol{x}_{rpjm} + \sum_{m \in \mathcal{M}} carbon_{rpjm} \cdot \boldsymbol{x}_{rpjm} \cdot \boldsymbol{x}_p \qquad r \in \mathcal{R},\, p \in \mathcal{P},\, j \in \mathcal{N}(p)^+ \qquad (4.47)$$

$$\boldsymbol{y}_{rd} \cdot \sum_{r' \in \mathcal{R}} \boldsymbol{x}_{r'd} = \sum_{i \in \mathcal{N}(d)^-} \sum_{m \in \mathcal{M}} \boldsymbol{y}_{ridm} \sum_{r' \in \mathcal{R}} \boldsymbol{x}_{r'd} + carbon_d^{fixed} \cdot \boldsymbol{x}_{rd} \qquad r \in \mathcal{R}, d \in \mathcal{D} \qquad (4.48)$$

$$\boldsymbol{y}_{rdj} \cdot \boldsymbol{x}_{rd} = \boldsymbol{y}_{rd} \cdot \sum_{m \in \mathcal{M}} x_{rdjm} + \sum_{m \in \mathcal{M}} carbon_{rdjm} \cdot \boldsymbol{x}_{rdjm} \cdot \boldsymbol{x}_{rd} \qquad r \in \mathcal{R},\, d \in \mathcal{D},\, j \in \mathcal{N}(d)^+ \qquad (4.49)$$

$$\boldsymbol{y}_{rt} = \sum_{i \in \mathcal{N}(t)^-} \boldsymbol{y}_{rit} \qquad r \in \mathcal{R},\, t \in \mathcal{T} \qquad (4.50)$$

$$\boldsymbol{y}_{rt} \leq CI_{rt}^{max} \cdot \boldsymbol{x}_{rt} \qquad r \in \mathcal{R},\, t \in \mathcal{T} \qquad (4.51)$$

Constraints (4.45) calculate the carbon flows leaving the sources. Constraints (4.46) calculate the total carbon flow that enters and is produced at a production unit. Constraints (4.47) distribute the total carbon flow at the production unit over the outgoing arcs. Constraints (4.48) calculate the incoming carbon flow for each resource at the depots. Constraints (4.49) distribute the carbon flows over the outgoing arcs of depots. Constraints (4.50) calculate the carbon flows entering the targets per resource. Constraints (4.51) induce restrictions on carbon intensities.

4.1.5 Carbon Capture & Storage Constraints

Next, we want to include the option for capturing carbon for the production units. To allow for the option of CCS, we add constraints (4.52)-(4.56) to the model for units $p \in \mathcal{P}'$.

$$\boldsymbol{c}_p \leq carbon_p \cdot \boldsymbol{x}_p \qquad p \in \mathcal{P}' \qquad (4.52)$$

$$\boldsymbol{c}_p \leq \sum_{l \in \mathcal{L}} capture_{pl}^{max} \cdot \boldsymbol{z}_{pl} \qquad p \in \mathcal{P}' \qquad (4.53)$$

$$\sum_{l \in \mathcal{L}} \boldsymbol{z}_{pl} \leq 1 \qquad p \in \mathcal{P}' \qquad (4.54)$$

$$\boldsymbol{c}_p \geq 0 \qquad p \in \mathcal{P}' \qquad (4.55)$$

$$\boldsymbol{z}_{pl} \in \{0, 1\} \qquad p \in \mathcal{P}',\, l \in \mathcal{L} \qquad (4.56)$$

Constraints (4.52) make sure the captured carbon is not more than the emissions that are actually emitted at the pool. Constraints (4.53) ensure that either nothing is captured if no investment is made or no more than the allowed capacity is captured for the chosen investment. Constraints (4.54) allow for at most one CCS investment per production unit. Constraints (4.55) preserve the non-negativity of the captured carbon and constraints (4.56) preserve the binary domain of the investment variables.

In some cases, we want to define production units in groups. For instance, one physical production unit with different modes of operation and different baseline energy requirements can be modeled as multiple separate production units in a group, like $p_G = \{p_1, p_2\}$. Now we can keep the amount of carbon captured per individual production unit, but make the CCS investment on a group level. Then constraints (4.53) should be replaced by (4.57) to make sure the total emissions of the group are not larger than the investment.

$$\sum_{p \in p_G} \boldsymbol{c}_p \leq \sum_{l \in \mathcal{L}} capture^{max}_{p_G l} \cdot \boldsymbol{z}_{p_G l} \qquad p_G \subseteq \mathcal{P}' \tag{4.57}$$

Some adaptations to the previously mentioned equations have to be made to include CCS as a decision option. First of all, a new cost equation (4.58) is introduced, which calculates the installation costs of CCS facilities (which can also be defined for installations on a group level). This should be added to the total cost calculations in equation (4.12).

$$\boldsymbol{cost}_{CCS} = \sum_{p \in \mathcal{P}'} \sum_{l \in \mathcal{L}} install^{fixed}_{pl} \cdot \boldsymbol{z}_{pl} \tag{4.58}$$

When calculating CI post-optimization, we have to subtract some terms from the equations, depending on the type of formulation. When using CI variables, we should subtract the amount of carbon captured divided by the amount produced at the respective production node p. To do so, Equations (4.28) should be replaced by Equations (4.59) for $p \in \mathcal{P}'$.

$$CI_{rp} := \sum_{\substack{r \in \mathcal{R}, \\ yield_{rp} < 0}} CI_{rp} \cdot (-1 \cdot yield_{rp}) + carbon_p - \frac{\bar{\boldsymbol{c}}_p}{\bar{\boldsymbol{x}}_p} \qquad r \in \mathcal{R},\, p \in \mathcal{P}',\, yield_{rp} > 0,\, \bar{\boldsymbol{x}}_p > 0 \tag{4.59}$$

When we calculate total emissions associated with a production node, we can simply subtract the amount of CO_2 captured from the total emissions y associated with production node p. Then equations (4.32) should be replaced by Equations (4.60) for $p \in \mathcal{P}'$.

$$y_p := \sum_{r \in \mathcal{R},\, yield_{rp} < 0} \sum_{i \in \mathcal{N}(p)^-} \sum_{m \in M} y_{ripm} + carbon_p \cdot \bar{\boldsymbol{x}}_p - \bar{\boldsymbol{c}}_p \qquad p \in \mathcal{P}' \tag{4.60}$$

When we incorporate CI during-optimization, we have to adapt the constraints similarly. Equations (4.40) from Option 1 should be replaced by Equations (4.61), where c^{unit}_p accounts for the amount of carbon captured per amount of product produced, and (4.62), the actual adapted balance constraint, for $p \in \mathcal{P}'$.

$$\boldsymbol{c}^{unit}_p \cdot \boldsymbol{x}_p = \boldsymbol{c}_p \qquad r \in \mathcal{R},\, p \in \mathcal{P}',\, yield_{rp} > 0 \tag{4.61}$$

$$\boldsymbol{CI}_{rp} = \sum_{r' \in \mathcal{R}, yield_{r'p} < 0} \boldsymbol{CI}_{r'p} \cdot yield_{r'p} + carbon_p - \boldsymbol{c}_p^{unit} \qquad r \in \mathcal{R},\, p \in \mathcal{P}',\, yield_{rp} > 0 \tag{4.62}$$

Finally, constraints (4.46) from Option 2 should be replaced by Equations (4.63) for $p \in \mathcal{P}'$.

$$\boldsymbol{y}_p = \sum_{r \in \mathcal{R},\, yield_{rp} < 0} \sum_{i \in \mathcal{N}(p)^-} \boldsymbol{y}_{rip} + carbon_p \cdot \boldsymbol{x}_p - \boldsymbol{c}_p \qquad p \in \mathcal{P}' \tag{4.63}$$

With this modeling strategy, only in constraints (4.61) additional nonlinear terms are introduced, while all other CCS constraints are linear or do not impose new nonlinearities.

4.1.6 Constraining Total Carbon Emissions Linearly

If one does not want to restrict a certain carbon intensity, but rather all carbon emissions in the network in absolute terms, one can add equations (4.64)-(4.69) to the basic model. Note that for CCS in equations (4.66), we actually multiply it by -1 to subtract the amount of CO_2 captured.

$$\boldsymbol{emissions}_{sources} = \sum_{r \in \mathcal{R}} \sum_{s \in \mathcal{S}} carbon_{rs} \cdot \boldsymbol{x}_{rs} \tag{4.64}$$

$$\boldsymbol{emissions}_{prod} = \sum_{p \in \mathcal{P}} carbon_p \cdot \boldsymbol{x}_p \tag{4.65}$$

$$\boldsymbol{emissions}_{CCS} = -1 \cdot \sum_{p \in \mathcal{P}'} \boldsymbol{c}_p \tag{4.66}$$

$$\boldsymbol{emissions}_{depots} = \sum_{d \in \mathcal{D}} carbon_d^{fixed} \cdot \boldsymbol{z}_d \tag{4.67}$$

$$\boldsymbol{emissions}_{transport} = \sum_{r \in \mathcal{R}} \sum_{(i,j) \in \mathcal{E}} \sum_{m \in \mathcal{M}} carbon_{rijm} \cdot \boldsymbol{x}_{rijm} \tag{4.68}$$

$$\sum_{loc \in \{sources, prod, CCS, depots, transport\}} \boldsymbol{emissions}_{loc} \leq emissions^{max} \tag{4.69}$$

As these constraints are all linear, the model can find the lowest-carbon solution much faster compared to carbon intensity restrictions. However, reducing the total amount of carbon emissions does not necessarily achieve specific carbon intensity restrictions most effectively.

4.1.7 Discussion of Multi-Resource, Multi-Transport Model

The discussed multi-resource, multi-transport model has made the following additional assumptions:

1. Scope 3 emissions are not explicitly accounted for. However, they could be incorporated in two ways. First of all, given that we know exactly what product we need, we can add the scope 3 emissions at the end of the network to its carbon intensity. For instance, we might know that 1 liter of diesel emits 3.23 kg of CO_2. This requires a precise approximation of the emissions of our product. Alternatively, if we know the carbon content of the feedstock and have some distribution rules during processing, this carbon content is 'passed' to our final products. This is especially useful if the composition of our product is not fixed: for example, blending biofuels

into fossil fuels leads to different scope 3 emissions. In this project, we do not go into detail regarding these exact scope 3 emissions of products.

2. There are no emissions at the target nodes. This could be included, for example to model the scope 3 emissions or the carbon emissions resulting from the storage of final products at the target nodes.

3. So far, we have assumed that there is a demand for all the products we produce. However, we might also produce byproducts for which there is no demand, which we should get rid of in the system. This can be done in practice by incorporating demand nodes with zero minimum demand and infinite maximum demand of the byproduct at a zero price.

4. The modeling framework is also applicable to networks where there are two directed arcs between two nodes, for example one arc from depot $D1$ to $D2$ and one arc from depot $D2$ to $D1$. As both arcs have an associated positive cost, there will only be flow from one depot to another.

5. All carbon intensities in the model are based on units or mass, while it could in fact also be based on volume or energy content. This requires conversion rules and correction factors at the units to redistribute carbon flows over our produced products. One could in fact use any arbitrary distribution of our total carbon flow over our final products, as long as no flow gets lost in the system. Whether this is also fair in a real-life context, we leave up to policymakers.

6. Carbon intensities can go up if we produce less and we have some fixed carbon emissions we have to distribute over less product. This is something to keep in the back of our minds, because the absolute amount of CO_2 decreases if we produce less.

7. For CCS, the model allows capturing a fraction of the emitted CO_2 at a unit, as long as that satisfies all the constraints and it is cost-optimal. However, in fact we would capture all emitted CO_2 at a unit up to the capacity of the CCS installment. Incorporating this 'all-or-nothing' would lead to extra nonlinearities, as the CO_2 emissions at the units are unknown quantities. However, if this would happen one can always correct the carbon intensities post-optimization such that all CO_2 was captured, resulting in a slightly lower carbon intensity than the model found. Additionally, it is reasonable to assume for CCS that not 100% but a somewhat lower percentage of the emitted CO_2 is captured, for example because of leaks, depending on the implemented CCS technology. How CCS is implemented with a fixed capture rate and without a capture capacity, we discuss in the next section.

4.2 Hydrogen Supply Chain Network Model

In the second part of the thesis, we apply the concept of carbon intensity to a hydrogen supply chain network (HSCN) optimization problem. We consider the case study environment of Konda et al. (2011), who studied the problem of satisfying nationwide hydrogen demand in a least-cost production and distribution network. In Section 4.2.1, we present a general description of the setup of the model. In Section 4.2.2, we go into more detail on the mathematical structure of the model and how to incorporate carbon intensity. This is a new model which is not directly associated with or compared to the MRMT model. The complete formulations can be found in Appendix B.

4.2.1 Case Study Description

We describe the case study by considering its main pathways, which are schematically presented in Figure 4.5.

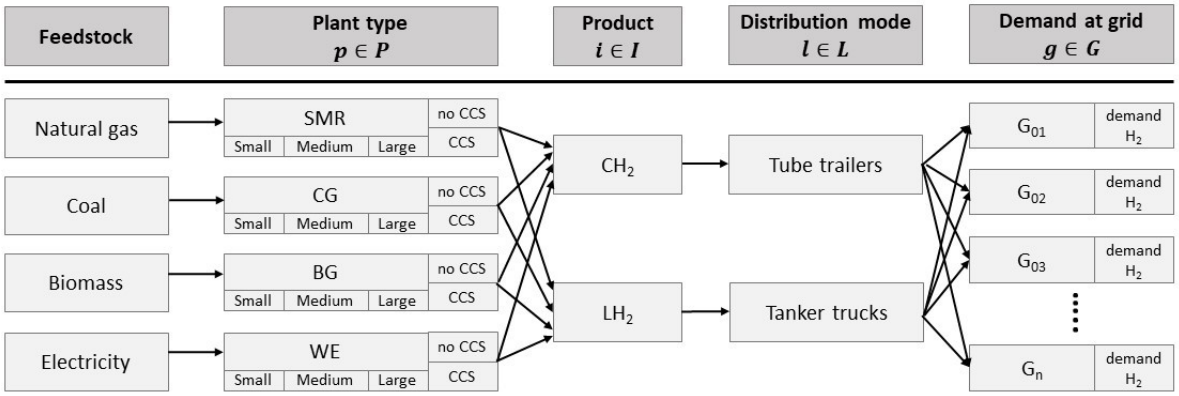

FIGURE 4.5: Hydrogen case study pathways superstructure.

The model components in 4.5 are further described as:

- Feedstock. There are four types of raw materials that can be used to produce hydrogen: natural gas, coal, biomass or electricity. For simplicity, we assume that these resources are available in unlimited quantities at any production location, such that only their cost per unit is considered in the optimization.
- Production plants $p \in \mathcal{P}$. The raw materials can be transformed into hydrogen under the following technologies: steam methane reforming (SMR), coal gasification (CG), biomass gasification (BG) and water electrolysis (WE). Production plants have a variable production capacity, generally split up into small, medium and large plants. Different sizes and technologies are associated with different costs and production efficiencies. Production plants can have a CCS structure on top of them, allowing to capture a certain fraction of the emitted CO_2 at the plants.
- Hydrogen products $i \in \mathcal{I}$. There are two types of physical hydrogen products: compressed/gasified hydrogen (CH_2) and liquefied hydrogen (LH_2). As hydrogen is a gas in its natural form, it is an intensive process to liquefy hydrogen. However, LH_2 has a higher energy density than CH_2 and can be transported in higher quantities. Therefore, the model should find a trade-off in the

production of both products. It is assumed that the customer is demanding hydrogen, regardless of whether that is CH_2 or LH_2, or possibly a combination of both.

- Modes of transport $l \in \mathcal{L}$. Hydrogen should be transported from production units to the customers. This can be done with different modes of transport. In this case study, we only consider road transport for simplicity, in particular tube trailers for CH_2 and tanker trucks for LH_2. Alternative modes of transport that can be considered are rail transport, in particular railway tube cars for CH_2 and railway tank cars for LH_2, and pipelines for CH_2.
- Demand at grid $g \in \mathcal{G}$. The country that is studied is split up into several grids, which in this case correspond to the largest cities in the country. Each grid has a certain daily demand for hydrogen, which increases over the different time periods that are considered. Demand is satisfied from production units at grids, for which we assume only a subset of grids is suitable to build production plants.

Firstly, we consider a static model, where the model solves one fixed time period. Then, we also consider a dynamic model, in which we consider demand over multiple time periods, meaning new production plants have to be built over time and/or existing plants have to extend their capacity. In the dynamic version of the model, we assume that larger plants can be built in earlier time periods in order to satisfy demand in later time periods. A comparison between the solutions of the static and dynamic models will be made.

The complete mathematical formulations are given in Appendix B. As the base models are mainly based on the models in Almansoori and Shah (2006) and Almansoori and Shah (2009), we chose to state the models in the appendix and give the main description here. One big assumption by Konda et al. (2011) compared to the base models is that there are no hydrogen storage locations. This is done because the Netherlands is considered, which is a relatively small country with the largest one-way distance between grids generally not larger than a three hours drive. The appendix also contains a detailed list of model changes compared to their respective papers. For example, Konda et al. (2011) consider refueling stations at demand locations, which we leave out for simplicity, and consider power equations for capital costs, which we simplify by considering fixed and variable capital costs. Also, some additions to the base models in Almansoori and Shah (2006) and Almansoori and Shah (2009) are made, for instance by introducing a parameter that holds information in which grids hydrogen production is allowed.

4.2.2 Case Study Model Structure and Adding Carbon Intensity

The basic models from Almansoori and Shah (2006) and Almansoori and Shah (2009) have a different structure than the MRMT model as described in Section 4.1. Both models have individual notations which are not linked to each other. On a structural level, the case study model is more 'zoomed-out' in the sense that it does not consider feedstock-to-production arcs, sees each plant as one big production unit and looks at locations in generalized grids rather than specific locations. The goal is to add carbon emissions, carbon intensity and CCS to this existing modeling framework, without changing fundamentally how the model works.

To explain the mathematics of the model, we consider the static variant. This model differentiates $\boldsymbol{D}^L_{ig}$, the locally satisfied demand of product i in grid g, and $\boldsymbol{D}^I_{ig}$, the imported hydrogen of

product i to grid g from another grid. The variable $\boldsymbol{P}_{pig}$ represents the daily hydrogen production of plant type p producing hydrogen type i in grid g, with corresponding total production in a grid $\boldsymbol{P}_{ig}^{T}$ of product i in grid g. Variable $\boldsymbol{Q}_{ilgg'}$ presents the transport of product i using mode of transport l from grid g to grid g', where it is the transportation in its own grid for $g' = g$. Each grid has a parameter for the total demand D_g^T that should be satisfied. The operational variables in the models are schematically shown in Figure 4.6, where the blue circles in the top-left corner of grid g correspond to one type of hydrogen, and the red circles in the bottom-right corner correspond to the other type of hydrogen.

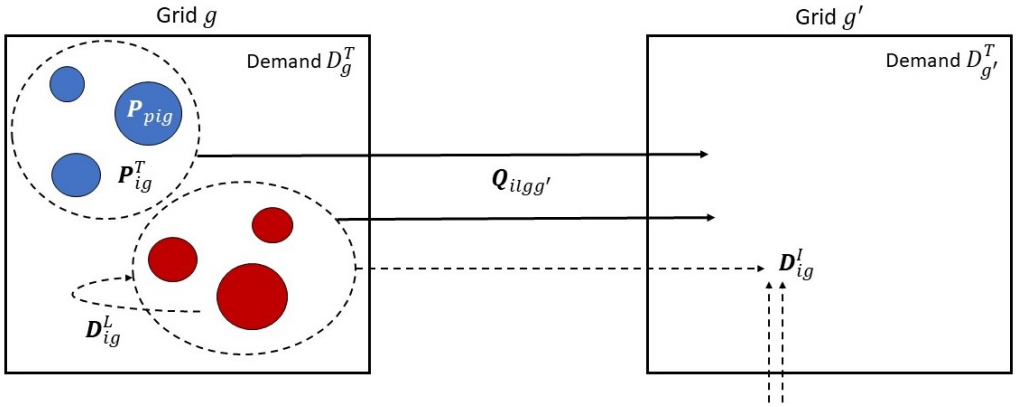

FIGURE 4.6: Schematic explanation of operational variables of the case study model.

The objective of the model is to minimize the total daily cost ($\boldsymbol{TDC}$) of the whole HSCN. For the hydrogen plants, facility capital costs ($\boldsymbol{FCC}$) are calculated as daily costs, on top of its facility operating costs ($\boldsymbol{FOC}$) and feedstock costs ($\boldsymbol{FSC}$). The number of transportation units ($\boldsymbol{NTU}$) is used to calculate the transport capital costs ($\boldsymbol{TCC}$), also calculated as daily costs. The transportation operation costs ($\boldsymbol{TOC}$) consist of fuel costs ($\boldsymbol{FC}$), labor costs ($\boldsymbol{LC}$), maintenance costs ($\boldsymbol{MC}$) and general costs ($\boldsymbol{GC}$), where the latter include transportation insurance, license and registration, and outstanding finances (Almansoori & Shah, 2006).

Three new elements are added to the base model. Firstly, we calculate the total chain emissions ($\boldsymbol{TCE}$), consisting of feedstock emissions ($\boldsymbol{TCE}^{Feed}$), production emissions ($\boldsymbol{TCE}^{Prod}$) and transportation emissions ($\boldsymbol{TCE}^{Trans}$). Feedstock and production emissions are calculated based on the hydrogen production of all plants, while transportation emissions are calculated based on the daily number of trips operational on each origin-destination pair (g, g') and the distance that is driven. These total emissions also include the second newly added feature: the option of CCS plants. We assume that each plant either has CCS implemented or not, where CCS plants capture a fixed amount of CO_2 without any maximum capture restrictions. Thirdly, we show how to calculate carbon intensity post-optimization, as well as during-optimizing based on the post-optimization calculation. Carbon intensity calculations are done using the existing operational variables in the model and the carbon parameters. Thus, the goal is not to reformulate the model in order to incorporate carbon intensity as efficiently as possible, but to show how to include carbon intensity in an existing model.

Each plant type has a fixed associated carbon intensity parameter CI_{pi}^{Start}, considering what the feedstock and production emissions are and if CCS is implemented. As feedstock and production

carbon parameters are expressed as ton CO_2 emitted per ton H_2 in Konda et al. (2011), this is easy to calculate. Then, to get the carbon intensity CI_{ig} of product i satisfied at grid location g, we separately calculate the carbon intensity CI_{ig}^{Prod} from production plants and the carbon intensity CI_{ig}^{Trans} coming from transportation. By definition, if product i is not satisfied in grid g, then $CI_{ig} = 0$. To get the CI of all hydrogen products at a location, we average over the carbon intensities based on the amount of product satisfied at a grid, which gives the total carbon intensity CI_g of all products satisfied at grid g. Thus, if $D_g^T > 0$, then $CI_g > 0$ and $CI_{ig} \geq 0$.

4.2.3 Discussion of Hydrogen Supply Chain Network Model

The HSCN model makes two big assumptions regarding carbon intensities. Firstly, as the model uses the variable $\boldsymbol{Q}_{ilgg'}$, the transport of product i using mode l from grid g to grid g', we do not explicitly state that grid g is satisfied by a particular plant in a grid, but just by all plants of that product type in a grid. Therefore, the carbon intensity of produced hydrogen products in a grid is averaged over the plant types in that grid, i.e., as CI_{ig}^{Plants}. This corresponds to the amount-of-product averaged CI of a striped circle in Figure 4.6, instead of individual carbon intensities CI_{pig}. This means for example, if in a grid we have a CG-Large-CH_2 plant and an SMR-Small-CCS-CH_2 plant, the carbon intensity of the CH_2 plants is the amount-of-product weighted average of the carbon intensity of both plants. Even though one grid with a strict CI restriction might be able to be completely satisfied by the SMR-Small-CCS-CH_2 plant, while other grids are satisfied by the CG-Large-CH_2 plants, we still consider the average carbon intensity of both plants. This can be avoided by considering a variable $\boldsymbol{Q}_{pilgg'}$ with an additional index p, but this would require a complete redesign of the model, as well as a lot more variables. Also, in real-life production planning we might not always be able to satisfy demand from exactly one plant in a grid, which also makes it a reasonable assumption to make.

Secondly, an assumption we can make is that every grid can only import one type of hydrogen product, so either CH_2 or LH_2, but not both. This still allows to produce both products in a grid, and even satisfy both products in grids where production is possible. However, this restriction might increase the speed of nonlinear carbon intensity models, as there is no longer a trade-off possible of how much CH_2 and LH_2 to import with different carbon intensities. The demand should then be completely satisfied by one product *or* the other. In Chapter 5, the speed increase with and without this assumption is investigated.

Finally, considering carbon emissions, we assume that CCS can be built on top of every type of plant. For water electrification this is technically not needed, as emissions mainly depend on how the electricity is generated. Nevertheless, we keep this option to be consistent with the other production types. Also, we do not consider the life-cycle emissions of biomass, meaning we do not account for the carbon emissions that are 'absorbed' by biomass.

Chapter 5

Results

In this chapter, we present the results of the multi-resource, multi-transport (MRMT) model (Section 5.1) and the hydrogen supply chain network (HSCN) model (Section 5.2). All code is executed using Gurobi 9.5.2 in Python 3.9 on a Dell Core i7 computer. The code can be found on GitHub[1].

5.1 Results Multi-Resource, Multi-Transport Model

In the first part of the results section, we discuss the topology, data and experiments that are performed for the MRMT model.

5.1.1 Topology

Figure 5.1 shows the topology of the experimental setup. In total, we have 24 node-resource pairs and 30 arc-resource-mode triples. Four source nodes supply four different resources, which are converted into a fifth and sixth resource at two different production units. CCS is defined on both production units individually. With two modes of transport options, the resources can be transported to two depots. From the depots, the resources are transported to four target nodes, which have different demands for different resources.

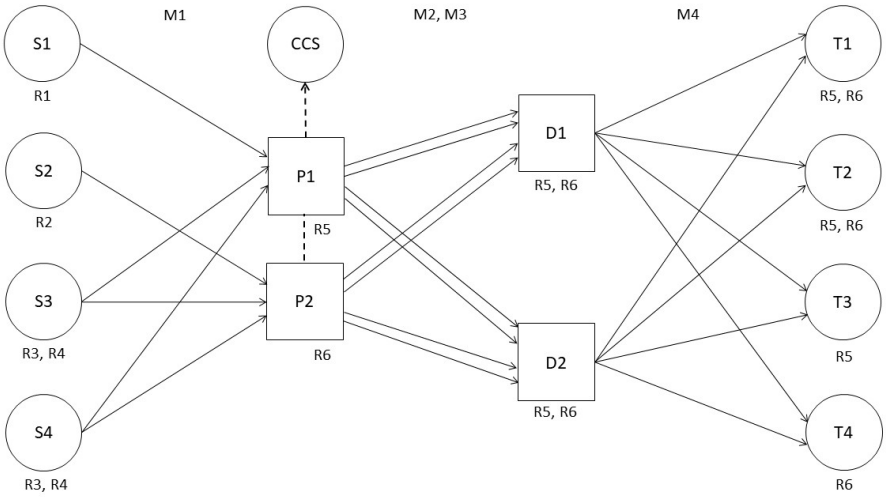

FIGURE 5.1: Topology for the computational experiments.

[1]https://github.com/erikvdheide/MSc-Thesis-Operations-Research

This topology is chosen, because it resembles different modeling components we have in practical models. The setup is deliberately kept small, such that we can get results from the nonlinear formulations in acceptable running times. The main goal is to show the correctness of the model and show some first run time results. In real-world problems, the scale of such a network is usually much bigger, containing thousands of nodes and arcs.

5.1.2 Data

The data chosen for the topology in Figure 5.1 is given in Tables 5.1-5.6. The data is chosen in such a way that every carbon reduction possibility becomes active for some type of carbon restriction. For this topology, we have that S3, P1, M2 and D1 are low-cost, high-carbon options and S4, P2, M3 and D2 high-cost, low-carbon alternatives. The data on the arcs, not presented in the table, is that every arc has a cost of 1, a carbon emission of 1 and an infinite throughput, except mode M2 which has a cost of 1 and carbon emissions of 3 and mode M3 with a cost of 2 and carbon emissions of 1. The capacity of mode M3 for resource R5 is 200 and 300 for resource R6.

TABLE 5.1: Source data table.

$s \in \mathcal{S}, r \in \mathcal{R}$	$supply_{rs}^{min}$	$supply_{rs}^{max}$	$cost_{rs}$	$carbon_{rs}$
(S1, R1)	0	1000	10	20
(S2, R2)	0	1000	15	15
(S3, R3)	0	1000	2	10
(S3, R4)	0	1000	2	10
(S4, R3)	20	1000	4	2
(S4, R4)	20	1000	4	2

TABLE 5.2: Production nodes data table.

$p \in \mathcal{P}$	$through_{p}^{max}$	$cost_p$	$carbon_p$
P1	∞	10	20
P2	500	12	15

TABLE 5.3: Yields of resources at production units data.

$yield_{rp}$		$r \in \mathcal{R}$					
		R1	R2	R3	R4	R5	R6
$p \in \mathcal{P}$	P1	-0.65	0	-0.25	-0.10	1.0	0
	P2	0	-0.70	-0.15	-0.15	0	1.0

TABLE 5.4: CCS units data.

$p \in \mathcal{P}', l \in \mathcal{L}$	$capture_{p}^{max}$	$install_{p}^{fixed}$
(P1, L1)	2000	1000
(P1, L2)	5000	2000
(P1, L3)	9000	3000
(P2, L1)	2000	1000
(P2, L2)	5000	2000

TABLE 5.5: Depot data.

$d \in \mathcal{D}, r \in \mathcal{R}$	$through_{d}^{min}$	$through_{rd}^{max}$	$cost_{d}^{fixed}$	$carbon_{d}^{fixed}$
D1	0		500	1500
(D1, R5)		∞		
(D1, R6)		∞		
D2	50		750	450
(D2, R5)		300		
(D2, R6)		300		

TABLE 5.6: Target data.

$t \in \mathcal{T}, r \in \mathcal{R}$	$demand_{rt}^{min}$	$demand_{rt}^{max}$	$price_{rt}$
(T1, R5)	70	80	40
(T1, R6)	80	90	50
(T2, R5)	85	95	40
(T2, R6)	65	75	50
(T3, R5)	70	80	40
(T4, R6)	85	95	50

5.1.3 Computational Experiments

This section presents several computational experiments to illustrate the complexity and behavior of various carbon intensity formulations. We also perform several configurations of linear models and compare their results with the nonlinear models.

Absolute Emission Restrictions Before we consider any nonlinear formulation, we assess the trajectory of carbon intensities if we impose progressively stricter *linear* restrictions, as in constraint (4.69). For the data as presented in Tables 5.1-5.6, we find that the pure profit maximization objective is 10,763.0 with associated total emissions in the whole chain of 20,792.5, which was found in 0.005 seconds. If we consider pure carbon emission minimization, the optimal solution reduces the emissions in the chain by 63.9% to 7500.5, but also reduced the profit to 4328.75 (-59.8%).

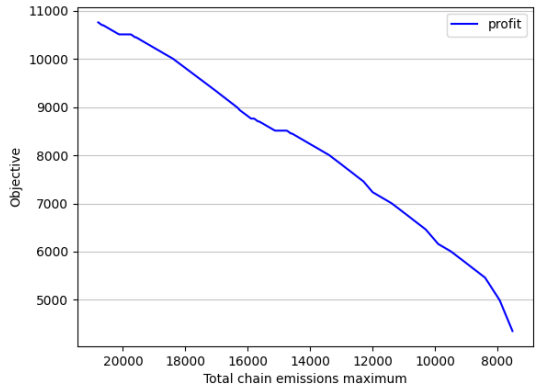

FIGURE 5.2: Profit objective for stricter linear emission restrictions.

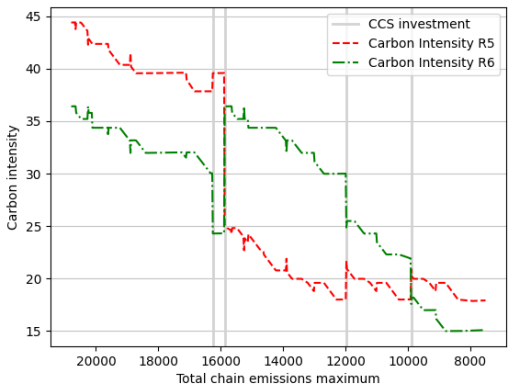

FIGURE 5.3: Carbon intensities of the resources at the targets for stricter linear emission restrictions.

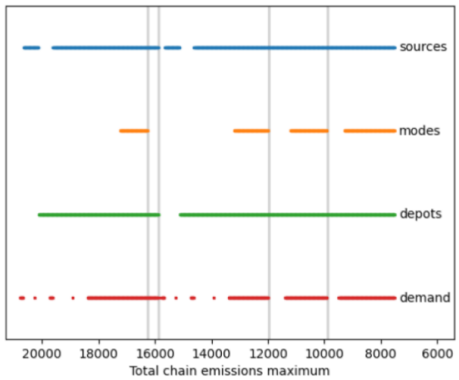

FIGURE 5.4: Indicators of whether a low-carbon alternative was used for stricter linear emission restrictions.

Figure 5.2 shows profit at progressively stricter emission restrictions between $emissions^{max} = 20,792.5$ and $emissions^{min} = 7500.5$. The objective is non-increasing, as can be expected when imposing stricter restrictions. Figure 5.3 shows the corresponding carbon intensities of resources $R5$ and $R6$ at the same linear restriction values. The carbon intensities have a general decreasing trend, but can also increase for lower absolute emissions. This can be explained by the fact that carbon intensities relate to each other, as carbon flows are distributed over multiple resources. This can

also be seen in the picture: generally, where we see sharp spikes up for one resource, we see a similar spike down for the other resource and vice versa. Solutions might not be unique: for instance, production units $P1$ and $P2$ can receive resource $R4$ from both S3 and S4, where the proportional amount that goes to each production unit impacts the carbon intensities of $R5$ and $R6$, but not the overall cost. Also the amount of resource produced plays a role: if less product is produced, more (fixed) emissions should be distributed over less product, increasing the carbon intensity. The vertical lines in Figure 5.3 show the moments there is a higher level of CCS investment. This goes together with sharp declines in carbon intensities. For this dataset in particular, the carbon intensities of the resources are the same across target locations.

Figure 5.4 shows if one of the low-carbon alternatives became active for that value of $emissions^{max}$. For example, at $emissions^{max} = 18,000$, we get that the low-carbon source $S4$ is used for some supply and low-carbon depot $D2$ is used to store the products, where low-carbon mode $M3$ was not utilized at all. In the case of demand, the definition is slightly different: it means the maximum demand was not produced at at least one of the targets. Figure 5.4 shows that the model seeks to find combinations of lower-carbon alternatives, which are not constantly needed. Using different modes of transport is here the low-carbon alternative that is used the fewest. Around CCS investments, other low-carbon alternatives are temporarily not needed. Towards the most strict emission restrictions, all low-carbon alternatives are needed.

All in all, we can conclude that linear restrictions are a fast way to reduce carbon intensities, but carbon intensities do not make the same linear trend downward.

Comparing CI Formulations Next, we use our nonlinear formulations to restrict carbon intensities. We perform both Option 1 using CI variables and Option 2 using y (carbon flow) variables. We set $CI_{R5}^{max} = \{44, 43, \ldots, 18\}$ and $CI_{R6}^{max} = \{36, 35, \ldots, 15\}$, as we know from Figure 5.3 those values are achievable. We also perform runs with restrictions on both $R5$ and $R6$ simultaneously, where we use the combinations of the five strictest carbon intensity restriction values. We always set a maximum run time of 100 seconds. The model without carbon intensity variables and balance constraints has 71 variables and 72 constraints, which becomes 99 variables and 80 constraints using Option 1 (CI variables) and 123 variables and 90 constraints using Option 2 (y variables).

In general, we find that both formulations find the optimal solutions in several milliseconds to seconds as long as CCS does not have to be used, which is up and until the cut-off points $CI_{R5}^{max} = 38$ and $CI_{R6}^{max} = 30$. The longest running times up and until these cut-off points are 1.32 seconds for $CI_{R6}^{max} = 32$ with Option 1 and 1.28 seconds for $CI_{R5}^{max} = 38$ with Option 2, all other running times were under a second. Although this is still very fast, going from about 10 milliseconds for the linear model to 1000 milliseconds for the nonlinear model means an upscale by a factor of 100. This becomes problematic if we have models that typically run for several minutes to hours. After the cut-off points, the model needs to determine the amount of carbon to capture at the production nodes, which leaves an optimality gap that cannot be reduced to (almost) zero within 100 seconds, though a feasible solution is always found in at most a few seconds. Thus, the more decision components are involved, the higher the running time is.

Table 5.7 shows the profit objective function values for different CI restriction values. Only those values are shown for which there was a difference in objective function value between the two

formulation options. As can be seen, for 7 out of 9 cases the first option gave the best result, while in 2 out of 9 cases the second option gave the best result. The differences between the solutions are relatively small, often not more than one percent, though there is one case with a difference of 4.44% and another case with a difference of 3.48%. Better objective function values seem to be for some consecutive CI^{max} values, which is most likely a coincidence, as previous solutions are, if even feasible, not chosen as a starting point for the next solution. The optimality gaps range from 8.0% to 59.6%, higher for stricter CI restrictions, so the solvers have difficulty proving optimality within the time limit of 100 seconds.

TABLE 5.7: Profit objective values using two different CI formulations for those CI restrictions where results differ.

CI^{max}_{R5}	32	31	30	22	21	19			21
CI^{max}_{R6}							24	22	18
Objective Option 1 (CI variables)	9175.49	8763.00	**8960.54**	**8494.64**	**8367.09**	**8122.08**	**9204.41**	**8805.49**	**6210.19**
(optimality gap in %)	(9.1)	(14.3)	**(11.7)**	**(17.9)**	**(19.7)**	**(23.3)**	**(8.8)**	**(12.6)**	**(27.6)**
Objective Option 2 (y variables)	**9271.01**	**9151.69**	8952.31	8494.17	8363.65	8121.95	9160.31	8763.00	6001.50
(optimality gap in %)	**(8.0)**	**(9.4)**	(11.8)	(17.9)	(19.7)	(23.3)	(9.3)	(14.3)	(59.6)
Difference in objective value (%)	1.04	4.44	0.09	0.01	0.04	0.002	0.48	0.48	3.48

All in all, the nonlinear models are relatively fast at this scale for not too high carbon intensity restrictions, and the formulation with CI variables more often finds the best solution, though the option with y variables is able to find a better solution as well.

Linear Approach to Satisfy CI Restrictions Next, we want to compare the solution values of the nonlinear model with a model with linear carbon restrictions like constraint (4.69) that satisfies carbon intensity restrictions. These results are given in Table 5.8. The results for the nonlinear models in the first row use a maximum running time of 100 seconds and the best solution out of the two formulation options is reported. In the second row, the solution is given when we tune the value of $emissions^{max}$ such that the carbon intensity restrictions are met. With tuning, we actually mean trial-and-error of increasing and decreasing $emissions^{max}$ until the desired values are met. As the linear models run in milliseconds, this can still be done quite quickly.

TABLE 5.8: Best-found solutions and linear approximations at different CI restrictions.

CI^{max}_{R5}	18		18
CI^{max}_{R6}		15	15
Best-found max. profit solution nonlinear model	7677.33	8022.41	5463.75
(optimality gap)	(30.4%)	(24.8%)	(65.0%)
Solution with linear restriction on *all* chain emissions	5617.00	5265.99	5265.99
(difference from best-found solution)	(-26.8%)	(-34.4%)	(-3.6%)
Solution with linear restriction on *sub*chain emissions	7718.50	7754.00	-
(reduction from best-found solution)	(+0.5%)	(-3.5%)	

From Table 5.8, we see a reduction in solution quality of 26.8% and 34.4% compared to the nonlinear model, except if we put a restriction on the carbon intensity of both resources, then the solution is only 3.6% worse. For the individual CI restrictions, we did put a linear restriction on *all* chain

emissions, which gives a worse result, as we also minimize emissions from the resources that do not need a CI restriction. For example, if we want to restrict the CI of $R5$, it does not make sense to consider CCS investments on $P2$, which only produces $R6$. Therefore, in the third row we also perform emission restrictions on *sub*chains, which are all components of the chain that are associated with that resource. Starting from target-resource pair ($t \in \mathcal{T}, r \in \mathcal{R}$), the subchain is all nodes and arcs that can be reached by going backward in the network. Now we see only a reduction of 3.5% in solution quality for $R6$ and even a slight solution improvement for $R5$ of 0.5%, showing the nonlinear model did not yet find an optimal solution. Earlier experimentation found that manually forcing the maximum amount of resources to produce even further improved the solutions, but for this data no feasible solutions existed for maximum production.

All in all, linear restrictions of subchains are able to find solution values close to solution values found by nonlinear models for the chosen topology, however one downside is that it is not obvious which $emissions^{max}$ value to choose, so it requires several runs of the model to find the right restriction value.

Scaled Up Experiments Finally, to have a further investigation on running times we scale up our topology from Figure 5.1 with five times as many nodes and consequently 5^2 as many arcs. Some arbitrary disturbances are made in the data, and the option for CCS is left out.

Some interesting results came out of experimenting with this setup. First of all, the model without carbon constraints finds the economic-optimal solution with a profit of 42,344.75 and chain emissions of 235,625.92 in 0.02 seconds. After that, we minimize the carbon emissions in the chain, which is also a linear model. The model finds the lowest emissions of 67,618.25 also in 0.02 seconds, a reduction of 71.3% compared to the economic-optimal solution emissions, and a corresponding profit of -7218.88, indicating a loss to arrive at this solution. If we then again consider the profit-maximizing model with a linear constraint of $emissions^{max} = 67,618.25$, we find a profit of 11,963.44 in 0.03 seconds, which is much higher than the pure carbon minimizing profit. Apparently, for this data there exists a much more economically profitable solution with the same carbon emissions. Therefore, a carbon minimizing model is useful to find the range of carbon emissions in the supply chain, but a more profitable solution might still be found by considering carbon emissions as a constraint.

For the disturbed data, the CIs at the targets are not equal for each target node. Therefore, if we put carbon restrictions on individual target nodes, the other target nodes do not necessarily decrease in carbon intensity. For a feasible restriction $CI^{max}_{R5,T1} = 40$, we find a solution of 42,278.12 within a second with an optimality gap of 0.16%, which does not improve in the remaining 99 seconds of running time. For the restriction $CI^{max}_{R6,T1} = 30$, we find a solution of 36,006.48 in two seconds with an optimality gap of 17.6%, also not improving in 100 seconds. For the combination of $CI^{max}_{R5,T1} = 40$ and $CI^{max}_{R6,T1} = 30$, the first feasible solution of 13,375.83 is found after five seconds, improving to 34,827.15 in ten seconds and staying on this solution with an optimality gap of 21.2%.

All in all, it is profitable to first minimize carbon emissions to know what is achievable, and then rerun the model with a linear restriction on emissions to find an economically better solution. Also, the nonlinear model finds feasible solutions still relatively fast, but has trouble proving optimality for these solutions.

5.2 Results Hydrogen Supply Chain Network Model

In this section, we discuss the results of the HSCN model. In Section 5.2.1, we briefly discuss the data that is used in the case study. In Section 5.2.2, we discuss the main results of the static model without any carbon intensity restrictions and in Section 5.2.3 we evaluate the results of nonlinear carbon intensity constraints. In Section 5.2.4 and Section 5.2.5, we do the same analysis for the dynamic version of the model.

5.2.1 Case Study Data

The data used in the case study is based on the data described by Konda et al. (2011). They performed a strategic study on the design of a hydrogen infrastructure network in the Netherlands, based on the projected trends in the hydrogen market. The full dataset where the models are evaluated on is given in Appendix C.

In the dataset by Konda et al. (2011), the Netherlands is split into 25 distinct regions, corresponding to the 25 biggest cities, as shown in Figure 5.5. For each region, the H_2 demand per day is calculated based on the vehicle density of the region, as well as the hydrogen market share as a whole. The latter is assumed to be increasing over time, where four time periods are considered: 2015-2020, 2021-2030, 2031-2040 and 2041-2050. The daily hydrogen demand is assumed to be the same across days within a time period. While Konda et al. (2011) use multiple demand scenarios, we fix one demand scenario: a hydrogen market share of 1%, 3%, 7.5% and 17.5% in the respective periods. Although this might be a too optimistic scenario according to up-to-date market predictions, it does provide us with a good demonstration of how the model works.

FIGURE 5.5: Locations in the Netherlands considered, including plant building options.

Some assumptions had to be made on top of the data from Konda et al. (2011). For example, we assume that a transportation vehicle emits 750 g CO_2/km, independent of the type of hydrogen and the weight of hydrogen transported. Also, instead of using power equations for the capital costs of hydrogen plants depending on the exact capacity of the plant, we introduce a fixed capital cost based on the size of the plant (small, medium, large) and the plant type, as well as a unit production cost. The distance between destinations is calculated by taking the longitude and latitude values of the center of the locations and calculating their absolute distances. Within a grid, it is assumed that the average one-way travel distance is 5 km.

5.2.2 Results Static Model

First, we look at the cost, emission and carbon intensity results without considering nonlinear carbon intensity restrictions.

Cost Minimization Table 5.9 shows the cost and emission values for the static model for the four different time periods. As can be seen, facility capital costs account for the largest share of the total daily cost, with a cost share between 38.6% and 53.0%. The total feedstock plus production costs account for 87.8%-98.2% of total costs, where the other 12.2%-1.8% accounts for transportation costs. Of transportation operating costs, the labor cost has the highest share with 66.1%-87.8%. Regarding the total chain emissions, the production emissions by far have the highest share between 93.3%-95.8%, with transportation emissions only 0.2%-1.9%. The running time is much lower than in the papers the model is based on: all four demand periods can be run under three seconds. Each linear model has 10,168 variables and 17,768 constraints.

TABLE 5.9: Total daily costs and total daily carbon emissions for demand in different time periods under the objective of **cost minimization**.

Abrev.	Cost or carbon type	Period T1	Period T2	Period T3	Period T4	Units
TDC	**Total daily cost**	**593,387.68**	**1,297,992.0**	**3,225,851.06**	**7,702,797.90**	\$/day
FSC	Feedstock cost	27,235.17 (4.6%)	87,664.86 (6.8%)	260,472.55 (8.1%)	728,918.42 (9.5%)	\$/day (% of TDC)
FCC	Facility capital cost	303,900.38 (51.2%)	501,207.78 (38.6%)	1,658,506.55 (51.4%)	4,080,497.07 (53.0%)	\$/day (% of TDC)
FOC	Facility operating cost	189,697.69 (32.0%)	610,601.02 (47.0%)	1,130,794.0 (35.1%)	2,748,822.1 (35.7%)	\$/day (% of TDC)
TCC	Transport capital cost	8630.14 (1.5%)	8520.55 (0.7%)	17,424.66 (0.5%)	212,60.27 (0.3%)	\$/day (% of TDC)
TOC	Transport operating cost	63,924.30 (10.8%)	89,997.79 (6.9%)	158,653.31 (4.9%)	123,300.03 (1.6%)	\$/day (% of TDC)
FC	Fueling cost	9089.02 (14.2%)	11,092.43 (12.3%)	15,131.49 (9.5%)	34,450.95 (27.9%)	\$/day (% of TOC)
LC	Labor cost	52,587.35 (82.3%)	76,045.48 (84.5%)	139,323.57 (87.8%)	81,465.11 (66.1%)	\$/day (% of TOC)
MC	Maintenance cost	1730.07 (2.7%)	2103.65 (2.3%)	2825.5 (1.8%)	6586.63 (5.3%)	\$/day (% of TOC)
GC	General cost	517.86 (0.8%)	756.24 (0.8%)	1372.74 (0.9%)	797.34 (0.6%)	\$/day (% of TOC)
TCE	**Total chain emissions**	**689.66**	**2559.55**	**9313.57**	**28,077.07**	ton CO_2/day
TCE^{Feed}	Total feedstock emissions	32.7 (4.7%)	105.4 (4.1%)	376.9 (4.0%)	1114.9 (4.0%)	ton CO_2/day (% of TCE)
TCE^{Prod}	Total production emissions	643.62 (93.3%)	2437.98 (95.3%)	8914.92 (95.7%)	26,911.55 (95.8%)	ton CO_2/day (% of TCE)
TCE^{Trans}	Total transport emissions	13.29 (1.9%)	16.17 (0.6%)	21.71 (0.2%)	50.61 (0.2%)	ton CO_2/day (% of TCE)
D_g^T	Total demand	56.46	181.73	649.88	1992.25	ton H_2/day
	Run time	0.04	2.52	1.12	0.14	seconds

Each time period is executed individually, meaning we do not assume that plants from previous time periods can or should be used in later time periods. In the first time period, an SMR-Small-CH_2 plant is built in Rotterdam, for which 63 tube trailers satisfy the demand of the whole country. In the second time period, one SMR-Small-CH_2 and one SMR-Small-LH_2 are built in Rotterdam. CH_2 is served in 8 grids, including Rotterdam, with 85 tube trailers, and LH_2 is served to 18 grids with

7 tanker trucks. Only Haarlem receives both CH_2 (6.77 ton H_2/day) and LH_2 (4.59 ton H_2/day). In the third period, one SMR-Medium-CH_2 plant which produces 150.88 tons of CH_2 per day and one SMR-Medium-LH_2 producing 499 tons of LH_2 per day are built in Rotterdam. Rotterdam and Zoetermeer are satisfied by CH_2 and Zoetermeer and all other locations are satisfied by LH_2, using 150 tube trailers and 27 tanker trucks. Finally, in the fourth period, two SMR-Large-LH_2 plants are built in Rotterdam, where 97 tanker trucks satisfy the demand of the whole country.

Although we use a static model instead of a dynamic model as in Konda et al. (2011), these results are in line with their results: mainly SMR units in the Rotterdam area are built, producing a combination of CH_2 and LH_2. If we would make the assumption that only one type of hydrogen can be imported into a grid, the solutions of periods T2 and T3 change slightly. For period two, a cost increase of 0.07% leads to a solution where 7 grids import CH_2 and 17 grids import LH_2 from Rotterdam, while Rotterdam itself uses both. For period three, a cost increase of 0.02% leads to a solution where Zoetermeer only receives CH_2 instead of both CH_2 and LH_2.

CO_2 Minimization To get an impression of the CO_2 reductions that are possible at which costs, we also run the model on pure CO_2 emissions minimization. These results are given in Table 5.10. Compared to the cost minimization case, the total daily costs become 1.5, 1.6, 1.7, and 1.6 times as large, while the total CO_2 emissions become 6.7, 7.4, 7.8 and 8.1 times as low respectively for the four time periods. The share of facility capital costs to total daily costs increases for CO_2 minimization compared to cost minimization, as carbon minimization requires building more plants in order to reduce transportation emissions. For total chain emissions, we see that the share of production emissions decreases, though still relatively high. This is because of the CCS plants that are built. For the first period, one SMR-CCS-CH_2 plant is built in Rotterdam and one in Amsterdam. For the second period, three SMR-CCS-CH_2 plants are built in Rotterdam, Amsterdam and Arnhem, and one SMR-CCS-LH_2 plant in Rotterdam. In the third period, 5 SMR-CCS-CH_2 plants are built across the five possible destinations, and one SMR-CCS-LH_2 plant is built in Rotterdam. Finally, in the last time period we have six SMR-CCS-CH_2 plants across the possible production locations (two in Amsterdam), and one SMR-CCS-LH_2 plant in Rotterdam.

TABLE 5.10: Total daily costs and total daily carbon emissions for demand in different time periods under the objective of **CO_2 minimization**.

Abrev.	Cost or carbon type	Period T1	Period T2	Period T3	Period T4	Units
TDC	**Total daily cost**	**900,879.49**	**2,061,347.06**	**5,499,763.06**	**12,587,043.53**	\$/day
FSC	Feedstock cost	27,235.17 (3.0%)	79,504.86 (3.9%)	265,098.89 (4.8%)	738,039.09 (5.9%)	\$/day (% of TDC)
FCC	Facility capital cost	607,800.77 (67.5%)	1,299,429.11 (63.0%)	325,4949.22 (59.2%)	6,958,874.35 (55.3%)	\$/day (% of TDC)
FOC	Facility operating cost	205,788.12 (22.8%)	501,286.79 (24.3%)	1,408,459.01 (25.6%)	3,426,228.97 (27.2%)	\$/day (% of TDC)
TCC	Transport capital cost	7671.23 (0.9%)	14,219.18 (0.7%)	46,246.58 (0.8%)	120,657.53 (1.0%)	\$/day (% of TDC)
TOC	Transport operating cost	52,384.2 (5.8%)	166,907.12 (8.1%)	525,009.35 (9.5%)	1,343,243.58 (10.7%)	\$/day (% of TDC)
FC	Fueling cost	4512.48 (8.6%)	21,112.55 (12.6%)	49,092.4 (9.4%)	118,980.12 (8.9%)	\$/day (% of TOC)
LC	Labor cost	46,561.88 (88.9%)	140,403.45 (84.1%)	462,126.08 (8.4%)	1,190,212.06 (88.6%)	\$/day (% of TOC)
MC	Maintenance cost	849.52 (1.6%)	4010.16 (2.4%)	9261.65 (1.8%)	22,395.44 (1.7%)	\$/day (% of TOC)
GC	General cost	460.32 (0.9%)	1380.96 (0.8%)	4529.22 (0.9%)	11,655.96 (0.9%)	\$/day (% of TOC)
TCE	**Total chain emissions**	**103.64**	**346.96**	**1191.38**	**3473.04**	ton CO_2/day
TCE^{Feed}	Total feedstock emissions	32.7 (31.6%)	105.4 (30.4%)	376.9 (31.6%)	1114.9 (32.1%)	ton CO_2/day (% of TCE)
TCE^{Prod}	Total production emissions	64.36 (62.1%)	210.74 (60.7%)	743.27 (62.4%)	2186.03 (62.9%)	ton CO_2/day (% of TCE)
TCE^{Trans}	Total transport emissions	6.53 (6.3%)	30.82 (8.9%)	71.17 (6.0%)	172.1 (5.0%)	ton CO_2/day (% of TCE)
D_g^T	Total demand	56.46	181.73	649.88	1992.25	ton H_2/day
	Run time	0.07	1.40	3.24	5.58	seconds

In general, we see that much more plants and only CCS plants are built in order to reduce transportation emissions. These solutions might not be realistic in real life, for example because it requires 1388 tube trailers to transport the much higher quantities of CH_2 in the last time period, which the model does not penalize as vehicles have no fixed associated carbon emissions. In practice, one can first run a CO_2 minimization and then a cost maximization with a linear CO_2 constraint, knowing the minimum CO_2 level achievable. However, as the cost improvements were so little doing this for the minimization of the CO_2 level, this was not done for the results in Table 5.10.

Corresponding CI Values Finally, we look at the range of carbon intensity values that can be achieved for this setup. We look at three problems: the CO_2 minimization problem, the cost minimization problem and the CO_2 maximization problem. Of course, the latter is something we want to avoid at all costs, but it is just to illustrate the range of carbon intensity values that are possible. These values are given in Figure 5.11. As can be seen, for pure cost minimization the values are around 14-15 ton CO_2 per ton H_2, which can be reduced to about 1.6-2.0 ton CO_2 per ton H_2, which means a carbon intensity close to zero is not possible to achieve for this data. In practice, if other assumptions are made, like only considering green electricity or assuming biomass to be carbon neutral, this actually might be possible. The carbon intensity can be as much as 45-46 tons of CO_2 per ton of H_2, but this also corresponds to a very inefficient supply chain.

TABLE 5.11: Carbon intensity CI_g values, weighted-averaged over hydrogen products i, under three model configurations for the fourth time period.

Problem	**Carbon intensity (ton CO_2/ton H_2) of grid g**																								
	G01	G02	G03	G04	G05	G06	G07	G08	G09	G10	G11	G12	G13	G14	G15	G16	G17	G18	G19	G20	G21	G22	G23	G24	G25
CO_2 min.	1.65	1.72	1.88	1.76	1.65	1.74	1.77	1.87	1.97	1.70	1.85	1.81	2.01	2.00	2.00	2.00	1.75	2.00	1.70	2.04	2.03	1.85	1.70	2.04	1.80
Cost min.	14.6	14.6	14.6	14.6	14.6	14.6	14.6	14.6	14.6	14.6	15.6	14.6	14.6	14.6	14.6	14.6	14.6	14.6	14.6	14.6	14.6	14.7	14.7	14.6	14.6
CO_2 max.	45.4	45.3	45.3	45.4	45.2	45.3	45.4	45.1	45.0	45.0	45.0	45.1	45.5	45.3	45.5	45.6	45.4	46.0	43.9	45.2	45.3	45.7	43.9	45.9	45.2

5.2.3 Carbon Intensity Constraints in Static Model

Next, we want to include specific carbon intensity constraints at specific locations, such that some customers can demand a hydrogen product with a lower carbon intensity, while others do not have to. We discuss the run times of the nonlinear models and show some typical solutions when imposing CI restrictions. For each experiment, we assume that there can only be import of one hydrogen product in each grid, unless stated otherwise.

CI Restrictions on Non-Production Cities First of all, we are interested in carbon intensity restrictions for cities that do not have the possibility to produce hydrogen. We focus on a CI restriction of both hydrogen products, i.e., no matter which type(s) of hydrogen a grid location receives, the average carbon intensity must be below the restriction value. If we put a restriction on a single hydrogen product, we generally see that the demand is satisfied by the other product, such that one carbon intensity becomes zero and always satisfies the constraint.

Table 5.12 shows how much time the nonlinear solver needs to find an optimal solution, and in case of no optimality after five minutes, what the remaining optimality gap is. Except for one situation, the model could always find an optimal solution within five minutes. The run times for

the linear model without CI restrictions are 2.5 and 0.2 for time periods T3 and T4 respectively. Table 5.12 shows that a stricter CI restriction of 5 results in a higher running time for Zoetermeer and Haarlem, but in a lower running time for Apeldoorn, Enschede and Leeuwarden, compared to a restriction value of 10. Out of all 20 runs from Table 5.12, the average cost increase to obtain the solution that satisfies the CI constraint is 2.68% (minimum 0.46%, maximum 6.09%) where the total emissions in the chain decrease on average by 14.59% (minimum 2.23%, maximum 41.39%). Including CI optimization introduces 225 additional variables and 95 additional variables compared to the linear model, for a single CI constraint.

TABLE 5.12: Run time complexity of cities without production possibility for two time periods and two CI restrictions. Maximum running time of 300 s.

Run time in seconds (optimality gap in %)	Zoetermeer	Haarlem	Apeldoorn	Enschede	Leeuwarden
T3 - CI $\leq$ 10	13.4	11.8	21.3	39.4	53.5
T3 - CI $\leq$ 5	15.5	12.3	4.6	6.2	25.3
T4 - CI $\leq$ 10	1.1	3.2	3.9	2.7	3.5
T4 - CI $\leq$ 5	1.9	300 (0.27)	1.8	1.7	1.7

We give a full example solution to demonstrate the choices that are made by the model. We take Zoetermeer in time period T4 with a CI restriction of 5. In the linear cost minimization problem, all of Zoetermeer's demand is satisfied from one of two SMR-Large-LH_2 plants in Rotterdam with a corresponding carbon intensity of 14.59. When imposing the CI restriction, an additional SMR-Small-CCS-CH_2 plant is built in Rotterdam on top of the two existing LH_2 plants, which increases the costs by 4.7% and decreases the CI of Zoetermeer to 1.83. By the assumption that production plants grouped by the same hydrogen product in the same grid have different carbon intensities, the restriction would not have been met if this CH_2-CCS plant would have been an LH_2-CCS plant. In that case, the CI would be averaged with the already established LH_2 plants in Rotterdam, which would not decrease the CI enough to satisfy the restriction.

We discuss some other notable results. For T4 and a CI restriction of 10, all five cities find the same solution where one of the two SMR-Large-LH_2 plants in Rotterdam is replaced by an SMR-Large-LH_2-CCS plant, such that the carbon intensities of all 25 locations become around 8.6. For the stricter CI restriction of 5, all five cities require a new SMR-Small-CCS-CH_2 plant to satisfy the restriction. For Haarlem, where the optimal solution was not found in 5 seconds, we find a solution where an SMR-Medium-CH_2-CSS plant is built, as a small CCS plant does not suffice to satisfy Haarlem's demand fully. For period T3, where we have one SMR-Medium-CH_2 and one SMR-Medium-LH_2 plant in Rotterdam, we generally see that one additional SMR-Small-CH_2-CCS plant is built, and one medium plant is downgraded to a small plant.

CI Restrictions on Production Cities Next, we consider restrictions on cities that can produce hydrogen and therefore also can have their demand satisfied by two types of hydrogen. The run time results are given in Table 5.13 for the five production locations and the same two time periods and CI restriction values. Compared to the cities without production possibilities, there are more cases

that do not solve to optimality in five minutes: four compared to one. However, the running time fluctuates quite a lot: for instance, a CI restriction of 10 in Arnhem in period T4 leads to the optimal solution in 2.5 seconds, but for a CI restriction of 5 the model cannot find the optimal solution in 5 minutes. For Maastricht en Groningen, quite in the corners of the country, the model finds very fast in T4 that it is most cost-efficient to build an additional SMR-Small-CH_2-CCS plant in their respective cities. Both cities import LH_2 and produce CH_2 for their own demand satisfaction.

TABLE 5.13: Run time complexity of cities with production possibility for two time periods and two CI restrictions. Maximum running time of 300 s.

Run time in seconds (optimality gap in %)	Rotterdam	Amsterdam	Arnhem	Maastricht	Groningen
T3 - CI $\leq$ 10	18.9	300 (0.74)	36.0	300 (0.67)	16.6
T3 - CI $\leq$ 5	4.4	4.3	6.7	5.7	5.7
T4 - CI $\leq$ 10	5.7	21.7	2.5	1.1	1.0
T4 - CI $\leq$ 5	46.1	300 (2.68)	300 (0.9)	6.39	1.3

Also here, we give a full example to demonstrate typical choices the model makes. We look at Rotterdam in the third time period, which is interesting as Rotterdam satisfies 128.88 tons of CH_2 (CI 11.42) and 5.67 tons of LH_2 (CI 15.18) from its own production. The optimal solution with the CI restriction is to partly satisfy demand from a CCS CH_2 plant in Amsterdam to get a CI of exactly 5. This plant might as well have been in Rotterdam, but by building it in Amsterdam the model 'escapes' the fact that it would otherwise be averaged with the already established CH_2 plant in Rotterdam with a higher CI. If we consider the same CI restriction in Amsterdam, a city that can build plants but does not do it in the cost minimization case, we find the same solution where a small CCS-CH_2 plant should be built in Amsterdam, but this time serving Amsterdam itself.

More CI Restrictions Simultaneously Next, we want to investigate whether having carbon intensity restrictions on more cities simultaneously increases or decreases the total running time. We consider pairs of cities that are far apart, including Rotterdam, Zoetermeer, Leeuwarden and Groningen. We again assume that only one type of hydrogen can be imported. Table 5.14 shows the results for these pairs, including for restrictions on all 25 grids.

TABLE 5.14: Run time complexity of a combination of cities with and without production possibility for two time periods and two CI restrictions. Maximum running time of 300 s.

Run time in seconds (optimality gap in %)	Zoetermeer, Leeuwarden (no prod., no prod.)	Rotterdam, Leeuwarden (prod., no prod.)	Zoetermeer, Groningen (no prod., prod.)	Rotterdam, Groningen (prod., prod.)	All
T3 - CI $\leq$ 10	36.1	27.8	20.1	88.5	17.0
T3 - CI $\leq$ 5	28.2	5.7	29.5	4.5	40.7
T4 - CI $\leq$ 10	1.0	2.7	3.6	3.1	1.4
T4 - CI $\leq$ 5	300 (0.4)	5.9	174.2	300 (0.66)	2.7

The running times from Table 5.14 are not drastically different than previously seen for single restrictions. Running times are most often in between the running times of both individual restrictions of the pair cities. A common solution seen is that an additional SMR-Medium-CH_2-CCS plant is

built to satisfy the CI restrictions of both locations. Putting a restriction on all 25 cities leads to a solution with only CCS plants. It still takes the model between 1.4 and 40.7 to find the optimal configuration with CCS plants.

With vs. Without Import Restriction Finally for the static model, we investigate the run time complexity of the nonlinear model if we let go of the assumption that only one type of hydrogen can be imported in a grid. This increases the solution space, specifically to balance the amount of each of the products to import such that the CI restriction can be met exactly. Table 5.15 demonstrates the running times for two cities where no hydrogen production is possible and two cities where production is possible. For 12 out of 16 cases, the model cannot find the optimal solution within five minutes. Most optimality gaps are under one percent, but the larger optimality gaps are around four percent, and the largest is 7.2%. Only for Rotterdam in periods T3 and T4 for CI ≤ 10, the solution is found quicker if we let go of the assumption. In total, the best-found solutions with the assumption are in 8 out of 16 cases better, the best-found solutions without the assumption are in 6 out of 16 cases better, and the solutions are the same in 2 out of 16 cases. The solutions with the assumption are on average 0.6% better. The assumption is not found to be better for either producing cities or non-producing cities. All in all, the run time increases if we let go of the import restriction assumption, and solution quality may or may not improve if the solver is terminated early.

TABLE 5.15: Run time complexity of cities with and without production possibility without the assumption of only one import product, for two time periods and two CI restrictions. Maximum running time of 300 s.

Run time in seconds (optimality gap in %)	Zoetermeer (no prod.)	Haarlem (no prod.)	Rotterdam (prod.)	Amsterdam (prod.)
T3 - CI ≤ 10	300 (0.63)	300 (0.72)	9.2	300 (0.4)
T3 - CI ≤ 5	300 (0.74)	300 (1.21)	300 (0.94)	300 (0.51)
T4 - CI ≤ 10	300 (0.07)	300 (1.17)	3.4	300 (4.48)
T4 - CI ≤ 5	63.9	300 (4.73)	300 (3.86)	300 (7.17)

5.2.4 Results Dynamic Model

Lastly, we evaluate the dynamic version of the model. With this model, we optimize all four time periods simultaneously. First, we compare the solutions of the linear model with that of the static model, after which we test carbon intensity constraints.

Table 5.16 demonstrates the solutions of the dynamic and static models. The types of solutions are different by the model assumptions that are made. For the dynamic model, we allow large plants to be built in early time periods to satisfy demand in later time periods. This is also what we see: an SMR-Large-LH_2 plant is built in periods 1 and 3. For the static model, the model does not know the demand in upcoming periods. Therefore, we enforce a constraint such that the plants that are already built in the previous period remain intact or get upgraded in size. The average daily cost over the entire time horizon is 10.9% lower than for the dynamic model, which is a significant amount, as this corresponds to a cost saving of 4.17 billion dollars over the complete time horizon. The optimal solution of the linear dynamic model was found in 0.45 seconds. The model has 48,790 variables and 81,810 constraints.

TABLE 5.16: Solutions of the dynamic and static model with rolling time horizon.

Total daily cost (TDC)	Period T1	Period T2	Period T3	Period T4	Avg. period
Dynamic model	3,505,486.75	341,025.60	3,259,133.49	3,615,506.31	**2,588,599.29**
$NP_{p,\mathrm{CH_2},\mathrm{G01}}$	-	-	-	-	
$NP_{p,\mathrm{LH_2},\mathrm{G01}}$	1 SMR-Large	1 SMR-Large	2 SMR-Large	2 SMR-Large	
Static model	593,387.68	1,115,651.77	2,724,762.30	6,265,703.07	2,906,152.71
$NP_{p,\mathrm{CH_2},\mathrm{G01}}$	1 SMR-Small	1 SMR-Small	1 SMR-Medium	1 SMR-Large	
$NP_{p,\mathrm{LH_2},\mathrm{G01}}$	-	1 SMR-Small	1 SMR-Medium	1 SMR-Large	

5.2.5 Carbon Intensity Constraints in Dynamic Model

Incorporating carbon intensity in the dynamic model leads to an even bigger set of possible combinations of restrictions to test on. Therefore, we demonstrate some interesting results for a limited number of cities, more focusing on time periods and restriction values. We assume that if a CI restriction is set in a time period before the last period, this restriction holds or gets stricter in the later periods. For instance, if we put a CI restriction of 5 in Zoetermeer in T2, then the CI of Zoetermeer must also be below 5 in T3 and T4. This is reasonable to assume, as carbon emission restrictions generally get stricter over the years, ultimately reaching net zero in 2050. We also again assume only one hydrogen product can be imported into a grid, unless stated otherwise.

CI Restrictions on a Non-Production City Table 5.17 shows the results of CI restrictions on a city without production possibility, Zoetermeer, for different time periods. The CI restriction value is kept the same over time at the value 5. The dynamic model results in larger running times than the static model. In this case, it took up to 20 seconds to find the first feasible solution, and the optimal solution was never found within five minutes. From Table 5.17, we can also conclude that CI restrictions on more time periods lead to a higher reduction of chain emissions. The big

difference in total emission reduction between the second-to-last and last column can be explained by the fact that for the T2-T3-T4 case a solution is found which builds an SMR-Large-CH_2-CCS which is used in the last period to satisfy the demand of multiple cities, where in the T1-T2-T3-T4 case only an SMR-Small-CH_2-CCS plant is built especially for Zoetermeer and the other cities are satisfied by two SMR-Large-LH_2 plants.

TABLE 5.17: Dynamic model results under the restriction of CI $\leq$ 5 for the city of Zoetermeer without production possibility.

	Zoetermeer T4	Zoetermeer T3-T4	Zoetermeer T2-T3-T4	Zoetermeer T1-T2-T3-T4
First feasible solution (s)	2	2	20	15
Total running time (s)	300	300	300	300
Optimality gap (%)	0.64	1.08	2.90	2.00
Cost increase (%)	3.88	4.62	6.02	4.91
Chain CO_2 decrease (%)	1.71	2.40	29.73	2.65

We give a full example of a typical solution for Zoetermeer with a CI restriction in T3 and T4. In the first time period, an SMR-Large-LH_2 and SMR-Small-CH_2-CCS are built in Rotterdam, but only the SMR-Large-LH_2 plant is operational in the first two time periods. In the third and fourth period, the SMR-Small-CH_2-CCS also becomes operational, reducing the CI of Zoetermeer from 14.59 to 1.83.

CI Restrictions on a Production City Table 5.18 presents the same CI restriction experiments for Rotterdam. Rotterdam knows higher running times and optimality gaps than Zoetermeer, where a restriction on all time periods even leads to the first feasible solution found after 54 seconds. The model might have a harder time finding the optimal solution for Rotterdam, as this is the key production city, influencing the transportation to most other cities. This table also clearly shows the increase in costs and the decrease in chain emissions when imposing restrictions for more periods. The total chain emissions have a larger decrease compared to Zoetermeer, as CCS plants that are built and used in Rotterdam also satisfy a part of the other demand.

TABLE 5.18: Dynamic model results under the restriction of CI $\leq$ 5 for the city of Rotterdam with production possibility.

	Rotterdam T4	Rotterdam T3-T4	Rotterdam T2-T3-T4	Rotterdam T1-T2-T3-T4
First feasible solution (s)	3	4	5	54
Total running time (s)	300	300	300	300
Optimality gap (%)	2.43	2.94	3.38	7.91
Cost increase (%)	4.97	6.18	6.86	12.18
Chain CO_2 decrease (%)	28.94	32.33	33.36	36.15

CI Restrictions on All Cities Table 5.19 shows the results if we put the same CI restriction on all cities. It takes on average somewhat longer to find the first feasible solution, but this time all optima were found within five minutes. This might be explained by the fact that there is less choice around the optimum: to satisfy a CI restriction of 5, all plants must have implemented CCS. The CO_2 emissions decrease is substantial, with a decrease of up to 80% for the most strict CI restrictions.

TABLE 5.19: Dynamic model results under the restriction of CI $\leq$ 5 for all grids.

	All grids T4	All grids T3-T4	All grids T2-T3-T4	All grids T1-T2-T3-T4
First feasible solution (s)	3	7	7	54
Total running time (s)	21.8	27.3	131.7	61.1
Optimality gap (%)	0	0	0	0
Cost increase (%)	7.72	9.09	9.61	9.71
Chain CO_2 decrease (%)	59.49	74.90	79.21	80.01

CI Restrictions Progressively Stricter Table 5.20 shows the results for Zoetermeer and Rotterdam if we impose progressively stricter restrictions. Feasible solutions can be found in just a few seconds, but there remains a substantial optimality gap, more so for the stricter than the looser restrictions. There is also a big difference in solution type, where for the first of Zoetermeer's columns a solution is found where an SMR-Small-CH_2-CCS plant is built to satisfy all Zoetermeer's demand, whereas in the last column of Rotterdam two SMR-Large-LH_2 plants are built, where one has CCS from the first period onward and one CCS only in the last period.

TABLE 5.20: Dynamic model results under progressively stricter CI restrictions for two different locations.

	Zoetermeer T1-T2-T3-T4 CI $\leq$ 10-8-6-4	Rotterdam T1-T2-T3-T4 CI $\leq$ 10-8-6-4	Zoetermeer T1-T2-T3-T4 CI $\leq$ 8-6-4-2	Rotterdam T1-T2-T3-T4 CI $\leq$ 8-6-4-2
First feasible solution (s)	3	7	2	1
Total running time (s)	300	300	300	300
Optimality gap (%)	1.98	3.88	2.87	5.19
Cost increase (%)	4.91	7.68	5.76	9.80
Chain CO_2 decrease (%)	2.65	35.15	29.83	80.75

CI Restrictions Without Import Assumption We also ran the same setups as in Table 5.20, but this time without the assumption that a grid can only import one hydrogen product. These results are given in Table 5.21. In total, 2 out of 4 solutions are worse, 1 out of 4 solutions is better and the last solution has the same objective function value. Especially remarkable is the solution for Zoetermeer and CI $\leq$ 10-8-6-4 where the first solution was only found only after 96 seconds, and the solution found after five minutes is of poor quality with a cost increase of almost 60%, while we know this can be at most 4.9% from Table 5.20.

TABLE 5.21: Dynamic model results under progressively stricter CI restrictions for two different locations without the assumption of only one imported hydrogen product.

	Zoetermeer T1-T2-T3-T4 CI $\leq$ 10-8-6-4	Rotterdam T1-T2-T3-T4 CI $\leq$ 10-8-6-4	Zoetermeer T1-T2-T3-T4 CI $\leq$ 8-6-4-2	Rotterdam T1-T2-T3-T4 CI $\leq$ 8-6-4-2
First feasible solution (s)	96	13	3	1
Total running time (s)	300	300	300	300
Optimality gap (%)	35.60	3.74	6.59	5.24
Cost increase (%)	59.32	7.43	9.80	9.80
Chain CO_2 decrease (%)	68.92	19.13	80.76	80.75

Solutions With Starting Solution Finally, we try to find a better solution for Zoetermeer with CI $\leq$ 10-8-6-4 by giving the model a starting solution. As starting solution, we provide a solution that minimizes the chain emissions, which we know for sure satisfies the carbon intensity restrictions. This solution is found in 11 seconds for the dynamic model. Figure 5.6 gives the solution values over time for ten minutes of run time if we do not give the model a start solution. Figure 5.7 shows the same results, but with the start solution. As can be seen, without the starting solution, the model finds after about 100 seconds a solution of around 400 thousand dollars, which gradually improves over time. However, if we give the model a starting solution, the model is able to find a solution of around 300 thousand dollars after about 65 seconds, which is better than the model can find without starting solution in 600 seconds. After 600 seconds, a solution is found that is 22.6% better when using a starting solution. This is an indication that it is useful to provide the model with a feasible starting solution if the solver has trouble finding an initial solution.

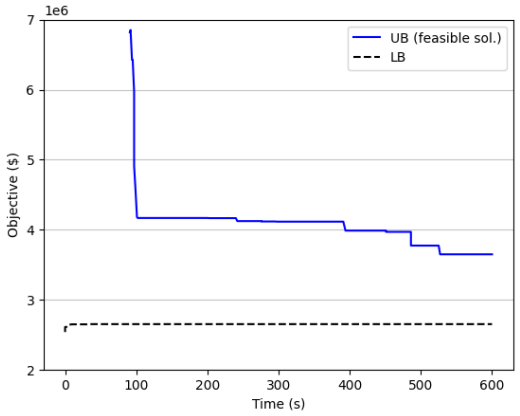

FIGURE 5.6: Upper and lower bound for Zoetermeer, CI $\leq$ 10-8-6-4, without starting solution.

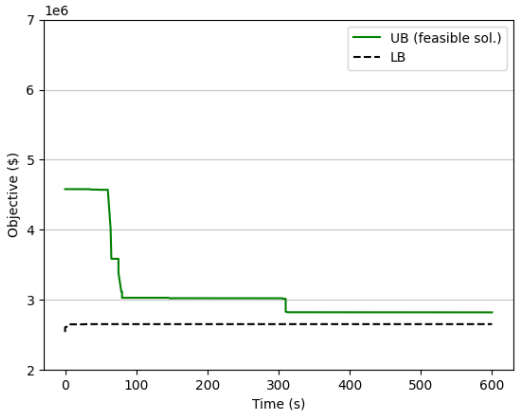

FIGURE 5.7: Upper and lower bound for Zoetermeer, CI $\leq$ 10-8-6-4, with starting solution.

We also provided a starting solution for a case where the initial solution can be found quicker. If we consider the exact same setup, but this time for Rotterdam instead of Zoetermeer, we find that using a starting solution ends up at a solution which is 14.7% worse than when using no starting solution. Using a so-called warm start therefore does not automatically lead to a better solution.

Chapter 6

Conclusion

This thesis aims to incorporate the property of carbon intensity (CI) into energy value chain optimization models. Carbon intensity is a measure of the accumulated emissions in the network that are associated with an energy product, usually expressed in gCO2e/x – grams of CO2-equivalent per volume, mass, or energy content of the product. In this thesis, we present a general modeling framework for a four-tier supply chain network including carbon intensity and carbon capture & storage (CCS), as well as an application on a hydrogen supply chain network case study.

6.1 Main Findings

The first question this thesis tries to answer is the following: *What is the most effective way to model carbon flows in mixed-integer linear programming production and distribution models in the energy value chain optimization domain?* To answer this question, we consider a generic model with supply, production, depot and target nodes, including multiple modes of transport and CCS.

Carbon intensity is included by considering CI variables of a resource (product) at each location. This way, carbon intensity can be tracked throughout the network, and eventually be restricted on the customer side. Balance equations make sure the carbon intensity at a node is the resource-weighted sum of the incoming carbon intensities. Specific constraints involving production processes and fixed carbon emissions at depots are presented as well. Carbon capture & storage is incorporated by including variables for the amount of CO_2 that is captured at a node, as well as binary variables for which level of CCS investment is made. Although carbon emissions at a node are unknown beforehand, this way of modeling allows to incorporate CCS linearly into carbon intensity constraints. Only at production nodes with multiple resources, some nonlinear constraints were needed to incorporate CCS.

Calculating carbon intensities post-optimization after product flows are optimized can be done relatively easily, given a set of rules on how to distribute carbon flows over products. If this is translated to CI restrictions during-optimization, we end up with a nonconvex quadratic optimization problem. The problem is nonconvex, as we have nonlinear equality constraints for carbon balancing. The problem is quadratic or bilinear, because we multiply carbon intensities with product flows to get carbon flows. State-of-the-art solvers are able to solve such problems to optimality. We find that optimal solutions can be found for small data instances where carbon intensities are restricted, provided that the carbon intensity restriction is not too strict. For CI intensity restrictions close to the minimum achievable carbon intensity, the model generally cannot prove what the optimal

solution is as it has to weigh many carbon reduction possibilities. Carbon intensities can much more easily be reduced by linear carbon restrictions defined on the whole supply chain, but those might not target carbon intensities of specific targets effectively. We have tried an alternative formulation using carbon flow variables, but based on the numerical experiments done in this study, neither of the two formulations consistently outperformed the other.

The second research question this thesis aims to answer is: *What is the performance in terms of running time of large models which include restrictions on carbon intensities?* To answer this question, we looked at a case study model from the literature specifically to assess the effect on models of a realistic real-life scale. We include carbon emissions, carbon intensity and CCS in the hydrogen supply chain network optimization model for the Netherlands by Konda et al. (2011). Compared to the cost minimization case, there can be up to eight times as little carbon emissions when we minimize the carbon emissions in the chain. For a static model, we find that CI restrictions on cities that can produce hydrogen have a larger effect on running times than for cities that can only receive hydrogen. If an assumption that only one type of hydrogen product can be imported is loosened, optimal solutions are rarely found within five minutes of running time. This is because there are significantly more options the model has to balance the import of hydrogen from different locations with different carbon intensities. A linear dynamic model reduces the average daily cost by 10.9% compared to a linear static model. Under the emission data that is provided by Konda et al. (2011), we typically find solutions where steam methane reforming plants are built in Rotterdam, and the installation of CCS allows a decrease in carbon intensities. Emissions of transportation have a very minor role compared to emissions from hydrogen production, which makes CCS the best investment to reduce CO_2 emissions in hydrogen supply chains.

More generally, where linear models of about ten thousand variables are able to find the optimal solution in up to two seconds, nonlinear models incorporating CI generally need longer and in some cases do not find optimal solutions within five minutes. For a dynamic model of several tens of thousands of variables, it generally takes up to ten seconds to find the first feasible solution satisfying a CI restriction. For one specific restriction, it took 96 seconds to find the first feasible solution, but this can be improved by providing a warm start with the pure carbon minimization solution which satisfies the CI restriction too. We can conclude that CI can be included in models of realistic scale, provided that the linear base model can be solved to optimality in a reasonable time, such that the nonlinear model most likely will find a feasible but not the optimal solution.

6.2 Discussion & Further Research

Finally, we discuss the work of this thesis and where further research can be performed.

Multi-Resource, Multi-Transport Model In this thesis we have looked at a generic multi-resource, multi-transport (MRMT) supply chain model with CCS components. These models reflect practical optimization models, but cannot incorporate all features that industry models have. Therefore, there remain plenty of challenges in carbon intensity modeling. Moreover, the focus of this thesis was not so much on the accounting aspects. In particular, we have looked at basic allocation rules of carbon flows based on a mass balance. If we consider biofuels in refinery processes, it becomes relevant to also consider energy content balancing. We also did not distinguish CO_2

emissions and more general greenhouse gas or CO_2-equivalent emissions. In addition, there was little focus in this thesis on scope 3 emissions, which is something to study further as there is a high share of scope 3 emissions for hydrocarbon energy sources compared to operational scope 1 and 2 emissions. The carbon flow formulation did not significantly outperform the formulation using CI variables. Other interesting alternatives to study are the Q-formulation and the multi-commodity flow formulation for generalized pooling problems as given by Alfaki and Haugland (2013). These have been shown to outperform the P-formulation for the pooling problem, which indicates it might also be beneficial for the carbon intensity modeling problem. However, these alternatives were not considered in this project as they are hard to generalize to less specific network structures.

Hydrogen Supply Chain Network Model Although the hydrogen case study has provided us with valuable results, one shortcoming of the original study is that the data is somewhat outdated. Today, the market share for low-duty hydrogen vehicles is only expected to be 1% in 2050 (DNV, 2022), which is much less than Konda et al. (2011) predicted back then. Also, the assumptions on production carbon emissions might not be accurate. The emissions for electrolysis assumed by Konda et al. (2011) are quite high, though a large share of electricity is generated from renewable sources nowadays. Also, the emissions for biomass do not reflect the complete life cycle of biomass. Using other emission data might result in completely different solutions, however in this thesis we aimed to stay as close to the paper by Konda et al. (2011) as possible. The run times of the linear case study model were relatively short, though these models consist of tens of thousands of variables and constraints. The model might not be too 'complex' in the sense that steam methane reforming is both the most cost-efficient option as well as the most carbon-efficient option, discarding the other three production technologies. The model still has the potential to be extended with more complexity considering multiple modes of transport (including pipelines), external import of feedstock, storage locations, uncertainty, etc. Also, some sensitivity analysis can be performed based on other factors. For instance, if we know that there is a high employment rate in Groningen, what is the network cost when building a plant in Groningen compared to the mathematically optimal solution that might not decide to build a plant in Groningen? Depending on these cost differences, one can still decide to build a plant in Groningen. These strategic models are usually only performed on a monthly or yearly basis, compared to daily operational models. Therefore, we can allow the solvers to have more running time than the few minutes that were used in this project, although you cannot say beforehand how much the solution quality improves if more hours of running time are provided. Finally, where for the MRMT model we found that linearly restricting subchains resulted in good CI approximations, this was not effective for the hydrogen case study model, as there are no real subchains - each demand location can receive any hydrogen product from any location.

Heuristics As there is little to find in the literature about carbon intensity optimization or restricting cost-to-serve, we would go as far as to say that this thesis can be seen as a starting point for research in the realm of carbon intensity. As seen throughout this thesis, nonlinear models generally find feasible solutions or can even be solved to optimality, but this is only compared to linear models that run in at most a few seconds. Therefore, heuristics can be designed to solve problems of larger scale. Most generally, some search algorithms might be defined to find those model components that have the largest effect on carbon intensity. For each main continuous and integer variable in

the model, we should know the associated carbon emissions. By iteratively putting different linear restrictions on each of the variables, we could end up at a solution satisfying CI restrictions without imposing a nonlinear structure. To iterate between solutions, a variable neighborhood descent structure might be defined. However, heuristics are usually very specific to a problem structure. Therefore, one can also think of heuristics that build solutions from scratch, for example by opening or closing production facilities with a genetic algorithm. In the case of the hydrogen case study, we saw that production emissions account by far for the largest share of total emissions. One idea is the following: first, define all possible technology-size-CCS-location combinations. Then, for one or multiple combinations, define how much production must be realized, such that the total production sums up to the total demand. Assign cities with the strictest carbon intensity restrictions to the production units with the lowest carbon intensities and continue until all cities are connected to production units. Then you can calculate the carbon intensities at the target locations and the total costs of the solution. Continue creating production schedules such that the solution is feasible according to CI restrictions and the costs are as low as possible. Another strategy which we do not recommend as it did not seem to work is fixing the carbon intensities at certain values and then calculating the corresponding network solution. Each solution was found to be very specific to certain CI values, and changing one CI value generally leads to an infeasible solution.

Vision for the Future Decarbonizing industry and accelerating a green economy are some of the most urgent issues of this century. Carbon intensity as a tool is not only relevant in the energy sector, but also in many other sectors like retail, where customers can actively become aware of the emissions that are associated with products they buy. Though the goal of this thesis was to look at carbon intensity restrictions for specific customers, we should keep in mind that under scarce resources a higher global reduction could be achieved if we restrict the carbon emissions of the entire supply chain. We should collaborate to achieve the most efficient decarbonization strategy.

Bibliography

Adhya, N., Tawarmalani, M., & Sahinidis, N. V. (1999). A lagrangian approach to the pooling problem. *Industrial & Engineering Chemistry Research*, *38*(5), 1956–1972.

Ahuja, R. K., Magnanti, T. L., & Orlin, J. B. (1988). Network flows.

Alfaki, M., & Haugland, D. (2013). A multi-commodity flow formulation for the generalized pooling problem. *Journal of Global Optimization*, *56*(3), 917–937.

Alfaki, M., & Haugland, D. (2014). A cost minimization heuristic for the pooling problem. *Annals of Operations Research*, *222*(1), 73–87.

Almansoori, A., & Betancourt-Torcat, A. (2016). Design of optimization model for a hydrogen supply chain under emission constraints - A case study of Germany. *Energy*, *111*, 414–429.

Almansoori, A., & Shah, N. (2009). Design and operation of a future hydrogen supply chain: multi-period model. *International Journal of Hydrogen Energy*, *34*(19), 7883–7897.

Almansoori, A., & Shah, N. (2012). Design and operation of a stochastic hydrogen supply chain network under demand uncertainty. *Int. Journal of Hydrogen Energy*, *37*(5), 3965–3977.

Almansoori, A., & Shah, N. (2006). Design and operation of a future hydrogen supply chain: snapshot model. *Chemical Engineering Research and Design*, *84*(6), 423–438.

Almutairi, H., & Elhedhli, S. (2009). A new lagrangean approach to the pooling problem. *Journal of Global Optimization*, *45*(2), 237–257.

Audet, C., Brimberg, J., Hansen, P., Digabel, S. L., & Mladenović, N. (2004). Pooling problem: Alternate formulations and solution methods. *Management Science*, *50*(6), 761–776.

Baker, T. E., & Lasdon, L. S. (1985). Successive linear programming at Exxon. *Management Science*, *31*(3), 264–274.

Belotti, P., Kirches, C., Leyffer, S., Linderoth, J., Luedtke, J., & Mahajan, A. (2013). Mixed-integer nonlinear optimization. *Acta Numerica*, *22*, 1–131.

Benjaafar, S., Li, Y., & Daskin, M. (2012). Carbon footprint and the management of supply chains: Insights from simple models. *IEEE Transactions on Automation Science and Engineering*, *10*(1), 99–116.

Ben-Tal, A., Eiger, G., & Gershovitz, V. (1994). Global minimization by reducing the duality gap. *Mathematical Programming*, *63*(1), 193–212.

Burer, S., & Letchford, A. N. (2012). Non-convex mixed-integer nonlinear programming: A survey. *Surveys in Operations Research and Management Science*, *17*(2), 97–106.

Calderón, A. J., Agnolucci, P., & Papageorgiou, L. G. (2017). An optimisation framework for the strategic design of synthetic natural gas supply chains. *Applied Energy*, *187*, 929–955.

Cantú, V. H., Azzaro-Pantel, C., & Ponsich, A. (2021). A Novel Matheuristic based on bi-level optimization for the multi-Objective design of hydrogen supply chains. *Computers & Chemical Engineering*, *152*, 107370.

DNV. (2022). Hydrogen Forecast to 2050.

Floudas, C. A., & Aggarwal, A. (1990). A decomposition strategy for global optimum search in the pooling problem. *ORSA Journal on Computing*, *2*(3), 225–235.

Foulds, L. R., Haugland, D., & Jørnsten, K. (1992). A bilinear approach to the pooling problem. *Optimization*, *24*(1-2), 165–180.

Garcia, D. J., & You, F. (2015). Supply chain design and optimization: Challenges and opportunities. *Computers & Chemical Engineering*, *81*, 153–170.

Gong, J., & You, F. (2014). Global optimization for sustainable design and synthesis of algae processing network for CO2 mitigation and biofuel production using life cycle optimization. *AIChE Journal*, *60*(9), 3195–3210.

Gupte, A., Ahmed, S., Dey, S. S., & Cheon, M. S. (2017). Relaxations and discretizations for the pooling problem. *Journal of Global Optimization*, *67*(3), 631–669.

Han, J.-H., Ryu, J.-H., & Lee, I.-B. (2012). Modeling the operation of hydrogen supply networks considering facility location. *International Journal of Hydrogen Energy*, *37*(6), 5328–5346.

Han, J.-H., Ryu, J.-H., & Lee, I.-B. (2013). Multi-objective optimization design of hydrogen infrastructures simultaneously considering economic cost, safety and CO2 emission. *Chemical Engineering Research and Design*, *91*(8), 1427–1439.

Hansen, P., & Jaumard, B. (1992). Reduction of indefinite quadratic programs to bilinear programs. *Journal of Global Optimization*, *2*(1), 41–60.

Kim, J., Lee, Y., & Moon, I. (2008). Optimization of a hydrogen supply chain under demand uncertainty. *International Journal of Hydrogen Energy*, *33*(18), 4715–4729.

Konda, N. M., Shah, N., & Brandon, N. P. (2011). Optimal transition towards a large-scale hydrogen infrastructure for the transport sector: The case for the Netherlands. *International Journal of Hydrogen Energy*, *36*(8), 4619–4635.

Lamb, W. F., Wiedmann, T., Pongratz, J., Andrew, R., Crippa, M., Olivier, J. G., Wiedenhofer, D., Mattioli, G., Al Khourdajie, A., House, J., et al. (2021). A review of trends and drivers of greenhouse gas emissions by sector from 1990 to 2018. *Environmental Research Letters*.

Middleton, R. S., & Bielicki, J. M. (2009). A comprehensive carbon capture and storage infrastructure model. *Energy Procedia*, *1*(1), 1611–1616.

Moreno-Benito, M., Agnolucci, P., & Papageorgiou, L. G. (2017). Towards a sustainable hydrogen economy: Optimisation-based framework for hydrogen infrastructure development. *Computers & Chemical Engineering*, *102*, 110–127.

Moro, A., & Lonza, L. (2018). Electricity carbon intensity in European Member States: Impacts on GHG emissions of electric vehicles. *Transportation Research Part D: Transport and Environment*, *64*, 5–14.

Nie, D., Li, H., Qu, T., Liu, Y., & Li, C. (2020). Optimizing supply chain configuration with low carbon emission. *Journal of Cleaner Production*, *271*, 122539.

Nouira, I., Hammami, R., Frein, Y., & Temponi, C. (2016). Design of forward supply chains: Impact of a carbon emissions-sensitive demand. *International Journal of Production Economics*, *173*, 80–98.

Nunes, P., Oliveira, F., Hamacher, S., & Almansoori, A. (2015). Design of a hydrogen supply chain with uncertainty. *International Journal of Hydrogen Energy*, *40*(46), 16408–16418.

Pörtner, H., Roberts, D., Adams, H., Adler, C., Aldunce, P., Ali, E., Ara Begum, R., Betts, R., Bezner Kerr, R., Biesbroek, R., Birkmann, J., Bowen, K., Castellanos, E., Cissé, G., Constable, A., Cramer, W., Dodman, D., Eriksen, S., Fischlin, A., ... Zaiton Ibrahim, Z. (2022). *Climate change 2022: impacts, adaptation and vulnerability.* IPCC.

Quarton, C. J., & Samsatli, S. (2020). The value of hydrogen and carbon capture, storage and utilisation in decarbonising energy: Insights from integrated value chain optimisation. *Applied Energy*, *257*, 113936.

Quesada, I., & Grossmann, I. E. (1995). Global optimization of bilinear process networks with multicomponent flows. *Computers & Chemical Engineering*, *19*(12), 1219–1242.

Ravi, N. K., Annaland, M. V. S., Fransoo, J. C., Grievink, J., & Zondervan, E. (2017). Development and implementation of supply chain optimization framework for CO2 capture and storage in the Netherlands. *Computers & Chemical Engineering*, *102*, 40–51.

Robles, J. O., Azzaro-Pantel, C., & Aguilar-Lasserre, A. (2020). Optimization of a hydrogen supply chain network design under demand uncertainty by multi-objective genetic algorithms. *Computers & Chemical Engineering*, *140*, 106853.

Ruvalcaba-Sandoval, D. A., Olivares-Benitez, E., Rojas, O., & Sosa-Gómez, G. (2021). Matheuristics for the Design of a Multi-Step, Multi-Product Supply Chain with Multimodal Transport. *Applied Sciences*, *11*(21), 10251.

Samsatli, S., & Samsatli, N. J. (2018). A multi-objective MILP model for the design and operation of future integrated multi-vector energy networks capturing detailed spatio-temporal dependencies. *Applied Energy*, *220*, 893–920.

Seo, S.-K., Yun, D.-Y., & Lee, C.-J. (2020). Design and optimization of a hydrogen supply chain using a centralized storage model. *Applied energy*, *262*, 114452.

Tan, R. R., Aviso, K. B., Bandyopadhyay, S., & Ng, D. K. (2013). Optimal source–sink matching in carbon capture and storage systems with time, injection rate, and capacity constraints. *Environmental Progress & Sustainable Energy*, *32*(2), 411–416.

Tawarmalani, M., & Sahinidis, N. V. (2013). *Convexification and global optimization in continuous and mixed-integer nonlinear programming: theory, algorithms, software, and applications.* (Vol. 65). Springer Science & Business Media.

Woo, Y.-B., & Kim, B. S. (2019). A genetic algorithm-based matheuristic for hydrogen supply chain network problem with two transportation modes and replenishment cycles. *Computers & Industrial Engineering*, *127*, 981–997.

Zamboni, A., Bezzo, F., & Shah, N. (2009). Spatially explicit static model for the strategic design of future bioethanol production systems. 2. Multi-objective environmental optimization. *Energy & Fuels*, *23*(10), 5134–5143.

Zarei, J., Amin-Naseri, M. R., Khorasani, A. H. F., & Kashan, A. H. (2020). A sustainable multi-objective framework for designing and planning the supply chain of natural gas components. *Journal of Cleaner Production*, *259*, 120649.

Zhang, S., Liu, L., Zhang, L., Zhuang, Y., & Du, J. (2018). An optimization model for carbon capture utilization and storage supply chain: A case study in Northeastern China. *Applied Energy*, *231*, 194–206.

Appendix A

Single-Resource, Multi-Transport Model

This appendix presents the single-resource, multi-transport (SRST) model, which is a special case of the multi-resource, multi-transport (MRMT) model. The reader can study this model if they want to start with an easier version of the MRMT model. We refer to Tables 4.1, 4.3 and 4.4 for the notation of the model, which is simplified for this model. In particular, we do not have the set of resources $r \in \mathcal{R}$ as we only consider one resource. Also, the set $p \in \mathcal{P}$ has a slightly different interpretation here: instead of production units and depots, we consider pools, which linearly blend all the resources that come in and produce one outgoing resource. This is in fact the same as a depot for which different streams for the same resource can mix. From the SRST model, it is relatively easy to arrive at the single-resource, single-transport (SRST) model, just by ignoring all indices and summations over $m \in \mathcal{M}$.

A.1 Exact Model Formulation

The following parts are discussed: the basic model without any carbon constraints (A.1.1); calculating carbon intensity post-optimization (A.1.2); incorporating carbon intensities during-optimization (A.1.3); carbon capture and storage (A.1.4); constraining carbon emissions linearly (A.1.5).

A.1.1 Linear Program Without Accounting for Carbon Emissions

If we do not account for any carbon flow calculations and restrictions in the model, we arrive at the MILP model as given in (A.1)-(A.13).

$$\max \quad \boldsymbol{revenue} - \boldsymbol{costs}_{nodes} - \boldsymbol{costs}_{arcs} \tag{A.1}$$

$$\text{s.t.} \quad \boldsymbol{revenue} = \sum_{t \in \mathcal{T}} \sum_{i \in \mathcal{N}(t)^-} \sum_{m \in \mathcal{M}} price_t \cdot \boldsymbol{x}_{itm} \tag{A.2}$$

$$\boldsymbol{costs}_{nodes} = \sum_{i \in S \cup P} \sum_{j \in \mathcal{N}(i)^+} \sum_{m \in \mathcal{M}} cost_i \cdot \boldsymbol{x}_{ijm} \tag{A.3}$$

$$\boldsymbol{cost}_{arcs} = \sum_{(i,j) \in \mathcal{E}} \sum_{m \in \mathcal{M}} cost_{ij} \cdot \boldsymbol{x}_{ijm} \tag{A.4}$$

$$\sum_{j \in \mathcal{N}(s)^+} \sum_{m \in \mathcal{M}} \boldsymbol{x}_{sjm} \geq supply_s^{min} \cdot \boldsymbol{z}_s \qquad s \in \mathcal{S} \tag{A.5}$$

$$\sum_{j\in\mathcal{N}(s)^+}\sum_{m\in\mathcal{M}} \boldsymbol{x}_{sjm} \leq \min\Big\{supply_s^{max}, M\Big\}\cdot \boldsymbol{z}_s \qquad s\in\mathcal{S} \tag{A.6}$$

$$\sum_{i\in\mathcal{N}(p)^-}\sum_{m\in\mathcal{M}} \boldsymbol{x}_{ipm} = \sum_{j\in\mathcal{N}(p)^+}\sum_{m\in\mathcal{M}} \boldsymbol{x}_{pjm} \qquad p\in\mathcal{P} \tag{A.7}$$

$$\sum_{i\in\mathcal{N}(p)^-}\sum_{m\in\mathcal{M}} \boldsymbol{x}_{ipm} \geq through_p^{min}\cdot \boldsymbol{z}_p \qquad p\in\mathcal{P} \tag{A.8}$$

$$\sum_{i\in\mathcal{N}(p)^-}\sum_{m\in\mathcal{M}} \boldsymbol{x}_{ipm} \leq \min\Big\{through_p^{max}, M\Big\}\cdot \boldsymbol{z}_p \qquad p\in\mathcal{P} \tag{A.9}$$

$$\boldsymbol{x}_{ijm} \leq through_{ijm}^{max} \qquad (i,j)\in\mathcal{E}, m\in\mathcal{M} \tag{A.10}$$

$$demand_t^{min} \leq \sum_{i\in\mathcal{N}(t)^-}\sum_{m\in\mathcal{M}} \boldsymbol{x}_{itm} \leq demand_t^{max} \qquad t\in\mathcal{T} \tag{A.11}$$

$$\boldsymbol{x}_{ijm} \geq 0 \qquad (i,j)\in\mathcal{E}, m\in\mathcal{M} \tag{A.12}$$

$$\boldsymbol{z}_i \in \{0,1\} \qquad i\in(S\cup P) \tag{A.13}$$

Objective (A.1) and constraints (A.2)-(A.4) regulate the profit that is maximized. Constraints (A.5) and (A.6) regulate the minimum and maximum supply. The big M that is used is $M = \sum_{t\in\mathcal{T}} demand_t^{max}$. Constraints (A.7) make sure the total flow into a pool equals to total flow out of a pool. Constraints (A.8)-(A.9) regulate the minimum and maximum throughput of the pool. Constraints (A.10) restrict how much flow can go on an arc. Constraints (A.11) make sure the necessary demand is satisfied. Constraints (A.12) and (A.13) specify the domain of the variables.

A.1.2 Calculating Carbon Intensities Post-Optimization

Two options to calculate carbon intensities post-optimization are discussed: using CI variables (Option 1) and carbon flow y variables (Option 2).

Calculation Option 1: Carbon Intensities at the Nodes

$$CI_s := carbon_s \qquad s\in\mathcal{S} \tag{A.14}$$

$$\bar{\boldsymbol{x}}_j := \sum_{i\in\mathcal{N}(j)^-}\sum_{m\in\mathcal{M}} \bar{\boldsymbol{x}}_{ijm} \qquad j\in\mathcal{P}\cup\mathcal{T} \tag{A.15}$$

$$CI_p := \sum_{i\in\mathcal{N}(p)^-}\sum_{m\in\mathcal{M}} \Big((CI_i + carbon_{ipm})\cdot \frac{\bar{\boldsymbol{x}}_{ipm}}{\bar{\boldsymbol{x}}_p}\Big) + carbon_p \qquad p\in\mathcal{P}, \bar{\boldsymbol{x}}_p > 0 \tag{A.16}$$

$$CI_t := \sum_{i\in\mathcal{N}(t)^-}\sum_{m\in\mathcal{M}} \Big((CI_i + carbon_{itm})\cdot \frac{\bar{\boldsymbol{x}}_{itm}}{\bar{\boldsymbol{x}}_t}\Big) \qquad t\in\mathcal{T}, \bar{\boldsymbol{x}}_t > 0 \tag{A.17}$$

Equations (A.14) set the carbon intensity per unit material at the source to its parameter value. Equations (A.15) are a shortcut to calculate the total resource flow going through a pool or target. Equations (A.16) set the carbon intensities at the pooling nodes as a resource-weighted sum of the incoming carbon intensities, plus the carbon emissions per product at the node itself. Equations

(A.17) set the carbon intensities at the target nodes as a resource-weighted sum of the incoming carbon intensities.

Calculation Option 2: Carbon Flows through the Nodes

$$y_{sj} := \sum_{m \in \mathcal{M}} (carbon_s + carbon_{sjm}) \cdot \bar{\boldsymbol{x}}_{sjm} \qquad s \in \mathcal{S}, j \in \mathcal{N}(s)^+ \tag{A.18}$$

$$\bar{\boldsymbol{x}}_j := \sum_{i \in \mathcal{N}(j)^-} \sum_{m \in \mathcal{M}} \bar{\boldsymbol{x}}_{ijm} \qquad j \in \mathcal{P} \cup \mathcal{T} \tag{A.19}$$

$$y_p := \sum_{i \in \mathcal{N}(p)^-} y_{ip} + carbon_p \cdot \bar{\boldsymbol{x}}_p \qquad p \in \mathcal{P} \tag{A.20}$$

$$y_{pj} := \sum_{m \in \mathcal{M}} \left(\frac{y_p}{\bar{\boldsymbol{x}}_i} + carbon_{pjm} \right) \cdot \bar{\boldsymbol{x}}_{pjm} \qquad p \in \mathcal{P}, j \in \mathcal{N}(p)^+, \bar{\boldsymbol{x}}_i > 0 \tag{A.21}$$

$$CI_t := \frac{\sum_{i \in \mathcal{N}(t)^-} y_{it}}{\bar{\boldsymbol{x}}_t} \qquad t \in \mathcal{T}, \bar{\boldsymbol{x}}_t > 0 \tag{A.22}$$

Equations (A.18) calculate the carbon flows on arcs leaving the source nodes. Equations (A.19) are a shortcut to calculate the resource flows through pools and target nodes. Equations (A.20) calculate the total carbon flow into the pool plus the emissions realized at the pool. Equations (A.21) calculate the carbon flows leaving the pooling nodes. Equations (A.22) calculate the carbon intensities at the target nodes.

A.1.3 Optimizing Carbon Intensities During-Optimization

To restrict carbon intensities during-optimization, we use nonlinear balance constraints at the nodes. We again consider two options: using CI variables (Option 1) and carbon flow y variables (Option 2), which we both discuss.

Optimization Option 1: Carbon Intensity Balance Equations

$$\boldsymbol{CI}_s = carbon_s \qquad s \in \mathcal{S} \tag{A.23}$$

$$\boldsymbol{CI}_p \sum_{i \in \mathcal{N}(p)^-} \sum_{m \in \mathcal{M}} \boldsymbol{x}_{ipm} = \sum_{i \in \mathcal{N}(p)^-} \sum_{m \in \mathcal{M}} (\boldsymbol{CI}_i + carbon_{ipm} + carbon_p) \cdot \boldsymbol{x}_{ipm} \qquad p \in \mathcal{P} \tag{A.24}$$

$$\boldsymbol{CI}_t \sum_{i \in \mathcal{N}(t)^-} \sum_{m \in \mathcal{M}} \boldsymbol{x}_{itm} = \sum_{i \in \mathcal{N}(t)^-} \sum_{m \in \mathcal{M}} (\boldsymbol{CI}_i + carbon_{itm}) \cdot \boldsymbol{x}_{itm} \qquad t \in \mathcal{T} \tag{A.25}$$

$$\boldsymbol{CI}_t \leq CI_t^{max} \qquad t \in \mathcal{T} \tag{A.26}$$

Constraints (A.23) set the carbon intensity per unit material at the source to its parameter value. Constraints (A.24) regulate the carbon intensity balancing at the pools. Notice that these constraints contain bilinear terms. Both the left-hand side and the right-hand side consider a summation over the incoming carbon flow at a pool, but as incoming and outgoing flow are equal, one can also consider a summation over outgoing flow. Constraints (A.25) calculate the total carbon intensities at the target nodes. Constraints (A.26) restrict the carbon intensities at the targets.

Optimization Option 2: Carbon Flow Balance Equations

$$\boldsymbol{y}_{sj} = \sum_{m \in \mathcal{M}} (carbon_s + carbon_{ijm}) \cdot \boldsymbol{x}_{sjm} \qquad s \in \mathcal{S}, j \in \mathcal{N}(s)^+ \tag{A.27}$$

$$\boldsymbol{x}_j = \sum_{i \in \mathcal{N}(j)^-} \sum_{m \in \mathcal{M}} \boldsymbol{x}_{ijm} \qquad j \in \mathcal{P} \cup \mathcal{T} \tag{A.28}$$

$$\boldsymbol{y}_p = \sum_{i \in \mathcal{N}(p)^-} \boldsymbol{y}_{ip} + carbon_p \cdot \boldsymbol{x}_p \qquad p \in \mathcal{P} \tag{A.29}$$

$$\boldsymbol{y}_{pj} \cdot \boldsymbol{x}_p = \boldsymbol{y}_p \sum_{m \in \mathcal{M}} \boldsymbol{x}_{pjm} + \sum_{m \in \mathcal{M}} carbon_{pjm} \cdot \boldsymbol{x}_{pjm} \cdot \boldsymbol{x}_p \qquad p \in \mathcal{P}, j \in \mathcal{N}(p)^+ \tag{A.30}$$

$$\boldsymbol{y}_t = \sum_{i \in \mathcal{N}(t)^-} \boldsymbol{y}_{it} \qquad t \in \mathcal{T} \tag{A.31}$$

$$\boldsymbol{y}_t \leq CI_t^{max} \cdot \boldsymbol{x}_t \qquad t \in \mathcal{T} \tag{A.32}$$

Constraints (A.27) calculate the carbon flow on arcs leaving the source nodes. Constraints (A.28) calculate the resource flow going through a pool or target. Constraints (A.29) calculate the total carbon flow going into a pool plus the emissions at the pooling node itself. Constraints (A.30) determine the carbon flows on the arcs leaving the pools. Notice that these constraints contain bilinear terms. Constraints (A.31) calculate the carbon flow entering the demand nodes. Constraints (A.32) restrict carbon flows according to carbon intensity restrictions.

A.1.4 Carbon Capture & Storage Constraints

To allow for the option of carbon capture & storage, add constraints (A.33)-(A.37) to the model.

$$\boldsymbol{c}_p \leq carbon_p \cdot \boldsymbol{x}_p \qquad p \in \mathcal{P}' \tag{A.33}$$

$$\boldsymbol{c}_p \leq \sum_{l \in \mathcal{L}} capture_{pl}^{max} \cdot \boldsymbol{z}_{pl} \qquad p \in \mathcal{P}' \tag{A.34}$$

$$\sum_{l \in \mathcal{L}} \boldsymbol{z}_{pl} \leq 1 \qquad p \in \mathcal{P}' \tag{A.35}$$

$$\boldsymbol{c}_p \geq 0 \qquad p \in \mathcal{P}' \tag{A.36}$$

$$\boldsymbol{z}_{pl} \in \{0, 1\} \qquad p \in \mathcal{P}', l \in \mathcal{L} \tag{A.37}$$

Constraints (A.33) make sure the captured carbon is not more than the emissions that are actually emitted at the pool. Constraints (A.34) ensure that either nothing is captured if no investment is made, and otherwise no more than the allowed capacity is captured for the chosen investment. Constraints (A.35) allow for at most one CCS investment per node. Constraints (A.36) and (A.37) specify the domain of the CCS variables.

Some adaptations to the previously mentioned equations have to be made to include CCS as a decision option. A new CCS cost equation (A.38) should be added to the total cost calculations as in the objective (A.1).

$$\boldsymbol{costs}_{CCS} = \sum_{p \in \mathcal{P}'} \sum_{l \in \mathcal{L}} install_{pl} \cdot \boldsymbol{z}_{pl} \tag{A.38}$$

Equations (A.16) should be replaced by Equations (A.39) for $p \in \mathcal{P}'$.

$$CI_p := \sum_{i \in \mathcal{N}(p)^-} \sum_{m \in \mathcal{M}} \left((CI_i + carbon_{ipm}) \cdot \frac{\bar{\boldsymbol{x}}_{ipm}}{\bar{\boldsymbol{x}}_p} \right) + carbon_p - \frac{\bar{\boldsymbol{c}}_p}{\bar{\boldsymbol{x}}_p} \qquad p \in \mathcal{P}', \bar{\boldsymbol{x}}_p > 0 \tag{A.39}$$

Equations (A.20) should be replaced by Equations (A.40) for $p \in \mathcal{P}'$.

$$y_p := \sum_{i \in \mathcal{N}(p)^-} \sum_{m \in \mathcal{M}} y_{ipm} + carbon_p \cdot \bar{\boldsymbol{x}}_p - \bar{\boldsymbol{c}}_p \qquad p \in \mathcal{P}' \tag{A.40}$$

Constraints (A.24) should be replaced by Equations (A.41) for $p \in \mathcal{P}'$.

$$\boldsymbol{CI}_p \sum_{i \in \mathcal{N}(p)^-} \sum_{m \in \mathcal{M}} \boldsymbol{x}_{ipm} = \sum_{i \in \mathcal{N}(p)^-} \sum_{m \in \mathcal{M}} (\boldsymbol{CI}_i + carbon_{ipm} + carbon_p) \cdot \boldsymbol{x}_{ipm} - \boldsymbol{c}_p \quad p \in \mathcal{P}' \tag{A.41}$$

Constraints (A.29) should be replaced by Equations (A.42) for $p \in \mathcal{P}'$.

$$\boldsymbol{y}_p = \sum_{i \in \mathcal{N}(p)^-} \boldsymbol{y}_{ip} + carbon_p \cdot \boldsymbol{x}_p - \boldsymbol{c}_p \qquad p \in \mathcal{P}' \tag{A.42}$$

A.1.5 Constraining Total Carbon Emissions Linearly

Adding equations (A.43)-(A.47) allows to put linear restrictions on the total amount of carbon emitted in the whole supply chain. Note that for CCS in equations (A.45), we actually multiply it by -1 to subtract the amount of CO_2 captured.

$$\boldsymbol{emissions}_{sources} = \sum_{s \in \mathcal{S}} \sum_{j \in \mathcal{N}(s)^+} \sum_{m \in \mathcal{M}} carbon_s \cdot \boldsymbol{x}_{sjm} \tag{A.43}$$

$$\boldsymbol{emissions}_{pools} = \sum_{p \in \mathcal{P}} \sum_{i \in \mathcal{N}(p)^-} \sum_{m \in \mathcal{M}} carbon_p \cdot \boldsymbol{x}_{ipm} \tag{A.44}$$

$$\boldsymbol{emissions}_{CCS} = -1 \cdot \sum_{p \in \mathcal{P}'} \boldsymbol{c}_p \tag{A.45}$$

$$\boldsymbol{emissions}_{transport} = \sum_{(i,j) \in \mathcal{E}} \sum_{m \in \mathcal{M}} carbon_{ijm} \cdot \boldsymbol{x}_{ijm} \tag{A.46}$$

$$\sum_{loc \in \{sources, pools, CCS, transport\}} \boldsymbol{emissions}_{loc} \leq emissions^{max} \tag{A.47}$$

Appendix B

Hydrogen Case Study: Full Model

This appendix presents the modeling framework for the hydrogen case study, which we largely base on the setup by Konda et al. (2011). As Konda et al. (2011) do not present a mathematical model, the actual mathematical formulations are based on the work by Almansoori and Shah (2006) and Almansoori and Shah (2009). We first present a static variant of the model in Section B.1 which optimizes the hydrogen supply chain network (HSCN) for one demand period. Then, we present the dynamic model in Section B.2 solving the HSCN for four time periods. The notation in these models is completely separate from the MRMT model as presented in Chapter 4.1.

B.1 Static Model

We first discuss the static model mainly based on the model by Almansoori and Shah (2006).

B.1.1 Indices, Sets, Parameters and Variables

The model consists of a set of grids $\mathcal{G}$, which are in our case cities in the Netherlands. In earlier papers, the map of the United Kingdom was split into several block grids, explaining the name grid, which we keep as notation. Each grid has a certain daily hydrogen demand. These can be different physical types of hydrogen, presented in the set $\mathcal{I}$. Hydrogen is produced at plants from the set $\mathcal{P}$, which are plants that technologically produce hydrogen in different ways. Each plant has a size and the option for CCS, and for ease of notation, we collect all those decisions in one set $\mathcal{P}$, which consists of technology-size-CCS triples. Additionally, a set of feedstock used by plants in $\mathcal{P}$ can be defined, but as we do not restrict feedstock availability, we can simplify by considering cost and carbon data of feedstock under the set $\mathcal{P}$. Finally, the set $\mathcal{L}$ presents the set of transportation modes. Table B.1 presents the full set of indices and sets for the static HSCN model.

Table B.1: Indices and sets of the hydrogen case study model.

Index & Set	Description
$g \in \mathcal{G}$	grid square or location;
$g' \in \mathcal{G}$	also a grid square;
$i \in \mathcal{I}$	physical form of hydrogen product;
$p \in \mathcal{P}$	plant type with corresponding technology, size and CCS decision;
$l \in \mathcal{L}$	type of transportation mode.

Table B.2 presents the full list of parameters for the static HSCN model.

TABLE B.2: Parameters of the hydrogen case study model.

Parameter	Description
CCF	capital charge factor, defined as the length of the time period (years);
$CCSCost$	cost of capturing CO_2 by CCS (\$/ton CO_2);
$CCSEF$	efficiency of CCS as the percentage of CO_2 that can be captured (%);
CI_{pi}^{Start}	start CI values of plant type p producing product i (ton CO_2/ton H_2);
CI_{ig}^{max}	maximum allowed CI of product i at grid g;
CI_{g}^{max}	maximum average allowed CI of all hydrogen products at grid g;
$CO2_{p}^{Feed}$	CO_2 emissions from feedstock preparation for plant p (ton CO_2/ton H_2);
$CO2_{pi}^{Prod}$	CO_2 emissions from production for plant p producing product i (ton CO_2/ton H_2);
$CO2^{Trans}$	CO_2 transportation emissions per distance driven (ton CO_2/km);
D_g^T	daily demand for hydrogen in grid g in some time period (ton H_2/day);
DW_l	driver wage of transportation mode l (\$/h);
FE_l^{within}	fuel economy mode l *within* a grid (km/L diesel);
$FE_l^{between}$	fuel economy mode l *between* grids (km/L diesel);
FP_l	fuel price of transportation mode l (\$/L diesel);
FSP_p	feedstock price for the main feedstock needed for plant p (\$/ton or \$/MWh);
GE_l	general expenses of transportation mode l (\$/day/vehicle);
$L_{lgg'}$	average delivery distance between grids g and g' by transportation mode l (km/trip)[1];
LUT_l	load/unload time for transportation mode l (h/trip);
ME_l	maintenance expenses of transportation mode l (\$/km);
$PCap_{pi}^{min}$	minimum production capacity of plant p for product form i (ton H_2/day);
$PCap_{pi}^{max}$	maximum production capacity of plant p for product form i (ton H_2/day);
PCC_{pi}	capital cost of establishing plant type p producing product form i (\$/plant);
PCR_p	production conversation rate out of main feedstock at plant p (ton feed/ton H_2 or MWh/ton H_2);
Q_{il}^{min}	minimum product flow of product i by transportation mode l (ton H_2/day);
Q_{il}^{max}	maximum product flow of product i by transportation mode l (ton H_2/day);
SP_l^{within}	average speed of transportation mode l *within* a grid (km/h);
$SP_l^{between}$	average speed of transportation mode l *between* grids (km/h);
$TCap_{il}$	capacity of transportation mode l transporting product form i (ton H_2/trip);
TMA_l	availability of transportation mode l (h/day);
TMC_{il}	capital cost of establishing transportation mode l transporting product form i (\$/vehicle);
TCE^{max}	maximum allowed total chain emissions (ton CO_2/day);
UPC_{pi}	unit production cost for product form i produced by plant type p (\$/ton H_2);
α	network operating period (days/year);
$\mathbb{1}_{ig}^{Prod}$	1 if product i can be produced in grid g, 0 otherwise;
$\mathbb{1}_{p}^{CCS}$	1 if plant p is a CCS plant, 0 otherwise.

[1] $L_{lgg'}$ is defined such that for $g' = g$ the parameter equals the estimated travel distance *within* a grid for mode l.

Table B.3 presents the full list of variables for the static HSCN model.

TABLE B.3: Variables of the case study model.

Variable	Description
	Continuous operational variables:
$\boldsymbol{D}_{ig}^{L}$	demand product i in grid g satisfied by *local* production in the same grid (ton H_2/day);
$\boldsymbol{D}_{ig}^{I}$	demand product i in grid g satisfied by *imported* production from another grid (ton H_2/day);
$\boldsymbol{P}_{pig}$	amount daily produced of product i from plant type p in grid g (ton H_2/day);
$\boldsymbol{P}_{ig}^{T}$	total daily production of product i in grid g (ton H_2/day);
$\boldsymbol{Q}_{ilgg'}$	daily amount of product i between grid g and g' per day using mode l (ton H_2/day)[1];
$\boldsymbol{NOT}_{ilgg'}$	number of trips daily of product i transported by mode l between grid g and g';
	Continuous cost variables:
$\boldsymbol{FC}$	fuel cost ($/day);
$\boldsymbol{FCC}$	facility capital cost ($);
$\boldsymbol{FOC}$	facility operating cost ($/day);
$\boldsymbol{FSC}$	feedstock cost ($/day);
$\boldsymbol{GC}$	general cost ($/day);
$\boldsymbol{LC}$	labor cost ($/day);
$\boldsymbol{MC}$	maintenance cost ($/day);
$\boldsymbol{TCC}$	transportation capital cost ($);
$\boldsymbol{TDC}$	total daily cost network ($/day);
$\boldsymbol{TOC}$	transportation operating cost ($/day);
	Continuous CO_2 variables:
$\boldsymbol{CI}_{ig}^{Plants}$	CI of the plants producing product i in grid g (ton CO_2/ton H_2);
$\boldsymbol{CI}_{ig}^{Prod}$	CI of product i satisfied at the customer in grid g due to production (ton CO_2/ton H_2);
$\boldsymbol{CI}_{ig}^{Trans}$	CI of product i satisfied at the customer in grid g due to transportation (ton CO_2/ton H_2);
$\boldsymbol{CI}_{ig}$	CI of product i satisfied at the customer in grid g (ton CO_2/ton H_2);
$\boldsymbol{CI}_{g}$	average CI of all products satisfied at the customer in grid g (ton CO_2/ton H_2);
$\boldsymbol{TCE}^{Feed}$	total feedstock emissions (ton CO_2/day);
$\boldsymbol{TCE}^{Prod}$	total production emissions (ton CO_2/day);
$\boldsymbol{TCE}^{Trans}$	total transportation emissions (ton CO_2/day);
$\boldsymbol{TCE}$	total chain emissions (ton CO_2/day);
	Integer variables:
$\boldsymbol{NP}_{pig}$	number of plants of type p producing product form i in grid g;
$\boldsymbol{NTU}_{il}$	number of daily transport units needed of mode l for product i;
	Binary variables:
$\boldsymbol{X}_{ilgg'}$	1 if at least some product i is transported from g to g' using mode l, 0 otherwise;
$\boldsymbol{Y}_{ig}$	1 if product i is exported to another grid from grid g, 0 otherwise;
$\boldsymbol{Z}_{ig}$	1 if product i is imported from another grid into grid g, 0 otherwise.

[1] $\boldsymbol{Q}_{ilgg'}$ is defined such that for $g' = g$ the variable equals the amount of product i satisfied *within* a grid by mode l.

B.1.2 Exact Model

Here we present the exact model formulation. The model is split up into three parts: the operational part, which makes sure that production, transportation and demand match; the cost part, which makes sure it is done in the most cost-efficient way; the CO_2 part, which demonstrates how to calculate total chain emissions and carbon intensities and how to restrict carbon intensity. For a detailed explanation of the operational and cost part, we refer to the paper of Almansoori and Shah (2006). In Section B.1.3, we discuss the changes made to their model. The domains of the variables are not explicitly taken care of in the constraints, as the domains can be seen in Table B.3.

Operational Part Constraints (B.1)-(B.15) present the operational part.

$$\boldsymbol{D}^L_{ig} \leq \boldsymbol{P}^T_{ig} \qquad \forall i, g \text{ if } \mathbb{1}^{Prod}_{ig} = 1 \tag{B.1}$$

$$\boldsymbol{D}^L_{ig} = \sum_{l} \boldsymbol{Q}_{ilgg} \qquad \forall i, g \tag{B.2}$$

$$\boldsymbol{D}^I_{ig} = \sum_{l,g',g' \neq g} \boldsymbol{Q}_{ilg'g} \qquad \forall i, g \tag{B.3}$$

$$D^T_g = \sum_{i} \left(\boldsymbol{D}^L_{ig} + \boldsymbol{D}^I_{ig}\right) \qquad \forall g \tag{B.4}$$

$$\boldsymbol{D}^L_{ig} = \boldsymbol{P}^T_{ig} - \sum_{l,g',g' \neq g} \boldsymbol{Q}_{ilgg'} \qquad \forall i, g \tag{B.5}$$

$$\boldsymbol{P}^T_{ig} = \sum_{p} \boldsymbol{P}_{pig} \qquad \forall i, g \text{ if } \mathbb{1}^{Prod}_{ig} = 1 \tag{B.6}$$

$$PCap^{min}_{pi} \cdot \boldsymbol{NP}_{pig} \leq \boldsymbol{P}_{pig} \leq PCap^{max}_{pi} \cdot \boldsymbol{NP}_{pig} \qquad \forall p, i, g \text{ if } \mathbb{1}^{Prod}_{ig} = 1 \tag{B.7}$$

$$\sum_{p} PCap^{min}_{pi} \cdot \boldsymbol{NP}_{pig} \leq \boldsymbol{P}^T_{ig} \leq \sum_{p} PCap^{max}_{pi} \cdot \boldsymbol{NP}_{pig} \qquad \forall i, g \text{ if } \mathbb{1}^{Prod}_{ig} = 1 \tag{B.8}$$

$$Q^{min}_{il} \cdot \boldsymbol{X}_{ilgg'} \leq \boldsymbol{Q}_{ilgg'} \leq Q^{max}_{il} \cdot \boldsymbol{X}_{ilgg'} \qquad \forall i, l, g, g'; g' \neq g \text{ if } \mathbb{1}^{Prod}_{ig} = 1 \tag{B.9}$$

$$\boldsymbol{X}_{ilgg'} + \boldsymbol{X}_{ilg'g} \leq 1 \qquad \forall i, l, g, g'; g' \neq g \tag{B.10}$$

$$\boldsymbol{Y}_{ig} \geq \boldsymbol{X}_{ilgg'} \qquad \forall i, l, g, g'; g' \neq g \text{ if } \mathbb{1}^{Prod}_{ig} = 1 \tag{B.11}$$

$$\boldsymbol{Z}_{ig} \geq \boldsymbol{X}_{ilg'g} \qquad \forall i, l, g, g'; g' \neq g \tag{B.12}$$

$$\boldsymbol{Y}_{ig} + \boldsymbol{Z}_{ig} \leq 1 \qquad \forall i, g \tag{B.13}$$

$$\sum_{i} \boldsymbol{Z}_{ig} \leq 1 \qquad \forall g \tag{B.14}$$

$$\boldsymbol{D}^L_{ig} = \boldsymbol{P}_{pig} = \boldsymbol{P}^T_{ig} = \boldsymbol{Q}_{ilgg'} = \boldsymbol{NP}_{pig} = \boldsymbol{X}_{ilgg'} = \boldsymbol{Y}_{ig} = 0 \qquad \forall p, i, l, g, g' \text{ if } \mathbb{1}^{Prod}_{ig} = 0 \tag{B.15}$$

Cost Part Constraints (B.16)-(B.28) present the cost part.

$$\boldsymbol{FCC} = \sum_{p,i,g} PCC_{pi} \cdot \boldsymbol{NP}_{pig} \tag{B.16}$$

$$\boldsymbol{FOC} = \sum_{i,g,p} (UPC_{pi} + \mathbb{1}_{p}^{CCS} \cdot CCSCost \cdot CO2Prod_{pi}) \cdot \boldsymbol{P}_{pig} \tag{B.17}$$

$$\boldsymbol{FSC} = \sum_{p} \left(FSP_p \cdot PCR_p \cdot \sum_{i,g} \boldsymbol{P}_{pig} \right) \tag{B.18}$$

$$\boldsymbol{NOT}_{ilgg'} = \frac{\boldsymbol{Q}_{ilgg'}}{TCap_{il}} \quad \forall i, l, g, g' \tag{B.19}$$

$$\boldsymbol{NTU}_{il} \geq \sum_{g,g',g' \neq g} \frac{\boldsymbol{NOT}_{ilgg'}}{TMA_l} \left(\frac{2L_{lgg'}}{SP_l^{between}} + LUT_l \right) + \sum_{g} \frac{\boldsymbol{NOT}_{ilgg}}{TCap_{il} \cdot TMA_l} \left(\frac{2L_{lgg}}{SP_l^{within}} + LUT_1 \right) \quad \forall i, l \tag{B.20}$$

$$\boldsymbol{TCC} = \sum_{i,l} TMC_{il} \cdot \boldsymbol{NTU}_{il} \tag{B.21}$$

$$\boldsymbol{FC} = \sum_{i,l,g,g',g' \neq g} FP_l \left(\frac{2L_{lgg'} \cdot \boldsymbol{Q}_{ilgg'}}{FE_l^{between} \cdot TCap_{il}} \right) + \sum_{i,l,g} FP_l \left(\frac{2L_{lgg} \cdot \boldsymbol{Q}_{ilgg}}{FE_l^{within} \cdot TCap_{il}} \right) \tag{B.22}$$

$$\boldsymbol{LC} = \sum_{i,l,g,g',g' \neq g} DW_l \left(\frac{\boldsymbol{Q}_{ilgg'}}{TCap_{il}} \left(\frac{2L_{lgg'}}{SP_l^{between}} + LUT_l \right) \right) + \sum_{i,l,g} DW_l \left(\frac{\boldsymbol{Q}_{ilgg}}{TCap_{il}} \left(\frac{2L_{lgg}}{SP_l^{within}} + LUT_l \right) \right) \tag{B.23}$$

$$\boldsymbol{MC} = \sum_{i,l,g,g'} ME_l \left(\frac{2L_{lgg'} \cdot \boldsymbol{Q}_{ilgg'}}{TCap_{il}} \right) \tag{B.24}$$

$$\boldsymbol{GC} = \sum_{i,l} GE_l \cdot \boldsymbol{NTU}_{il} \tag{B.25}$$

$$\boldsymbol{TOC} = \boldsymbol{FC} + \boldsymbol{LC} + \boldsymbol{MC} + \boldsymbol{GC} \tag{B.26}$$

$$\boldsymbol{TDC} = \frac{\boldsymbol{FCC} + \boldsymbol{TCC}}{\alpha \cdot CCF} + \boldsymbol{FOC} + \boldsymbol{TOC} + \boldsymbol{FSC} \tag{B.27}$$

$$\min\{\boldsymbol{TDC}\} \tag{B.28}$$

CO_2 Part Constraints (B.29)-(B.33) calculate the total feedstock, production and transportation carbon emissions and put restrictions on the total emissions.

$$\boldsymbol{TCE}^{Feed} = \sum_{p} CO2_{p}^{Feed} \sum_{i,g} \boldsymbol{P}_{pig} \tag{B.29}$$

$$\boldsymbol{TCE}^{Prod} = \sum_{p,i,g} \Big((1 - \mathbb{1}_{p}^{CCS}) \cdot CO2_{pi}^{Prod} + \mathbb{1}_{p}^{CCS} \cdot (1 - CCSEF) \cdot CO2_{pi}^{Prod} \Big) \boldsymbol{P}_{pig} \tag{B.30}$$

$$\boldsymbol{TCE}^{Trans} = CO2^{Trans} \sum_{i,l,g,g'} \boldsymbol{NOT}_{ilgg'} \cdot 2L_{lgg'} \tag{B.31}$$

$$\boldsymbol{TCE} = \boldsymbol{TCE}^{Feed} + \boldsymbol{TCE}^{Prod} + \boldsymbol{TCE}^{Trans} \tag{B.32}$$

$$\boldsymbol{TCE} \leq TCE^{max} \tag{B.33}$$

Constraints (B.34)-(B.41) show how to calculate carbon intensities post-optimization using the existing model variables, using several intermediate steps. $Carbon_{ig}$ and $Carbon_{g}$ represent total emissions, if we multiply by the amount of product satisfied.

$$CI_{pi}^{Start} := \big(CO2_{p}^{Feed} + (1 - \mathbb{1}_{p}^{CCS}) \cdot CO2_{pi}^{Prod} + \mathbb{1}_{p}^{CCS} \cdot (1 - CCSEF) \cdot CO2_{pi}^{Prod} \big) \quad \forall p, i \tag{B.34}$$

$$CI_{ig}^{Plants} := \sum_{p} \frac{\bar{\boldsymbol{P}}_{pig}}{\bar{\boldsymbol{P}}_{ig}^{T}} \cdot CI_{pi}^{Start} \quad \forall i, g \tag{B.35}$$

$$CI_{ig}^{Prod} := \sum_{l,g'} \frac{\bar{\boldsymbol{Q}}_{ilg'g}}{\sum_{l^*,g'^*} \bar{\boldsymbol{Q}}_{il^*g'^*g}} \cdot CI_{ig'}^{Plants} \quad \forall i, g \tag{B.36}$$

$$CI_{ig}^{Trans} := \frac{CO2^{Trans} \sum_{l,g'} \bar{\boldsymbol{NOT}}_{ilg'g} \cdot 2L_{lg'g}}{\bar{\boldsymbol{D}}_{ig}^{L} + \bar{\boldsymbol{D}}_{ig}^{I}} \quad \forall i, g \tag{B.37}$$

$$CI_{ig} := CI_{ig}^{Prod} + CI_{ig}^{Trans} \quad \forall i, g \tag{B.38}$$

$$CI_{g} := \sum_{i} CI_{ig} \cdot \frac{(\bar{\boldsymbol{D}}_{ig}^{L} + \bar{\boldsymbol{D}}_{ig}^{I})}{D_{g}^{T}} \quad \forall g \tag{B.39}$$

$$Carbon_{ig} := CI_{ig} \cdot (\bar{\boldsymbol{D}}_{ig}^{L} + \bar{\boldsymbol{D}}_{ig}^{I}) \quad \forall i, g \tag{B.40}$$

$$Carbon_{g} := CI_{g} \cdot D_{g}^{T} \quad \forall g \tag{B.41}$$

Constraints (B.42)-(B.51) show an option to incorporate carbon intensity during-optimization using balance constraints and restriction constraints. This is inspired by the post-calculation option by multiplying the terms in the denominator on both sides of the equation, resulting in quadratic equality constraints.

$$CI_{pi}^{Start} = \big(CO2_{p}^{Feed} + (1 - \mathbb{1}_{p}^{CCS}) \cdot CO2_{pi}^{Prod} + \mathbb{1}_{p}^{CCS} \cdot (1 - CCSEF) \cdot CO2_{pi}^{Prod} \big) \quad \forall p, i \tag{B.42}$$

$$\boldsymbol{CI}_{ig}^{Plants} \cdot \boldsymbol{P}_{ig}^{T} = \sum_{p} \boldsymbol{P}_{pig} \cdot CI_{pi}^{Start} \quad \forall i, g \tag{B.43}$$

$$\boldsymbol{CI}_{ig}^{Prod} \cdot \sum_{l^*,g'^*} \boldsymbol{Q}_{il^*g'^*g} = \sum_{l,g'} \boldsymbol{Q}_{ilg'g} \cdot \boldsymbol{CI}_{ig'}^{Plants} \quad \forall i,g \tag{B.44}$$

$$\boldsymbol{CI}_{ig}^{Trans} \cdot (\boldsymbol{D}_{ig}^{L} + \boldsymbol{D}_{ig}^{I}) = CO2^{Trans} \sum_{l,g'} \boldsymbol{NOT}_{ilg'g} \cdot 2L_{lg'g} \quad \forall i,g \tag{B.45}$$

$$\boldsymbol{CI}_{ig} = \boldsymbol{CI}_{ig}^{Prod} + \boldsymbol{CI}_{ig}^{Trans} \quad \forall i,g \tag{B.46}$$

$$\boldsymbol{CI}_{g} = \sum_{i} \boldsymbol{CI}_{ig} \cdot (\boldsymbol{D}_{ig}^{L} + \boldsymbol{D}_{ig}^{I}) \cdot \frac{1}{D_g^T} \quad \forall g \tag{B.47}$$

$$\boldsymbol{CI}_{ig} \leq CI_{ig}^{max} \quad \forall i,g \tag{B.48}$$

$$\boldsymbol{CI}_{g} \leq CI_{g}^{max} \quad \forall g \tag{B.49}$$

$$\boldsymbol{CI}_{ig}^{Plants} = 0 \quad \forall i,g \text{ if } \mathbb{1}_{ig}^{Prod} = 0 \tag{B.50}$$

$$\boldsymbol{CI}_{ig} = \boldsymbol{CI}_{g} = 0 \quad \forall i,g \text{ if } D_g^T = 0 \tag{B.51}$$

B.1.3 Model Changes and Assumptions

The model is based on the framework by Konda et al. (2011) and is mainly based on the formulation by Almansoori and Shah (2006). However, some changes are made to accompany the setup and to add carbon emissions. These are explained here:

- The parameter D_{ig} is replaced by D_g, as for customers it does not matter whether they receive CH_2, LH_2 or both, as long as they receive some type of hydrogen. This is the same in the data by Almansoori and Shah (2006), but still they defined a variable D_{ig}, presumably for the generality of the model. As a consequence, constraints (B.4) and (B.5) are adapted.
- Almansoori and Shah (2006) are not very specific about the definition of $\boldsymbol{Q}_{ilgg'}$ for $g' = g$. Therefore, we define it as the locally satisfied demand of product i with mode l, making $L_{lgg'}$ for $g' = g$ the average distance traveled within a grid. Consequently, constraints (B.2) are added to define $\boldsymbol{Q}_{ilgg}$. Also constraints (B.20), (B.22) and (B.23) are adapted, additionally taking into account $SP_l^{between}$, SP_l^{within}, $FE_l^{between}$ and $FE_l^{between}$.
- Constraints (B.14) are added to make sure only one type of hydrogen product is imported in each grid. This assumption can be dropped for example if you consider multiple fueling stations per grid, but it improves the speed of the model. It still allows having both products satisfied in a grid that produces hydrogen. In this report, we show results both with and without this constraint.
- Almansoori and Shah (2006) consider storage facilities, as they consider the United Kingdom, which is larger than the Netherlands. However, as the Netherlands studied by Konda et al. (2011) is sufficiently small, storage facilities are not considered here.
- As given in the data by Konda et al. (2011), plants can only be built on a subset of locations. To reflect that, we introduce parameter $\mathbb{1}_{ig}^{Prod}$, which is used in constraints (B.1), (B.6), (B.7), (B.8), (B.9), (B.11) and (B.15).
- Almansoori and Shah (2006) use the variable $\boldsymbol{NTU}$ as the number of transportation units. However, as we have different costs for different transportation units, we extend this variable

to the variables $\boldsymbol{NTU}_{il}$. Consequently, constraints (B.20)-(B.21) are changed. These $\boldsymbol{NTU}_{il}$ variables actually serve as an underestimation of the number of units needed, assuming vehicles can perfectly route all (partial) trips, where $\boldsymbol{NTU}_{ilgg}$ would be an overestimation, as that assumes vehicles must only drive on one (g, g') route. We will use the underestimation, as we have a strategic model, thus our goal is not to solve a corresponding operational vehicle routing problem. To account for carbon emissions, we explicitly use a variable for the number of trips $\boldsymbol{NOT}_{ilgg}$ between grids.

- While Konda et al. (2011) use a power equation for $\boldsymbol{FOC}$ and take $\boldsymbol{FFC}$ as a percentage of $\boldsymbol{FOC}$, we fix $\boldsymbol{FCC}$ based on the average size of the plant and introduce a unit production cost $\boldsymbol{UPC}$ as used in Almansoori and Shah (2009).
- Scenarios from Konda et al. (2011) are not incorporated, as well as forecourt production and refueling stations.
- On top of Almansoori and Shah (2006), parameters for feedstock cost FSP_p and production conversation rate PCR_p are added to calculate the feedstock costs $\boldsymbol{FSC}$ in constraint (B.18).
- The carbon emission parameters $CO2_p^{Feed}$, $CO2_{pi}^{Prod}$ and $CO2^{Trans}$, the carbon intensity parameters CI_{pi}^{Start}, CI_{ig}^{max} and CI_g^{max} and the CCS parameters $CCSCost$, $CCSEF$ and $\mathbb{1}_p^{CCS}$ are added to the model. Variables $\boldsymbol{TCE}^{Feed}$, $\boldsymbol{TCE}^{Prod}$, $\boldsymbol{TCE}^{Trans}$ and $\boldsymbol{TCE}$ are added to reflect carbon emissions and variables $\boldsymbol{CI}_{ig}^{Plants}$, $\boldsymbol{CI}_{ig}^{Prod}$, $\boldsymbol{CI}_{ig}^{Trans}$, $\boldsymbol{CI}_{ig}$ and $\boldsymbol{CI}_g$ to reflect carbon intensities. CO_2 constraints (B.29)-(B.51) are added and constraint (B.17) is adapted to account for CCS.
- Carbon intensity is defined as CI_{ig}, which is the carbon intensity of product i at grid g. If a customer does not receive some product i, the corresponding CI is assumed to be 0. As the HSCN model is on a higher level than the MRMT model, i.e., we work with plants in grids rather than explicit locations of grids, some more generalized assumptions are made. This includes how carbon intensity is 'averaged' over different plants. This is where CI_{ig}^{Plants} comes in place. We assume that different plants p producing the same product i in grid g have an averaged CI. Therefore, it might happen that one customer is served by an SMR-CH_2-CCS plant to have a low CI, while other customers are served by an SMR-LH_2 plant in the same grid with a lower cost but higher CI. However, if we would have an SMR-CH_2-CCS and SMR-CH_2 plant in the same grid, the carbon intensity of both would be averaged. This could be changed by defining the carbon intensity of plants as CI_{pig}^{Plants}, but this also requires a variable $Q_{pilgg'}$, which is not implemented in the model by Almansoori and Shah (2006) and requires a lot more variables.

B.2 Dynamic Model

The dynamic model, where we optimize the four time periods simultaneously, has a lot of resemblances with the static model. The approach taken here is different than the time period model of Almansoori and Shah (2009), in particular the time periods are incorporated in a simpler manner. First we discuss how the indices, sets, parameters and variables change compared to the static model, after which we present the complete mathematical formulation.

B.2.1 Indices, Sets, Parameters and Variables

Compared to the static model, we only need one new index and set for the dynamic model, which is time period t in the set of time periods $\mathcal{T}$. To optimize over time periods, we need to define the parameters NP^0_{pig}, the initial number of plants of type p producing product i in grid g, and NTU^0_{il}, the initial number of transportation units of mode l for product i. Every variable from Table B.3 gets an additional time index t. Next to the new variables $\boldsymbol{TDC}_t$ and $\boldsymbol{TCE}_t$, we also keep the variables $\boldsymbol{TDC}$ and $\boldsymbol{TCE}$, such that we can calculate and optimize over the entire time horizon. We also introduce the variables $\boldsymbol{IP}_{pigt} \in \mathbb{N}$ (Investment Plants), indicating the number of new plants built of type p producing product i in grid g at time period t. Variables $\boldsymbol{ITU}_{ilt} \in \mathbb{N}$ (Investment Transportation Units) represent how many new transportation units of type i and mode l are bought in period t. For the dynamic model, we assume plants do not have a minimum capacity. This allows building larger plants in earlier time periods. An alternative strategy is to allow plant upgrades between time periods, for instance from a small to a medium plant. However, this asks for much more variables, as we should account for every possible upgrade. Therefore, we only assume that plants can be upgraded with CCS between time periods. We introduce the variables $\boldsymbol{UP}^{CCS}_{p'igt} \in \mathbb{N}$ (Upgrade Plants), which is 1 if plant p' producing product i in grid g is upgraded with CCS in time period t, 0 otherwise. The index p' is a specific case of p, which indicates the production technology and the size, but not whether CCS is implemented. There is no fixed upgrade cost for CCS, however upgrading with CCS does increase the unit production cost.

B.2.2 Exact Model

We present the exact formulation of the dynamic HSCN model.

Operational Part Constraints (B.52)-(B.69) present the operational part of the dynamic HSCN model. Constraints (B.66)-(B.68) make sure previously built plants remain operational in later time periods, possibly with an upgrade of CCS.

$$\boldsymbol{D}^L_{igt} \leq \boldsymbol{P}^T_{igt} \qquad \forall i, g, t \text{ if } \mathbb{1}^{Prod}_{ig} = 1 \tag{B.52}$$

$$\boldsymbol{D}^L_{igt} = \sum_l \boldsymbol{Q}_{ilggt} \qquad \forall i, g, t \tag{B.53}$$

$$\boldsymbol{D}^I_{igt} = \sum_{l, g', g' \neq g} \boldsymbol{Q}_{ilg'gt} \qquad \forall i, g, t \tag{B.54}$$

$$D^T_{gt} = \sum_i \left(\boldsymbol{D}^L_{igt} + \boldsymbol{D}^I_{igt}\right) \qquad \forall g, t \tag{B.55}$$

$$\boldsymbol{D}^L_{igt} = \boldsymbol{P}^T_{igt} - \sum_{l,g',g'\neq g} \boldsymbol{Q}_{ilgg't} \qquad \forall i,g,t \tag{B.56}$$

$$\boldsymbol{P}^T_{igt} = \sum_p \boldsymbol{P}_{pigt} \qquad \forall i,g,t \text{ if } \mathbb{1}^{Prod}_{ig}=1 \tag{B.57}$$

$$PCap^{min}_{pi} \cdot \boldsymbol{NP}_{pigt} \leq \boldsymbol{P}_{pigt} \leq PCap^{max}_{pi} \cdot \boldsymbol{NP}_{pigt} \qquad \forall p,i,g,t \text{ if } \mathbb{1}^{Prod}_{ig}=1 \tag{B.58}$$

$$\sum_p PCap^{min}_{pi} \cdot \boldsymbol{NP}_{pigt} \leq \boldsymbol{P}^T_{igt} \leq \sum_p PCap^{max}_{pi} \cdot \boldsymbol{NP}_{pigt} \qquad \forall i,g,t \text{ if } \mathbb{1}^{Prod}_{ig}=1 \tag{B.59}$$

$$Q^{min}_{il} \cdot \boldsymbol{X}_{ilgg't} \leq \boldsymbol{Q}_{ilgg't} \leq Q^{max}_{il} \cdot \boldsymbol{X}_{ilgg't} \qquad \forall i,l,g,g',t; g'\neq g \text{ if } \mathbb{1}^{Prod}_{ig}=1 \tag{B.60}$$

$$\boldsymbol{X}_{ilgg't} + \boldsymbol{X}_{ilg'gt} \leq 1 \qquad \forall i,l,g,g',t; g'\neq g \tag{B.61}$$

$$\boldsymbol{Y}_{igt} \geq \boldsymbol{X}_{ilgg't} \qquad \forall i,l,g,g',t; g'\neq g \text{ if } \mathbb{1}^{Prod}_{ig}=1 \tag{B.62}$$

$$\boldsymbol{Z}_{igt} \geq \boldsymbol{X}_{ilg'gt} \qquad \forall i,l,g,g',t; g'\neq g \tag{B.63}$$

$$\boldsymbol{Y}_{igt} + \boldsymbol{Z}_{igt} \leq 1 \qquad \forall i,g,t \tag{B.64}$$

$$\sum_i \boldsymbol{Z}_{igt} \leq 1 \qquad \forall g,t \tag{B.65}$$

$$\boldsymbol{NP}_{pigt_1} = \boldsymbol{NP}^0_{pig} + \boldsymbol{IP}_{pigt_1} \qquad \forall p,i,g \tag{B.66}$$

$$\boldsymbol{NP}_{pigt} = \boldsymbol{NP}_{pig(t-1)} + \boldsymbol{IP}_{pigt} - \boldsymbol{UP}^{CCS}_{p'igt} \qquad \forall p,\, p'\subseteq p,i,g,t\neq t_1 \text{ if } \mathbb{1}^{CCS}_{p}=0 \tag{B.67}$$

$$\boldsymbol{NP}_{pigt} = \boldsymbol{NP}_{pig(t-1)} + \boldsymbol{IP}_{pigt} + \boldsymbol{UP}^{CCS}_{p'igt} \qquad \forall p,\, p'\subseteq p,i,g,t\neq t_1 \text{ if } \mathbb{1}^{CCS}_{p}=1 \tag{B.68}$$

$$\boldsymbol{D}^L_{igt}=\boldsymbol{P}_{pigt}=\boldsymbol{P}^T_{igt}=\boldsymbol{Q}_{ilgg't}=\boldsymbol{NP}_{pigt}=\boldsymbol{IP}_{pigt}=\boldsymbol{UP}^{CCS}_{p'igt}=\boldsymbol{X}_{ilgg't}=\boldsymbol{Y}_{igt}=0 \qquad \forall p,\, p'\subseteq p,i,l,g,g',t \text{ if } \mathbb{1}^{Prod}_{ig}=0 \tag{B.69}$$

Cost Part Constraints (B.70)-(B.88) present the cost part of the dynamic HSCN model. Constraints (B.75)-(B.76) make sure previously acquired transportation units remain available; constraints (B.77)-(B.78) define if and how many new transportation units should be acquired.

$$\boldsymbol{FCC}_{t_1} = \sum_{p,i,g} PCC_{pi} \cdot NP^0_{pig} + \sum_{p,i,g} PCC_{pi} \cdot \boldsymbol{IP}_{pigt_1} \tag{B.70}$$

$$\boldsymbol{FCC}_{t} = \sum_{p,i,g} PCC_{pi} \cdot \boldsymbol{IP}_{pigt} \quad \forall t\neq t_1 \tag{B.71}$$

$$\boldsymbol{FOC}_t = \sum_{i,g,p} (UPC_{pi} + \mathbb{1}^{CCS}_{p} \cdot CCSCost \cdot CO2Prod_{pi}) \cdot \boldsymbol{P}_{pigt} \quad \forall t \tag{B.72}$$

$$\boldsymbol{FSC}_t = \sum_p \left(FSP_p \cdot PCR_p \cdot \sum_{i,g} \boldsymbol{P}_{pigt} \right) \quad \forall t \tag{B.73}$$

$$\boldsymbol{NOT}_{ilgg't} = \frac{\boldsymbol{Q}_{ilgg't}}{TCap_{il}} \quad \forall i,l,g,g',t \tag{B.74}$$

$$\boldsymbol{NTU}_{ilt_1} = NTU^0_{il} + \boldsymbol{ITU}_{ilt_1} \quad \forall i,l \tag{B.75}$$

$$\boldsymbol{NTU}_{ilt} = \boldsymbol{NTU}_{il(t-1)} + \boldsymbol{ITU}_{ilt} \quad \forall i, l, t \neq t_1 \tag{B.76}$$

$$\boldsymbol{ITU}_{ilt_1} \geq \sum_{g,g',g' \neq g} \frac{\boldsymbol{NOT}_{ilgg't_1}}{TMA_l} \left(\frac{2L_{lgg'}}{SP_l^{between}} + LUT_l \right) + \sum_g \frac{\boldsymbol{NOT}_{ilggt_1}}{TCap_{il} \cdot TMA_l} \left(\frac{2L_{lgg}}{SP_l^{within}} + LUT_1 \right) - NTU^0{}_{il} \quad \forall i, l \tag{B.77}$$

$$\boldsymbol{ITU}_{ilt} \geq \sum_{g,g',g' \neq g} \frac{\boldsymbol{NOT}_{ilgg't}}{TMA_l} \left(\frac{2L_{lgg'}}{SP_l^{between}} + LUT_l \right) + \sum_g \frac{\boldsymbol{NOT}_{ilggt}}{TCap_{il} \cdot TMA_l} \left(\frac{2L_{lgg}}{SP_l^{within}} + LUT_1 \right) - \boldsymbol{NTU}_{il(t-1)} \quad \forall i, l, t \neq t_1 \tag{B.78}$$

$$\boldsymbol{TCC}_{t1} = \sum_{i,l} TMC_{il} \cdot (NTU_{il}^0 + \boldsymbol{ITU}_{ilt_1}) \tag{B.79}$$

$$\boldsymbol{TCC}_t = \sum_{i,l} TMC_{il} \cdot \boldsymbol{ITU}_{il} \quad \forall t \neq t \tag{B.80}$$

$$\boldsymbol{FC}_t = \sum_{i,l,g,g',g' \neq g} FP_l \left(\frac{2L_{lgg'} \cdot \boldsymbol{Q}_{ilgg't}}{FE_l^{between} \cdot TCap_{il}} \right) + \sum_{i,l,g} FP_l \left(\frac{2L_{lgg} \cdot \boldsymbol{Q}_{ilggt}}{FE_l^{within} \cdot TCap_{il}} \right) \quad \forall t \tag{B.81}$$

$$\boldsymbol{LC}_t = \sum_{i,l,g,g',g' \neq g} DW_l \left(\frac{\boldsymbol{Q}_{ilgg't}}{TCap_{il}} \left(\frac{2L_{lgg'}}{SP_l^{between}} + LUT_l \right) \right) + \sum_{i,l,g} DW_l \left(\frac{\boldsymbol{Q}_{ilggt}}{TCap_{il}} \left(\frac{2L_{lgg}}{SP_l^{within}} + LUT_l \right) \right) \quad \forall t \tag{B.82}$$

$$\boldsymbol{MC}_t = \sum_{i,l,g,g'} ME_l \left(\frac{2L_{lgg'} \cdot \boldsymbol{Q}_{ilgg't}}{TCap_{il}} \right) \quad \forall t \tag{B.83}$$

$$\boldsymbol{GC}_t = \sum_{i,l} GE_l \cdot \boldsymbol{NTU}_{ilt} \quad \forall t \tag{B.84}$$

$$\boldsymbol{TOC}_t = \boldsymbol{FC}_t + \boldsymbol{LC}_t + \boldsymbol{MC}_t + \boldsymbol{GC}_t \quad \forall t \tag{B.85}$$

$$\boldsymbol{TDC_t} = \frac{\boldsymbol{FCC_t} + \boldsymbol{TCC_t}}{\alpha \cdot CCF_t} + \boldsymbol{FOC_t} + \boldsymbol{TOC_t} + \boldsymbol{FSC_t} \quad \forall t \tag{B.86}$$

$$\boldsymbol{TDC} = \sum_t \frac{CFF_t}{\sum_{t^*} CFF_t} \boldsymbol{TDC}_t \tag{B.87}$$

$$\min\{\boldsymbol{TDC}\} \tag{B.88}$$

CO_2 Part Constraints (B.89)-(B.95) present the total chain emissions for the dynamic HSCN model.

$$\boldsymbol{TCE}_t^{Feed} = \sum_p CO2_p^{Feed} \sum_{i,g} \boldsymbol{P}_{pigt} \quad \forall t \tag{B.89}$$

$$\boldsymbol{TCE}_t^{Prod} = \sum_{p,i,g} \left((1 - \mathbb{1}_p^{CCS}) \cdot CO2_{pi}^{Prod} + \mathbb{1}_p^{CCS} \cdot (1 - CCSEF) \cdot CO2_{pi}^{Prod} \right) \boldsymbol{P}_{pigt} \quad \forall t \tag{B.90}$$

$$\boldsymbol{TCE}_t^{Trans} = CO2^{Trans} \sum_{i,l,g,g'} \boldsymbol{NOT}_{ilgg't} \cdot 2L_{lgg'} \quad \forall t \tag{B.91}$$

$$\boldsymbol{TCE_t} = \boldsymbol{TCE}_t^{Feed} + \boldsymbol{TCE}_t^{Prod} + \boldsymbol{TCE}_t^{Trans} \quad \forall t \tag{B.92}$$

$$\boldsymbol{TCE} = \sum_t \frac{CFF_t}{\sum_{t^*} CFF_t} \boldsymbol{TCE}_t \tag{B.93}$$

$$\boldsymbol{TCE}_t \leq TCE_t^{max} \quad \forall t \tag{B.94}$$

$$\boldsymbol{TCE} \leq TCE^{max} \tag{B.95}$$

Constraints (B.96)-(B.103) present the calculation of CI post-optimization for the dynamic HSCN model.

$$CI_{pi}^{Start} := \left(CO2_p^{Feed} + (1 - \mathbb{1}_p^{CCS}) \cdot CO2_{pi}^{Prod} + \mathbb{1}_p^{CCS} \cdot (1 - CCSEF) \cdot CO2_{pi}^{Prod}\right) \quad \forall p, i \tag{B.96}$$

$$CI_{igt}^{Plants} := \sum_p \frac{\bar{\boldsymbol{P}}_{pigt}}{\bar{\boldsymbol{P}}_{igt}^T} \cdot CI_{pi}^{Start} \quad \forall i, g, t \tag{B.97}$$

$$CI_{igt}^{Prod} := \sum_{l,g'} \frac{\bar{\boldsymbol{Q}}_{ilg'gt}}{\sum_{l^*,g'^*} \bar{\boldsymbol{Q}}_{il^*g'^*gt}} \cdot CI_{ig't}^{Plants} \quad \forall i, g, t \tag{B.98}$$

$$CI_{igt}^{Trans} := \frac{CO2^{Trans} \sum_{l,g'} \boldsymbol{N\bar{O}T}_{ilg'gt} \cdot 2L_{lg'g}}{\bar{\boldsymbol{D}}_{igt}^L + \bar{\boldsymbol{D}}_{igt}^I} \quad \forall i, g, t \tag{B.99}$$

$$CI_{igt} := CI_{igt}^{Prod} + CI_{igt}^{Trans} \quad \forall i, g, t \tag{B.100}$$

$$CI_{gt} := \sum_i CI_{igt} \cdot \frac{(\bar{\boldsymbol{D}}_{igt}^L + \bar{\boldsymbol{D}}_{igt}^I)}{D_{gt}^T} \quad \forall g, t \tag{B.101}$$

$$Carbon_{igt} := CI_{igt} \cdot (\bar{\boldsymbol{D}}_{igt}^L + \bar{\boldsymbol{D}}_{igt}^I) \quad \forall i, g, t \tag{B.102}$$

$$Carbon_{gt} := CI_{gt} \cdot D_{gt}^T \quad \forall g, t \tag{B.103}$$

Constraints (B.104)-(B.113) present the calculation of CI during-optimization for the dynamic HSCN model.

$$CI_{pi}^{Start} = \left(CO2_p^{Feed} + (1 - \mathbb{1}_p^{CCS}) \cdot CO2_{pi}^{Prod} + \mathbb{1}_p^{CCS} \cdot (1 - CCSEF) \cdot CO2_{pi}^{Prod}\right) \quad \forall p, i \tag{B.104}$$

$$\boldsymbol{CI}_{igt}^{Plants} \cdot \boldsymbol{P}_{igt}^T = \sum_p \boldsymbol{P}_{pigt} \cdot CI_{pi}^{Start} \quad \forall i, g, t \tag{B.105}$$

$$\boldsymbol{CI}_{igt}^{Prod} \cdot \sum_{l^*,g'^*} \boldsymbol{Q}_{il^*g'^*gt} = \sum_{l,g'} \boldsymbol{Q}_{ilg'gt} \cdot \boldsymbol{CI}_{ig't}^{Plants} \quad \forall i, g, t \tag{B.106}$$

$$\boldsymbol{CI}_{igt}^{Trans} \cdot (\boldsymbol{D}_{igt}^L + \boldsymbol{D}_{igt}^I) = CO2^{Trans} \sum_{l,g'} \boldsymbol{NOT}_{ilg'gt} \cdot 2L_{lg'g} \quad \forall i, g, t \tag{B.107}$$

$$\boldsymbol{CI}_{igt} = \boldsymbol{CI}_{igt}^{Prod} + \boldsymbol{CI}_{igt}^{Trans} \quad \forall i, g, t \tag{B.108}$$

$$\boldsymbol{CI}_{gt} = \sum_i \boldsymbol{CI}_{igt} \cdot (\boldsymbol{D}_{igt}^L + \boldsymbol{D}_{igt}^I) \cdot \frac{1}{D_{gt}^T} \quad \forall g, t \tag{B.109}$$

$$\boldsymbol{CI}_{igt} \leq CI_{igt}^{max} \quad \forall i, g, t \tag{B.110}$$

$$\boldsymbol{CI}_{gt} \leq CI_{gt}^{max} \quad \forall g, t \tag{B.111}$$

$$\boldsymbol{CI}_{igt}^{Plants} = 0 \quad \forall i, g, t \text{ if } \mathbb{1}_{igt}^{Prod} = 0 \tag{B.112}$$

$$\boldsymbol{CI}_{igt} = \boldsymbol{CI}_{gt} = 0 \quad \forall i, g, t \text{ if } D_{gt}^T = 0 \tag{B.113}$$

Appendix C

Hydrogen Case Study: Full Data Set

This appendix presents the full dataset of the case study for both the static and dynamic model. Most of the data is based on Konda et al. (2011), but in a few cases some data is utilized from other papers or the internet, either to simplify the model or in case the paper was lacking data.

C.1 Sets

The elements of the sets are given below.

- G = {Rotterdam, Zoetermeer, Leiden, The Hague, Amsterdam, Haarlem, IJmuiden, Utrecht, Amersfoort, Arnhem, Apeldoorn, Nijmegen, Eindhoven, 's-Hertogenbosch, Tilburg, Breda, Dordrecht, Middelburg, Maastricht, Enschede, Zwolle, Assen, Groningen, Leeuwarden, Almere};
- I = {CH_2, LH_2};
- L = {tube trailer (CH_2 only), tanker truck (LH_2 only)};
- P = {SMR-Small, SMR-Medium, SMR-Large, CG-Small, CG-Medium, CG-Large, BG-Small, BG-Medium, BG-Large, WE-Small, WE-Medium, WE-Large, SMR-Small-CCS, SMR-Medium-CCS, SMR-Large-CCS, CG-Small-CCS, CG-Medium-CCS, CG-Large-CCS, BG-Small-CCS, BG-Medium-CCS, BG-Large-CCS, WE-Small-CCS, WE-Medium-CCS, WE-Large-CCS}.
- T = {2015-2020, 2021-2030, 2031-2040, 2041-2050}.

C.2 Parameters

The parameter values are given below.

- CCF = 6 years for period T1, 10 years for period T2, T3 and T4;
- $CCSCost$ = 25 \$/ton CO2 (optional range of 5-55 in case of further analysis);
- $CCSEF$ = 90%;
- CO_2Feed_p = given Table C.1;
- CO_2Prod_{pi} = given in Table C.1;
- CO_2Trans = 0.00075 ton CO_2/km (750 g CO_2/km);

- D_g^T = given in Table C.2, same as D_{gt}^T. The daily hydrogen demand in a grid in a given time period is calculated by the formula below.

  $$D_g^T(kg/day) = NumVeh \cdot MarketShare \cdot Density_g \cdot DistTrav(km/day) \cdot FuelEconomy(kg/km)$$

  The total number of vehicles $NumVeh$ in a time period is calculated by assuming 6,865,000 vehicles in 2004 with an annual growth rate of 2.4%, then averaging the number of vehicles over the length of the time period. The hydrogen market shares $MarketShare$ are assumed to be 1% in T1, 3% in T2, 7.5% in T3 and 17.5% in T4. The density of cars in each grid $Density_g$ is calculated based on the percentage of cars and FCV market penetration in the regions as given in Konda et al. (2011). It is assumed that the average distance traveled $DistTrav$ = 52.5 km/day and the fuel economy $FuelEconomy$ = 0.011 kg/km.

- DW_l = 35 \$/h $\forall l$;
- FE_l^{within} = 2.30 km/L diesel $\forall l$;
- $FE_l^{between}$ = 2.55 km/L diesel $\forall l$;
- FP_l = 1.3 \$/L diesel $\forall l$;
- FSP_p = 120 \$/ton NG for $p = SMR$, 30 \$/ton coal for $p = CG$, 50 \$/ton biomass for $p = BG$, 50 \$/MWh for $p = WE$, which is based on Almansoori and Shah (2012);
- GE_l = 8.22 \$/day/vehicle $\forall l$;
- $L_{lgg'}$ = is given in Table C.3. The distances between grids are calculated based on the longitude and latitude values of the centers of the regions. The distance traveled within in a grid is assumed to be 5 km.
- LUT_l = 4 h for l = tube tanker and 2 h for l = tanker truck;
- NP_{pig}^0 = 0 $\forall p, i, g$;
- NTU_{il}^0 = 0 $\forall i, l$;
- ME_l = 0.0976 \$/km $\forall l$;
- $PCap_{pi}^{min}$ = 20 ton H_2/day for small plants, 100 ton H_2/day for medium plants, 500 ton H_2/day for large plants, and 0 in case of the dynamic model;
- $PCap_{pi}^{max}$ = 99 ton H_2/day for small plants, 499 ton H_2/day for medium plants, 1000 ton H_2/day for large plants;
- PCC_{pi} = given in Table C.4. These values are calculated by taking the middle value of the minimum and maximum capacity of plants (60 for small plants, 300 for medium plants, 750 for large plants) and plugging these in the formulas given in Konda et al. (2011).
- PCR_p = given in Table C.5. These values are a rough estimate by considering the corresponding values from Almansoori and Shah (2012). For the missing values in their paper, a linear extrapolation is done;

- UPC_{pi} = given in Table C.4. These values are a rough estimate by considering the corresponding values from Almansoori and Shah (2009). For the missing values in their paper, a linear extrapolation is done;
- $Q_{il}^{min} = 0 \ \forall i, l$;
- $Q_{il}^{max} = \sum_g D_g^T \ \forall i, l$;
- $SP_l^{within} = 25$ km/h $\forall l$;
- $SP_l^{between} = 50$ km/h $\forall l$;
- $TCap_{il} = 0.2$ ton H_2/trip for $= l$ tube trailer & $i = CH_2$ and 4 ton H_2/trip for $l =$ tanker truck, $i = LH_2$;
- $TMA_l = 24$ h/day $\forall l$;
- $TMC_{il} = 300{,}000$ \$/vehicle for $l =$ tube trailer & $i = CH_2$ and 800,000 \$/vehicle for $l =$ tanker truck & $i = LH_2$;
- $\alpha = 365$ days/year;
- $\mathbb{1}_{ig}^{Prod}$ = given in Table C.2.

TABLE C.1: Production emissions ($CO2_{pi}^{Prod}$) and feedstock preparation emissions ($CO2_p^{Feed}$) at plants.

Product Technology	Production emissions in ton CO_2/ton H_2 ($CO2_{pi}^{Prod}$)						Feed emissions in ton CO_2/ton H_2 ($CO2_p^{Feed}$)
	CH_2 plant			LH_2 plant			
	Small	Medium	Large	Small	Medium	Large	
SMR	11.4	10.8	10.3	15.1	14.6	14.0	0.58
CG	24.8	23.8	22.9	27.6	26.6	25.7	1.31
BG	26.9	25.4	24.0	29.0	27.5	26.2	0.21
WE	43.9	41.1	38.6	26.2	24.5	23.0	0

TABLE C.2: Hydrogen demand per time period (D_g^T) and possible plant building locations ($\mathbb{1}_{ig}$).

Grid	Location	Hydrogen demand in ton/day (D_g^T)				Possible building site for CH_2 ($\mathbb{1}_{\{CH_2\}g}$)	Possible building site for LH_2 ($\mathbb{1}_{\{LH_2\}g}$)
		T1 (2015-2020)	T2 (2021-2030)	T3 (2031-2040)	T4 (2041-2050)		
G01	Rotterdam	18.82	37.62	134.55	334.58	1	1
G02	Zoetermeer	3.08	6.15	22.00	54.71	0	0
G03	Leiden	3.08	6.15	22.00	54.71	0	0
G04	The Hague	3.08	6.15	22.00	54.71	0	0
G05	Amsterdam	8.29	16.56	59.23	147.30	1	0
G06	Haarlem	5.68	11.36	40.62	101.01	0	0
G07	IJmuiden	2.37	4.73	16.92	42.09	0	0
G08	Utrecht	4.50	8.99	32.16	79.96	0	0
G09	Amersfoort	4.50	8.99	32.16	79.96	0	0
G10	Arnhem	0	5.68	20.31	75.75	1	0
G11	Apeldoorn	0	5.09	18.19	67.86	0	0
G12	Nijmegen	0	5.09	18.19	67.86	0	0
G13	Eindhoven	0	4.73	16.92	63.13	0	0
G14	's-Hertogenbosch	0	4.73	16.92	63.13	0	0
G15	Tilburg	0	4.73	16.92	63.13	0	0
G16	Breda	0	4.73	16.92	63.13	0	0
G17	Dordrecht	3.08	6.15	22.00	54.71	0	0
G18	Middelburg	0	3.08	11.00	41.03	0	0
G19	Maastricht	0	8.16	29.19	108.90	1	0
G20	Enschede	0	3.79	13.54	50.50	0	0
G21	Zwolle	0	3.67	13.12	48.92	0	0
G22	Assen	0	3.55	12.69	47.35	0	0
G23	Groningen	0	4.14	14.81	55.24	1	0
G24	Leeuwarden	0	4.50	16.08	59.97	0	0
G25	Almere	0	3.19	11.42	42.61	0	0
Total demand/sites		56.46	181.73	649.88	1922.25	5	1

TABLE C.3: Distance matrix between grids, rounded, in km/trip ($L_{lgg'}\ \forall l$).

$L_{lgg'}$	G01	G02	G03	G04	G05	G06	G07	G08	G09	G10	G11	G12	G13	G14	G15	G16	G17	G18	G19	G20	G21	G22	G23	G24	G25
G01	5	15	26	20	57	53	60	48	67	98	107	94	87	62	55	44	18	76	146	168	128	185	202	168	72
G02	15	5	11	13	44	38	45	43	62	97	102	96	96	69	66	58	30	87	158	165	119	174	190	154	62
G03	26	11	5	16	36	27	34	44	61	98	101	100	105	76	75	68	41	95	168	164	115	168	183	146	57
G04	20	13	16	5	52	42	48	56	75	110	115	109	107	80	75	64	38	79	166	178	131	184	199	161	73
G05	57	44	36	52	5	17	22	35	41	81	75	89	111	80	88	89	64	131	178	137	82	132	147	111	25
G06	53	38	27	42	17	5	8	46	57	96	92	103	119	89	94	91	64	122	185	154	98	146	159	119	42
G07	60	45	34	48	22	8	5	54	63	103	97	110	127	97	102	99	72	126	194	158	100	145	157	115	46
G08	48	43	44	56	35	46	54	5	20	54	59	58	76	45	56	63	44	123	143	122	81	140	159	132	31
G09	67	62	61	75	41	57	63	20	5	40	40	49	80	51	67	78	63	142	147	103	62	122	142	119	23
G10	98	97	98	110	81	96	103	54	40	5	26	20	67	52	73	90	87	167	127	73	60	121	144	135	59
G11	107	102	101	115	75	92	97	59	40	26	5	45	92	73	94	109	100	180	152	63	35	96	119	111	50
G12	94	96	100	109	89	103	110	58	49	20	45	5	48	39	59	78	80	157	107	85	80	140	164	154	71
G13	87	96	105	107	111	119	127	76	80	67	92	48	5	31	33	51	69	129	67	131	127	188	211	197	102
G14	62	69	76	80	80	89	97	45	51	52	73	39	31	5	21	40	46	119	98	124	105	168	190	171	73
G15	55	66	75	75	88	94	102	56	67	73	94	59	33	21	5	20	37	100	93	145	125	187	209	187	86
G16	44	58	68	64	89	91	99	63	78	90	109	78	51	40	20	5	28	80	103	163	138	200	220	194	93
G17	18	30	41	38	64	64	72	44	63	87	100	80	69	46	37	28	5	81	128	159	124	184	203	173	73
G18	76	87	95	79	131	122	126	123	142	167	180	157	129	119	100	80	81	5	162	239	204	261	277	241	148
G19	146	158	168	166	178	185	194	143	147	127	152	107	67	98	93	103	128	162	5	174	187	246	270	261	169
G20	168	165	164	178	137	154	158	122	103	73	63	85	131	124	145	163	159	239	174	5	64	89	113	132	112
G21	128	119	115	131	82	98	100	81	62	60	35	80	127	105	125	138	124	204	187	64	5	62	85	78	58
G22	185	174	168	184	132	146	145	140	122	121	96	140	188	168	187	200	184	261	246	89	62	5	25	56	113
G23	202	190	183	199	147	159	157	159	142	144	119	164	211	190	209	220	203	277	270	113	85	25	5	51	130
G24	168	154	146	161	111	119	115	132	119	135	111	154	197	171	187	194	173	241	261	132	78	56	51	5	101
G25	72	62	57	73	25	42	46	31	23	59	50	71	102	73	86	93	73	148	169	112	58	113	130	101	5

TABLE C.4: Plant capital costs (PCC_{pi}) and unit production costs (UPC_{pi}).

Product Technology	Plant capital cost in 10^6\$ (PCC_{pi})						Unit production cost in \$/ton H_2 (UPC_{pi})		
	CH_2 plant			LH_2 plant			CH_2 & LH_2 plant		
	Small	Medium	Large	Small	Medium	Large	Small	Medium	Large
SMR	666	2248	4481	1164	3806	7447	3360	1740	1430
CG	1716	5987	12,154	2263	7770	15,631	2500	2030	1560
BG	1788	6039	12,037	2298	7395	14,337	4890	3520	2150
WE	2706	10,748	23,487	3128	12,228	26,474	6820	5030	3240

TABLE C.5: Production conversation rate from feedstock at plants (PCR_p).

Product Technology	Production conversation rate (PCR_p)			Unit/ton H_2
	Small	Medium	Large	
SMR	4.02	3.34	3.16	ton NG/ton H_2
CG	5.95	5.64	5.33	ton coal/ton H_2
BG	25.5	18.4	11.3	ton biomass/ton H_2
WE	52.5	52.5	52.5	MWh/ton H_2